Technical Report CERC-95-14
September 1995

US Army Corps of Engineers
Waterways Experiment Station

Effectiveness of Spur Jetties at Siuslaw River, Oregon

Report 2

Localized Current Flow Patterns Induced by Spur Jetties: Airborne Current Measurement System and Prototype/Physical Model Correlation

by Cheryl E. Pollock

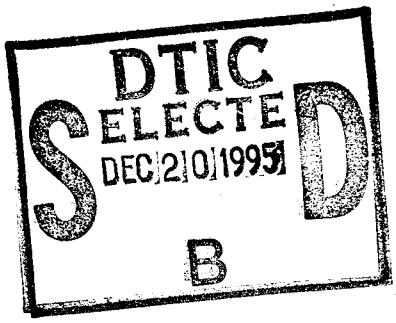

Prepared for Headquarters, U.S. Army Corps of Engineers

Technical Report CERC-95-14
September 1995

Effectiveness of Spur Jetties at Siuslaw River, Oregon

Report 2

Localized Current Flow Patterns Induced by Spur Jetties: Airborne Current Measurement System and Prototype/Physical Model Correlation

by Cheryl E. Pollock

U.S. Army Corps of Engineers
Waterways Experiment Station
3909 Halls Ferry Road
Vicksburg, MS 39180-6199

Report 2 of a series

Approved for public release; distribution is unlimited

Prepared for U.S. Army Corps of Engineers
Washington, DC 20314-1000

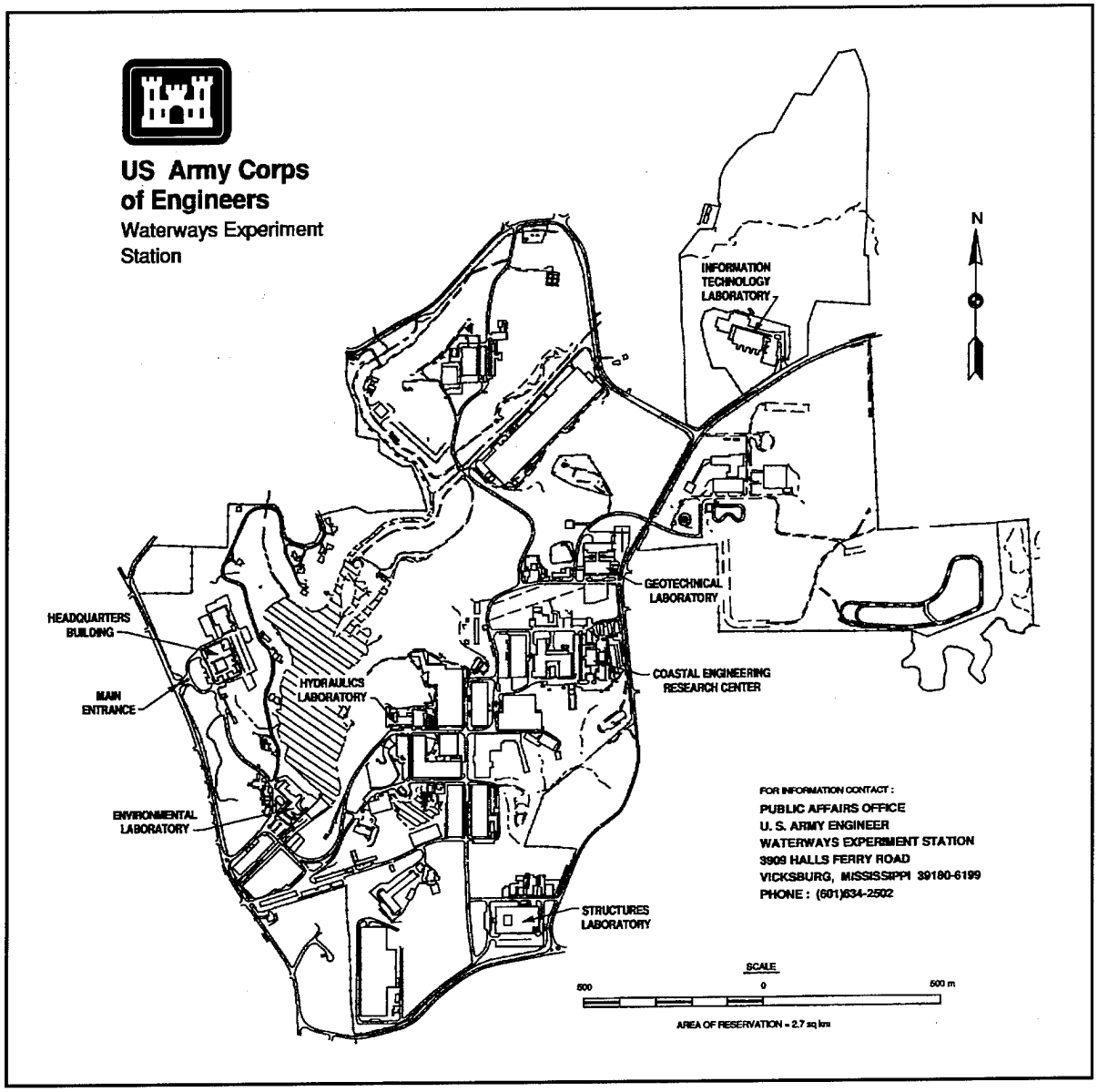

Waterways Experiment Station Cataloging-in-Publication Data

Pollock, Cheryl E.

Effectiveness of spur jetties at Siuslaw River, Oregon. Report 2, Localized current flow patterns induced by spur jetties : airborne current measurement system and prototype/ physical model correlation / by Cheryl E. Pollock ; prepared for U.S. Army Corps of Engineers.

117 p. : ill. ; 28 cm. — (Technical report ; CERC-95-14 rept.2)

Includes bibliographic references.

Report 2 of a series.

1. Ocean currents — Measurement. 2. Jetties — Siuslaw River (Or.) I. United States. Army. Corps of Engineers. II. U.S. Army Engineer Waterways Experiment Station. III. Coastal Engineering Research Center (U.S. Army Engineer Waterways Experiment Station) IV. Title. V. Title: Localized current flow patterns induced by spur jetties. VI. Title: Airborne current measurement system and prototype/physical model correlation. VII. Series: Technical report (U.S. Army Engineer Waterways Experiment Station) ; CERC-95-14 rept. 2.

TA7 W34 no.CERC-95-14 rept.2

Contents

List of Figures

Preface

The study summarized in this report was conducted jointly by the U.S. Army Engineer Waterways Experiment Station's (WES) Coastal Engineering Research Center (CERC) and the U.S. Army Engineer District, Portland (NPP). The effectiveness of spur jetties at the mouth of the Siuslaw River, Oregon, was selected for study by the CERC Monitoring Completed Coastal Projects (MCCP) Program. The MCCP Program Manager was Ms. Carolyn Holmes. This program was sponsored by Headquarters, U.S. Army Corps of Engineers (HQUSACE). The HQUSACE Technical Monitors were Messrs. John H. Lockhart, Jr., John G. Housley, and Barry W. Holliday.

Work was performed under the CERC general administrative supervision of Dr. Yen-hsi Chu, Chief, Engineering Applications Unit; Ms. Joan Pope, Chief, Coastal Structures and Evaluation Branch; Mr. Thomas W. Richardson, Chief, Engineering Development Division; Mr. Charles C. Calhoun, Jr., Assistant Director; and Dr. James R. Houston, Director, CERC.

This report was prepared by Ms. Cheryl E. Pollock, CERC. Field tests, directed by Ms. Pollock and Mr. Steve Chesser, NPP, were conducted jointly by CERC and NPP. Ms. Pollock and Mr. Mike Carpenter (formerly of CERC) were the principal developers of the airborne current measurement system. Assistance and air support were provided by the U.S. Coast Guard at North Bend and Florence, OR, and by the Blue Max Flying Service. Assistance in planning this study was also provided by Ms. Carolyn Holmes, and Messrs. Thomas W. Richardson, Mike Hemsley (formerly CERC), William Kucharski, David McGehee, and Gregory Williams (all of CERC). Messrs. Williams and Carpenter developed the data manipulation computer programs. Figures were prepared by Mses. Mary Allison and Melissa Moore (both of CERC). Ms. Jane Daughtry (CERC) assisted with final report preparation. Technical review was provided by Dr. Robert Randal and Prof. Robert Reid (both of Texas A&M University) and Drs. Steven Hughes (CERC) and Nicholas Kraus (formerly CERC).

Director of WES during publication of this report was Dr. Robert W. Whalin. Commander was COL Bruce K. Howard, EN.

1 Introduction

Background

In 1985 the entrance channel jetties at Siuslaw River, OR, were reconfigured to deflect away from the channel opening sediments carried there by river currents, thereby reducing shoaling in the channel. The project was selected for study as part of the Monitoring Completed Coastal Projects (MCCP) program of the U.S. Army Engineer Waterways Experiment Station (WES) Coastal Engineering Research Center (CERC). The goal of the MCCP program is the advancement of coastal engineering technology. It is designed to determine how well projects are accomplishing their designed purpose and withstanding waves and currents. These determinations, combined with concepts and understanding already available, will lead to solutions of coastal problems; strengthening and improving design criteria and methodology; improving construction practices; and improving operation and maintenance techniques. One aspect of the MCCP study required prototype verification of near-bottom localized current circulation patterns induced by the spur jetty configuration and qualitative comparison with physical model testing conducted by Bottin (1981, 1982).

Engineers and planners are often faced with a lack of knowledge of currents in the nearshore region. Quantitative information about currents is very important for the planning, design, construction, and evaluation of coastal structures. Many methods exist to measure near-bottom currents; however, very few of them can perform well in the adverse and dynamic nearshore environment. High-energy waves, coastal structures, shallow water, and changing bathymetry can individually, or in combination, make existing current measurement systems impractical or unable to provide synoptic views of near-bottom currents.

The most common methods for synoptic delineation of currents employ either the use of dyes and/or surface floats to follow fluid flow or an array of stationary-mounted current meters to measure fluid flow. Although dyes and/or surface floats generally provide a comprehensive picture of surface or near-surface currents, they are not necessarily indicative of near-bottom currents.

The operation of a large array of in situ current meters can simultaneously measure velocities at several points, providing a synoptic picture of flow

patterns near the bottom or at any depth. Under high-energy wave conditions, this method is often unsatisfactory because heavy surf conditions make deployment of sensors difficult, and the extensive scour and deposition associated with high-energy events undermine or bury stationary fixtures and may damage instruments (Sallenger et al. 1983). Additionally, this method requires numerous meters and extensive time expenditures in deployment and recovery of the instruments. Also, flexibility of sampling point locations and rates is not possible once the meters are in place. The adverse situations described above and problems associated with other systems have motivated the development of an airborne current measurement system for use at Siuslaw River, OR. This system maneuvers easily in coastal areas that are difficult to access and is capable of providing a near-synoptic picture of near-bottom currents.

Literature Review of Alternative Current Measurement Systems

A review of the literature provides several examples of current monitoring systems and studies. At Ajigaura Beach, Japan, Sasaki, Horikawa, and Hotta (1976) employed synchronized photogrammetry from two stationary helium-filled balloons to track Lagrangian floats in successive pictures and document nearshore surface flow fields. Figure 1 is a schematic of the balloon system. Sasaki and Sakuramoto (1984) evaluated shore-parallel rip current barriers using the same system with balloons and helicopters as support vehicles to photograph successive dye patch dispersions at Taito and Katagai fishing harbors in Japan. Figure 2 is a schematic diagram of the synchronized helicopter photogrammetry system, and Figure 3 shows circulation patterns obtained from photographs of successive dye patch dispersion patterns for Taito Harbor. Horikawa and Sasaki (1972) used the fixed-balloon and the helicopter systems to observe nearshore current patterns induced by waves on the Shonan Coast in Kanagawa Prefecture, Japan. During these studies, they found the balloon system to be limited to winds less than 7-8 m/s (23-26 ft/s), and both systems suffered from the inability of the boats to maneuver to designated deployment locations for the dye injection or surface float releases.

Prior to the design of structures to stabilize the eroding shoreline of North Bull Island, South Carolina, Knoth and Nummedal (1977) used fluorescent, dyed sand as a tracer to estimate the annual rate of longshore sediment transport. Tracer concentrations over time and space were determined from samples obtained in a grid pattern, and along a transect downdrift of dyed sand injection points. From this data set, sediment transport rates were estimated.

In eight experiments, Kraus et al. (1982) also used florescent, dyed sand as tracers to estimate short-term longshore sand transport rates on natural beaches and on beaches near structures. Sediment tracers of up to four different colors were injected along a transect perpendicular to the beach. A grid pattern of sampling locations extended downdrift of the injections and offshore the same distance as the injections. Stationary bottom-mounted electromagnetic current

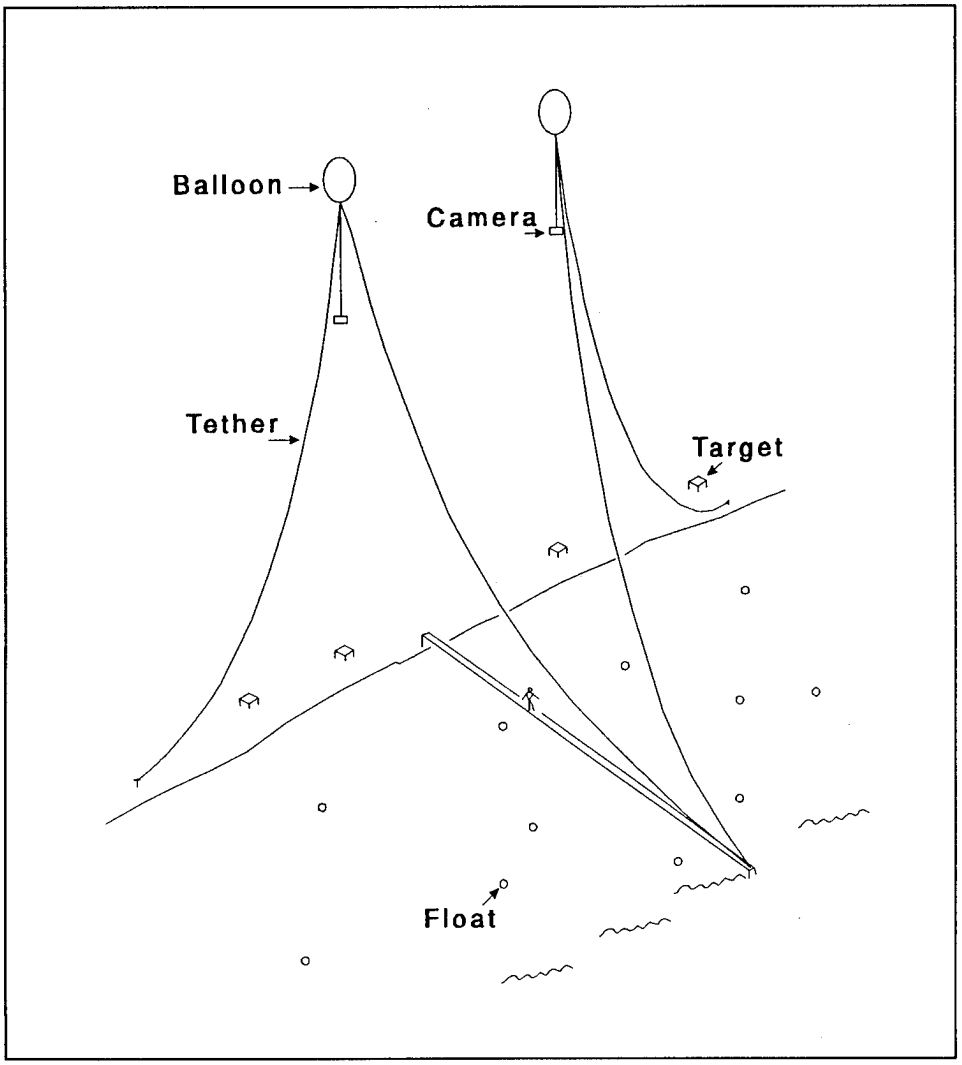

Figure 1. Schematic diagram of balloon system (after Sasaki, Horikawa, and Hotta (1976))

meters collected data within the grid pattern from which currents and sediment transport rates were inferred.

According to Wright, Sonu, and Kielhorn (1972), density contrasts between the water of Choctawhatchee Bay and the Gulf of Mexico resulted in sharp vertical and horizontal stratification in the northern part of East Pass near Destin, FL, during the flood and a portion of the ebb tidal phases. Circulation patterns associated with the saltwater/freshwater interface were investigated by means of drogues (Lagrangian indicators) and Rhodamine BA dye injected on either side of the interface. Two drogues, with vanes situated 0.3 and 1.6 m (1.0 and 5.2 ft) below the surface, were deployed at a point 46 m (150.9 ft) seaward of the visible front edge of the interface. Another drogue with a vane at a depth of 0.3 m (1.0 ft) was released simultaneously 46 m (150.9 ft) bayward of the interface. The shallow drogues approached the density interface

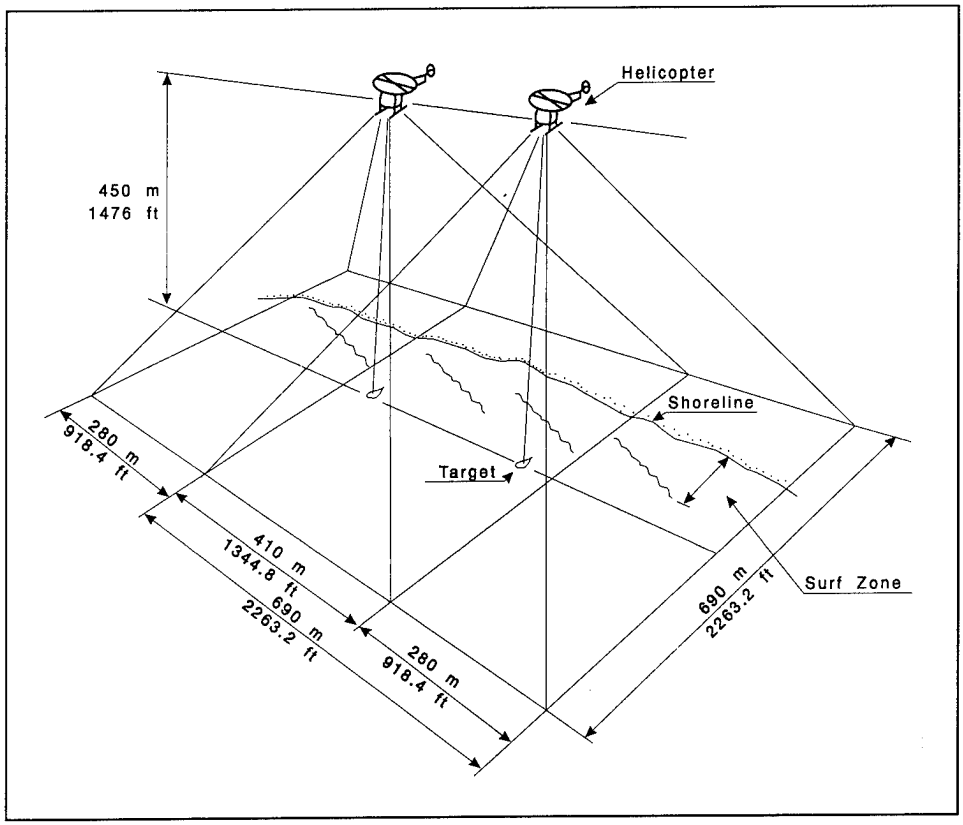

Figure 2. Schematic diagram of synchronized helicopter photogrammetry system (after Horikawa and Sasaki (1972))

from opposite directions; and both drogues stagnated upon reaching the interface. The 1.6-m-draft (5.2-ft-draft) drogue drifted bayward more rapidly than the simultaneously released shallower draft drogue, indicating higher flood velocities at depth. The deeper draft drogue was not hindered by the saltwater/freshwater interface and drifted about 91 m (298.5 ft) beyond the density interface into Choctawhatchee Bay. Similar convergence of the salt water and fresh water at the interface was demonstrated on four different occasions by dye experiments conducted during flood tide. Dye injected on both sides of the interface was tracked using a time-lapse sequence of aerial photographs.

As part of an investigation for the placement of dredged material off the coast of South Padre Island, TX, bottom-trailing drogues called seabed drifters were deployed, and their beach recovery documented (McLellan and Burke, in preparation). Seabed drifters were released at the ocean floor and allowed to flow with currents until they beached. Their recovery location was then recorded. The drifters were released in groupings of 25 from 8 sites that formed a grid over the proposed dredged material placement site and at 2 control sites. Four releases were made during a tidal cycle at each site. In studies of this type the deployment and recovery locations are clear, but current paths and transit rates between the two points can only be implied.

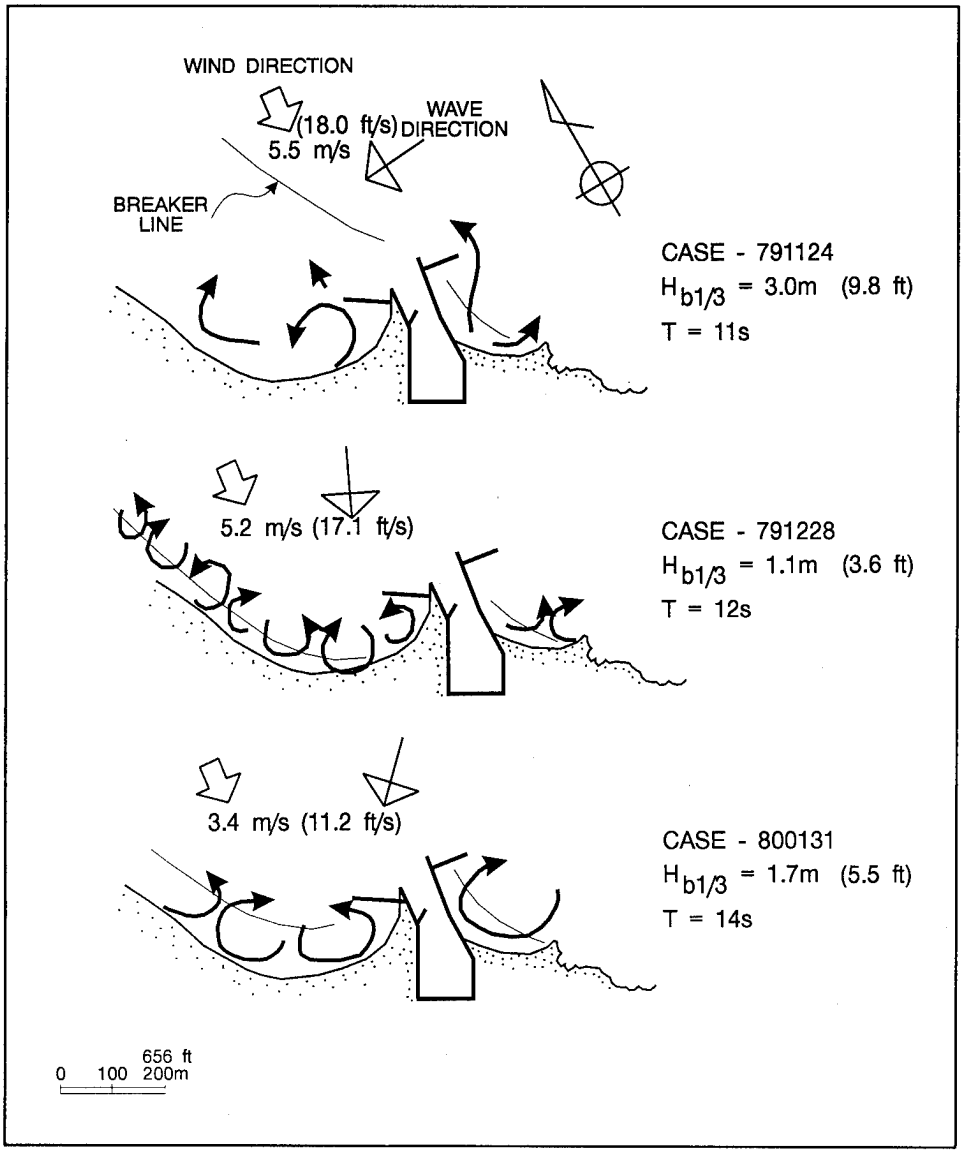

Figure 3. Circulation patterns of successive dye patch dispersion patterns at Taito Harbor, Japan (after Sasaki and Sakuramoto (1984))

Chu and Nersesian (1992) measured currents at Shinnecock and Moriches Inlets, New York, to investigate the development of scour holes. At each inlet three marker buoys were placed across the inlets and one in the scour hole. A survey boat moved from buoy to buoy. At each location, the boat was moored at the buoy while a vertical profile of the currents was obtained by raising an electromagnetic current meter incrementally through the water column.

As part of the Nearshore Sediment Transport Studies (NSTS), field studies were performed at several locations including Leadbetter and Torrey Pines Beaches, CA, and Duck, NC. The objective of NSTS was to use field experiments to formulate and improve littoral transport equations for topographically simple beaches. Verification and calibration of longshore current models were

integral parts of the studies. Field sites were selected where waves were usually nearly normal to the longshore direction, and the bottom contours were relatively straight and parallel to the shoreline. At Leadbetter Beach, Santa Barbara, CA, steady surf-zone longshore currents and directional properties of the nearshore incident wave field were measured for a beach with nearly straight and parallel depth contours. Instrumentation included Marsh-McBirney Model 512 electromagnetic 4-cm-diam (1.6-in.-diam) spherical probes. Figure 4 shows instrument deployment for an experiment at Leadbetter Beach, CA. In addition, an instrument array composed of four pressure sensors and a current meter were placed at water depths of 9 m and 5 m (29.5 ft and 16.4 ft), respectively (Thornton and Guza 1986; Guza, Thornton, and Christensen 1986).

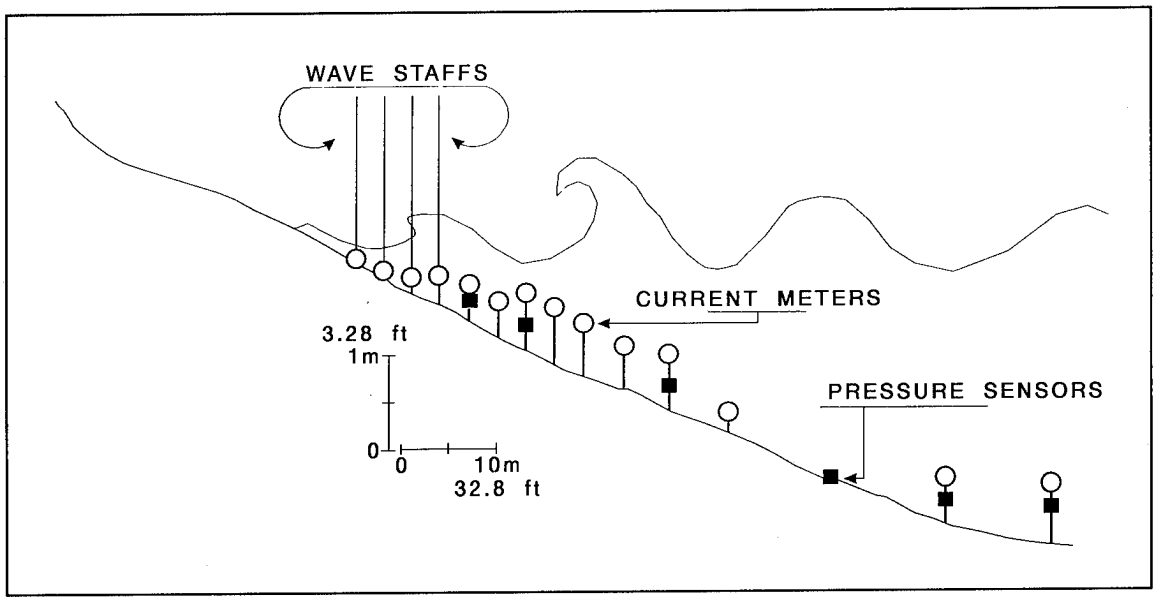

Figure 4. Instrument deployment for experiment at Leadbetter Beach, CA (after Thornton and Guza (1986))

At Torrey Pines Beach, San Diego, CA, an extensive array of instruments was deployed to study nearshore wave dynamics. Sea surface elevations, or pressures, and flow velocities were measured at closely spaced locations in a line extending from a depth of 10 m (32.8 ft) to inside the surf zone (Guza and Thornton 1978, 1980). These measurements were collected for intercomparison with a linear theory description of nearshore wave dynamics. Locations of instruments used in this study, in relation to onshore-offshore profiles, are shown in Figure 5. The suite of instruments deployed included six Marsh-McBirney electromagnetic current meters placed between depths of 0 m and 5 m ((0 ft and 16.4 ft), five Stathem temperature-compensated pressure transducers placed between the 3- and 10-m (9.8- and 32.8-ft) depth contours, and five wave staffs placed to depths of 4 m (13.1 ft). The Torrey Pines Beach topography as described by Guza, Thornton, and Christensen (1986) is a planar beach with straight and parallel contours.

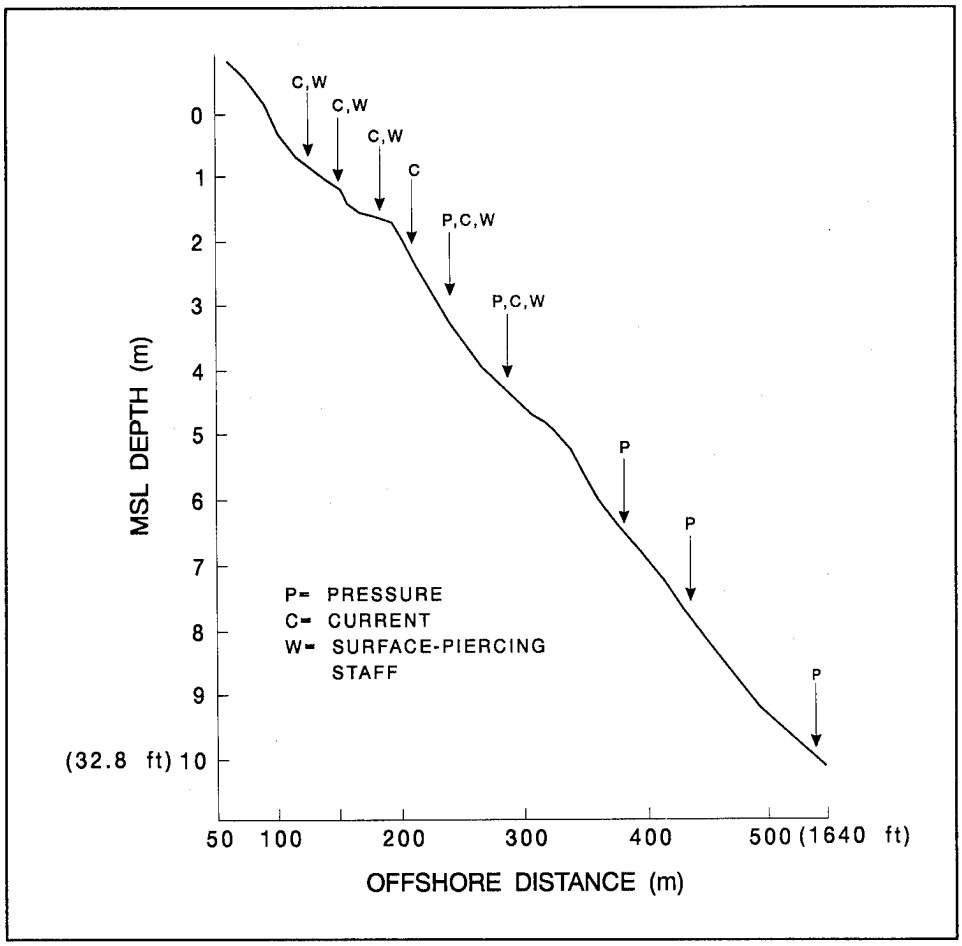

Figure 5. Instrument location used in onshore-offshore profiles study at Torrey Pines Beach, CA (after Guza and Thornton (1980))

During the SUPERDUCK experiment held at the CERC Field Research Facility (FRF), Duck, NC, currents were measured at various locations across the surf zone in October of 1986 (Whitford 1988, Whitford and Thornton 1988). A movable sled, instrumented with three Marsh-McBirney (4-cm- (1.6-in.-) diam sensor) electromagnetic current meters, and pressure and wind sensors, was used to transect sections of the surf zone to obtain field measurements for comparison with numerically predicted longshore current profiles. The sled was towed seaward along each transect by the FRF Coastal Research Amphibious Buggy, and onshore by a four-wheel-drive fork lift located on the beach. Along each transect, measurement positions included the point of maximum breaking, a point just beyond the breaker zone, on top of the nearshore bar, and in the nearshore trough. Measurements on each transect required approximately 35 min. Precise orientation of the sled was obtained using a Zeiss Elta-2 electronic survey system that reflected its signals off optical prisms mounted atop the mast of the sled.

Additionally, during SUPERDUCK, currents were measured in the surf zone for comparison with sand transport experiments (Rosati, Gingerich, and

Kraus 1990). Marsh-McBirney electromagnetic (4-cm- (1.6-in.-) diam sphere sensor) current meters were mounted on 1.5-m-high (4.9-ft-high) tripods and were connected to shore by cable. The lower ends of the tripods' legs were partially buried 10 cm (3.9 in.) into the seabed by shaking the tripod back and forth and applying downward pressure.

Observations during the NSTS and the SUPERDUCK experiments were used by Dodd, Oltman-Shay, and Thornton (1992) to investigate low-frequency oscillations in the surf zone longshore current, with wavelengths shorter than usual infra-gravity waves at the same frequency. The local topography during SUPERDUCK exhibited a barred beach with reasonably parallel contours. An alongshore array of seven current meters, 290 m (951 ft) in length, located in the trough shoreward of the bar was used in the analysis. The cross-shore profile of the longshore current was measured by moving a sled in a transect across the surf zone, stopping at each location for at least 35 min. Typically, measurements were made at three to five locations, concurrent with the hourly measurement period of the fixed array. In addition to the current measurements, an offshore (8-m (26.2-ft) depth) linear array of nine bottom-mounted pressure sensors was used to measure the incident wave field. Measurements were made around low tide to minimize the effects of tidal variation.

The mechanism responsible for onshore and offshore sediment fluxes across the surf zone was examined in a 3-year field study (Wright 1991). The study was conducted in the southern part of the middle Atlantic Bight in the depth region of 7 to 17 m (23 to 55.8 ft) using instrumented tripods supporting electromagnetic current meters, pressure sensors, suspended sediment concentration sensors, and sonar altimeters. The more comprehensive of these tripods supported four Marsh-McBirney two-component electromagnetic current meters (4-cm (1.6-in.) spheres) at different elevations, along with other instruments. Three field experiments were conducted over the shoreface regions of the FRF, Duck, NC, and one was conducted off Sandbridge Beach, VA. The Duck experiments were conducted in September 1985, July 1987, and January 1988. The Sandbridge experiment was conducted in October and November, 1988. Figure 6 shows the tripod location relative to the beach profile for the four experiments. The instruments were located on the portion of the profile that remained stable between experiments.

A tidal circulation study of Los Angeles and Long Beach Harbors was conducted by WES (McGehee, McKinney, and Dickey 1989; Coastal Engineering Research Center 1990). The data were used for calibration and verification of a numerical circulation model. Field data collection included a 30-day continuous record of the vertical velocity profile measured with in situ meters at nine locations covering the major tidal exchange openings inside the harbor and at the harbor-complex perimeter. In situ current profiles were obtained by deploying up to three current meters on a vertical string supported by a surface buoy on a taut mooring (Figure 7). Additionally, current profiles were taken at hourly intervals at eight locations directly inside harbor channel openings where in situ meters would have hindered boat traffic. At each of these locations, a boat maneuvered to the designated site and measured

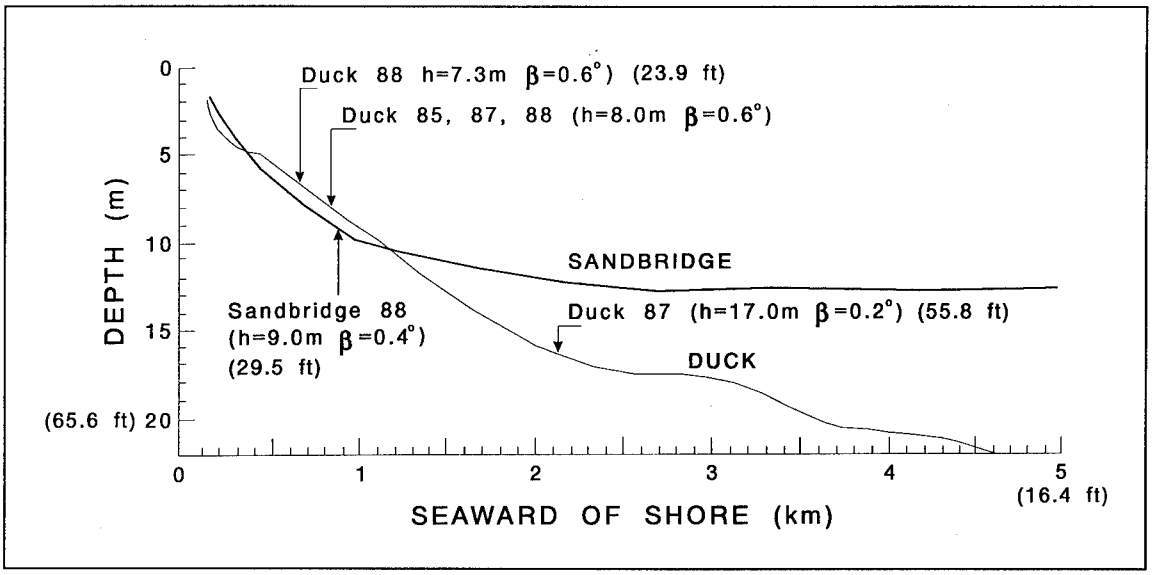

Figure 6. Tripod location for four beach profile experiments, North Carolina and Virginia (after Wright et al. (1991))

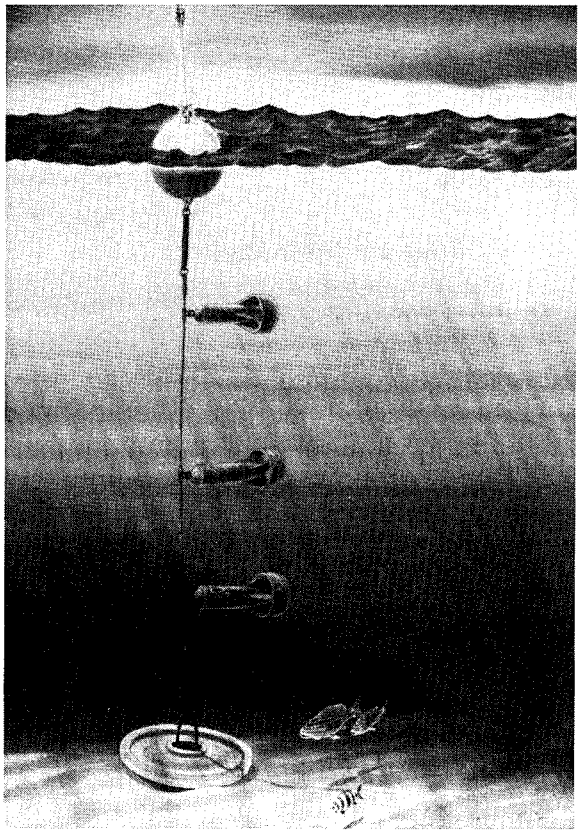

Figure 7. In situ current profiles obtained by deploying current meters (after McGehee, McKinney, and Dickey (1989))

currents near the bottom, mid-depth, and near the water surface. The instruments used for data collection were ducted-impeller meters with an internal compass for measuring direction.

At Prince Inlet, SC, electromagnetic current meters were used to assess the importance of wave contributions to flood dominance in the flood channel of an ebb tidal delta (Huntley and Nummedal 1978). Three Marsh-McBirney two- component electromagnetic sensors were mounted on a single tripod and deployed in the flood channel (Figure 8). Two meters simultaneously measured vertical and along-channel flow at 0.75 and 0.35 m (2.5 and 1.1 ft) above the channel floor, and the third flowmeter measured along-channel flow. For this

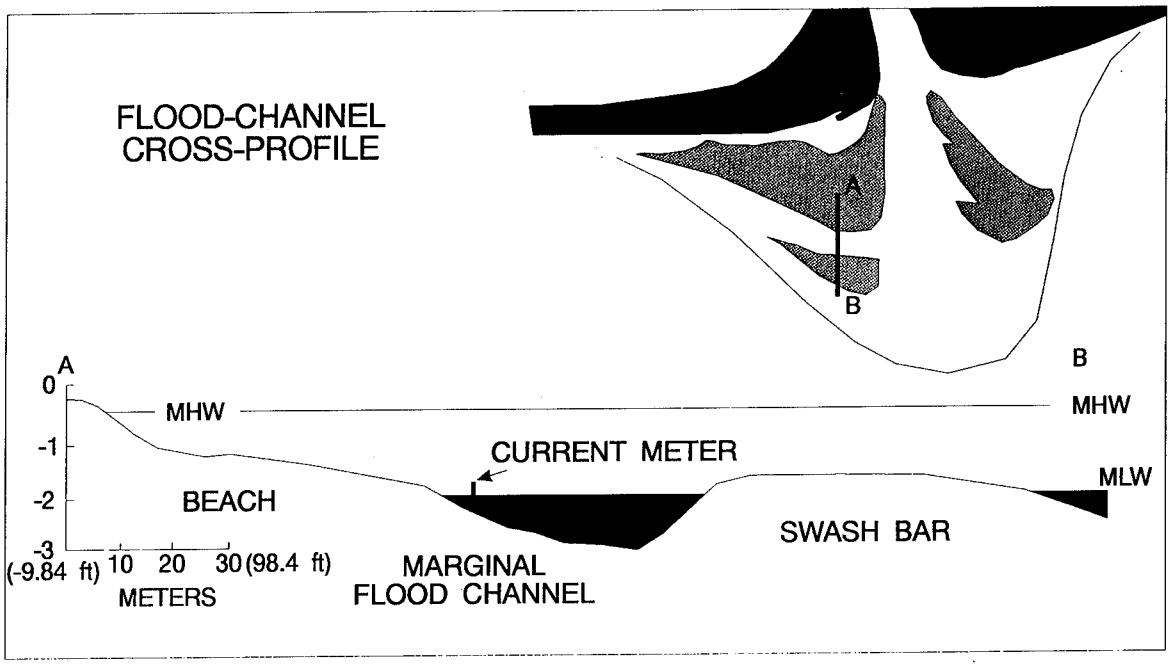

Figure 8. Marsh-McBirney two-component electromagnetic sensors deployed at Prince Inlet, SC (after Huntley and Nummedal (1978))

study, it was assumed that the flow past the meters was representative of the cross-sectional average. The tripod was placed during low water and anchored to the channel floor by lead weights. Alignment of the sensor was achieved using a visual navigational range on the shore. Cables were laid up the beach from the sensors to a telemetry system at the crest of the beach for data storage. The system was powered by 12-V batteries located on a boat anchored in the channel.

Sallenger et al. (1983) developed a system for measuring bottom profiles, waves, and currents in high-energy nearshore environments. The system utilized a sled equipped with a pressure sensor and a two-axis electromagnetic current meter. The sled was pulled across the nearshore zone by a double-drum and pulley system (Figure 9). The drum winch was located on land, and a line ran from one drum winch around three blocks and back to the other drum winch. The blocks form the corners of a right triangle. The sled was attached to the shore-normal side of the triangle line arrangement, and it was pulled offshore by one drum winch and onshore by the other. Location and depth of the sled were monitored using an infrared range-finder mounted onshore and optical prisms mounted atop the sled's mast. The system has been used in breaking waves up to 5 m (16.4 ft); however, it is limited to data acquisition along a single profile. Most previous uses of sea sleds required a boat to tow the sled offshore and a winch or vehicle to tow the sled onshore. The system also experienced problems when sand deposited on the sled and lines during high-energy swell conditions made it difficult to move the sled. Marsh-McBirney (4-cm-diam (1.6-in.-diam) sensor) analog signals were cabled to an underwater housing containing an encoding device and transmitter. The data are transmitted through an antenna at the top of the mast to a receiving

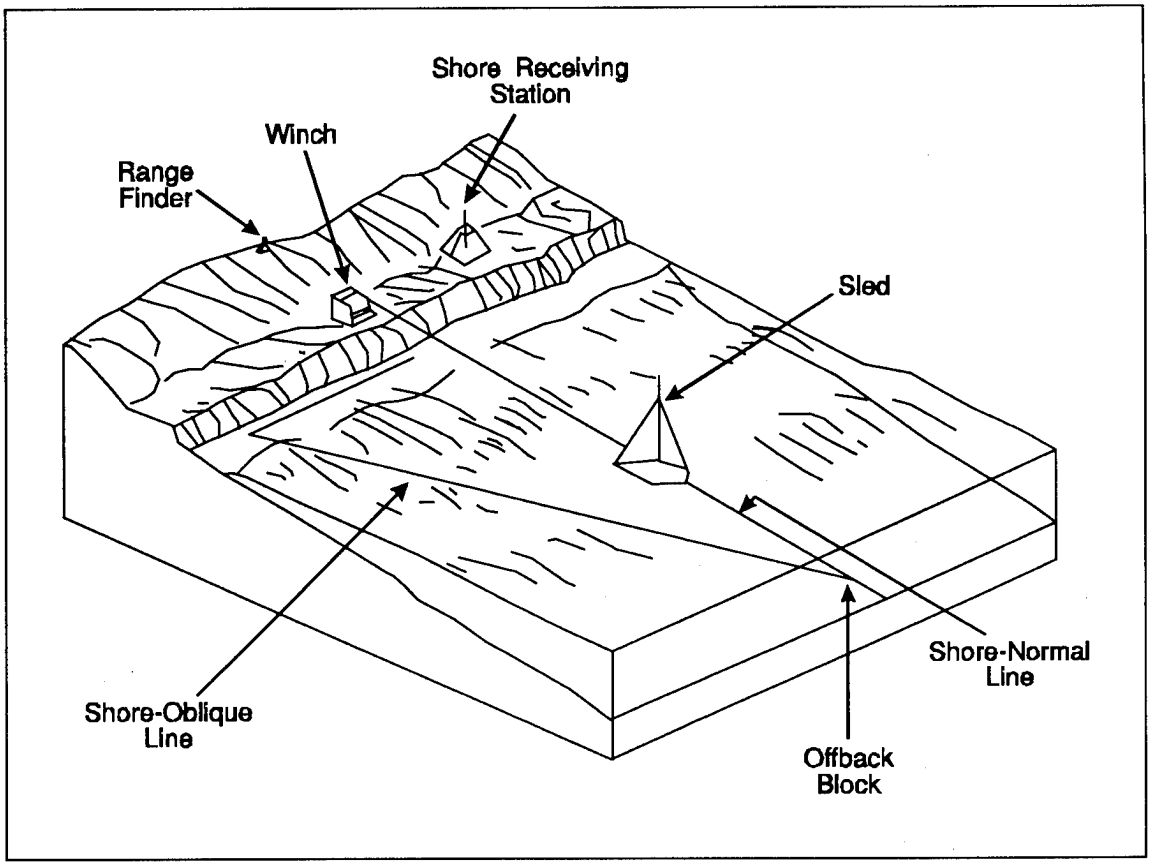

Figure 9. System for measuring bottom profiles, waves, and currents in high-energy nearshore environments (after Sallenger et al. (1983))

station onshore. Two 12-V batteries encased in a waterproof housing powered the data acquisition system.

During the DELILAH experiment at Duck, NC, three-dimensional nearshore dynamics were measured using 18 Marsh-McBirney electromagnetic current meters attached to stationary mounts (Birkemeier et al. 1991). Nine of these meters formed a line perpendicular to the shore, ranging in depth from 0 to 4 m (0 to 13.1 ft). The other nine meters were placed mostly along the 1.5- and 3.0-m- (4.9- and 9.8-ft-) depth contours. Figure 10 provides a schematic of the meter placement. The meters were cabled to an onshore computer, and current data were collected for 21 days.

Although there are several methods to measure currents, they can generally be classified as either Lagrangian or Eulerian. The Lagrangian method follows an individual fluid particle as it moves in time and space (Roberson and Crowe 1965), and generally flow tracers are required to obtain synoptic records of currents. Tracers such as dyes and surface floats are valuable in delineating surface currents. Subsurface floats with tags can be used to document intermediate depths, but do not work well in surf zones or shallow areas (Mimura 1988). Bottom trailing drogues and tracer sediments provide information

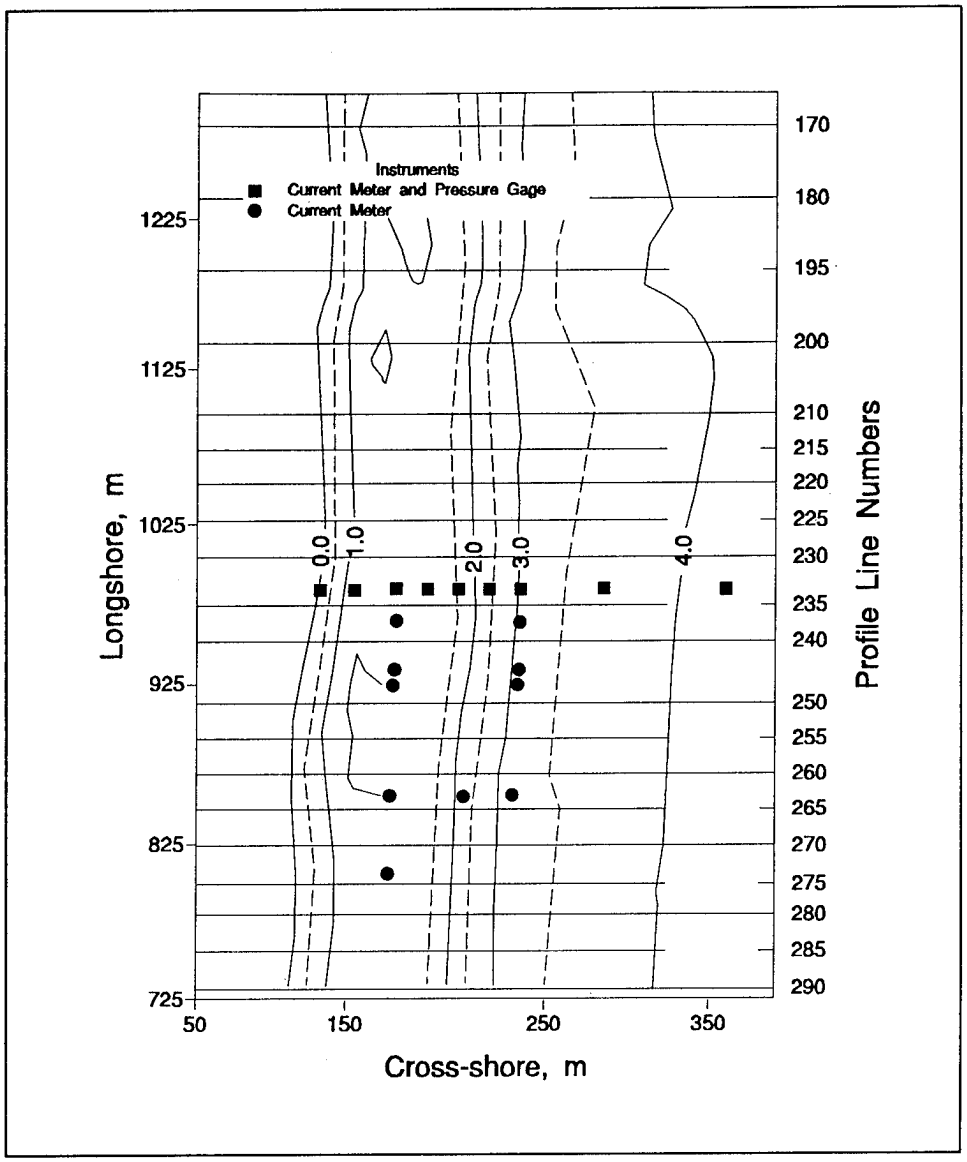

Figure 10. Schematic of the meter placement at Duck, NC, during the DELILAH experiment (Birkemeier et al. 1991)

regarding time-averaged near-bottom currents. Because these Lagrangian near-bottom current indicators do not have surface markers, only two data points are returned, the release and recovery locations. The path traveled between these two points can only be inferred (Hands 1987; McLellan and Burke, in preparation). Tides, breaking waves, flow reversals, and detainment by other obstacles increase the time between tracer release and return, and prevent associating elapsed time with the mean speed of the current. Drogues equipped with sonic devices offer an improvement, but are unsatisfactory near structures in the surf zone due to the inability to hear and track the sonic devices in a breaking wave environment. None of these Lagrangian methods provide synoptic delineation of near-bottom currents in the nearshore.

The Eulerian approach focuses on a fixed point in space and considers the motion of fluid particles that pass the point over time (Roberson and Crowe 1965). The Eulerian method generally uses instruments to measure currents at a location, and it requires several current meters at several points to provide a synoptic view of currents (Mimura 1988). The most effective method for providing spatial coverage of bottom current patterns requires placement of a suite of instruments to blanket an area and collect data simultaneously. Often this stationary bottom current acquisition technique is not used because of the number of instruments required, the enormous expense in time and money associated with placement, maintenance, and calibration of the large array of meters (Mimura 1988), and because of the difficulty of instrument deployment and recovery in the surf zone. Additionally, instruments may become covered with sand in areas of dynamic topographic change, and the location of the sampling points as well as the sampling rates cannot be easily altered once the instruments have been deployed.

Another option is to use several boats and instruments to collect data. Each boat is equipped with instruments and remains onsite for the duration of the measurement interval (McGehee, McKinney, and Dickey 1989). The required number of boats, instruments, and operators is a function of the size of the area to be surveyed and the spatial resolution dictated by the study. The use of boats provides the potential for excellent synoptic views of currents, but it is also expensive and labor-intensive. Using only one boat and current meter and maneuvering from point to point expends time while maneuvering and anchoring. This allows measurements to be taken at only a few points over a short period of time, thus preventing a synoptic view of currents. Additionally, boats are often limited by water depth, wave and current conditions, or the inability to navigate near structures.

The temporary placement of current meters mounted on tripods in the surf zone has also been used to document currents in the nearshore, but the approach has been limited to depths less than 3 m, requires numerous instruments, and is also labor-intensive (Birkemeier et al. 1991).

Systems presently employed to document current flow patterns in rivers and coastal areas use either dyes and/or surface floats to follow fluid flow or an array of stationary-mounted current meters to measure fluid flow. Surface current measuring devices are deployed by aircraft, boat, and/or wading, and are tracked by photographic methods. Mid-depth and bottom-trailing floats have been used to identify currents but these methods only yield drop and recovery location and times. They do not identify temporal or spatial current patterns. Stationary-mounted meters can measure current flows, and by placing several meters in an area, a synoptic picture of the currents can be inferred. Stationary deployment of instruments is generally achieved by boats or by wading. Additionally, this method requires deployment of several instruments to obtain spatial coverage.

The investigative techniques discussed above are generally capable of portraying currents in most areas, but are inadequate for measuring near-bottom

currents in areas where high waves, strong currents, nearby structures, and/or varying bathymetry prevent access to the area by boat or wading, or in cases where multiple meters are unavailable. A study at Siuslaw River, OR, requiring the identification of near-bottom current patterns in the vicinity of rubble-mound spur jetties during large wave events necessitated the development of a system that overcomes the limitations of the data collection methods previously described.

Objectives

Objectives of this research were as follows:

a. Develop an airborne current measurement system that can provide qualitative spatial coverage of near-bottom currents in nearshore areas which are difficult to access. The system must be able to operate in high-wave (3 m (9.8 ft)) and strong-current (2 m/s (6.6 ft/s)) environments, around coastal structures, in the surf zone, in drastically variant or rapidly changing bathymetry, and in water depths of 2-15 m (6.6-49.2 ft). It must be able to representatively measure currents approximately 1 m (3.3 ft) above the seabed at several points within a short period of time. The number and location of points, and the time constraints, are a function of the survey site and objectives. An example is the measurement of currents at 15 locations within 2 hr over a 1-km^2 (0.39 square-mile) area. The measured currents are plotted to create a vector mosaic providing a near-synoptic view of near-bottom currents in the area.

b. Test and use the airborne current meter system to measure currents at Siuslaw River, Florence, OR, and create vector mosaics of local near-bottom currents.

c. Qualitatively compare the current patterns illustrated in the Siuslaw current-vector mosaic with current patterns inferred from photographs of sediment tracer movement taken in a physical model study (Bottin 1981, 1982).

2 Description of Airborne Coastal Current Measurement System

This chapter describes WES's development of an Airborne Coastal Current Measurement System that can provide qualitative spatial coverage of currents 1 m above the bottom in nearshore areas which are difficult to access. The system is operable in high-wave and strong-current environments, around coastal structures, in the surf zone, and in a drastically variant or rapidly changing bathymetry. A helicopter, used as the support platform from which an electromagnetic current meter is suspended, hovers above the sea surface while data acquisition is accomplished. The quick maneuverability and versatility of the helicopter allow currents to be measured at several points approximately 1 m above the seabed within a short period of time. This flexibility also allows the sampling scheme to be altered in the field to meet changing study needs. The number and location of points, and the time constraints, are a function of the survey site and study objectives. Although measurements are quantitative, the short duration of the sampling period introduces statistical uncertainties that limit the information to being considered qualitative. As an example, the system can measure bottom currents at 15 points within 2 hr over a 1-km^2 (0.39-square-mile) area. Measured currents can be plotted to create a vector mosaic providing a near-synoptic view of near-bottom currents in the area.

Near-bottom currents are measured using an InterOcean electromagnetic current meter (S-4) suspended by cable from a helicopter. Currents are measured at several locations over a short period of time. Although the system does not provide simultaneous collection of data, it does provide quick sequencing of data collection from point to point. Near-bottom current mosaics developed from the measurements can be used to infer local flow patterns around inlet structures such as jetties.

The Airborne Coastal Current Meter System was used to measure currents at the structured entrance to the Siuslaw River, Florence, OR. From these data, a vector map of local bottom currents was created and qualitative comparisons of the current patterns were made with photographs of sediment tracer movement taken in a physical model study (Bottin 1981, 1982).

Equipment

Helicopter

A helicopter is used as the work platform because of its ability to operate above the high-energy wave environments in the nearshore zone and around coastal structures and because of its ability to transit quickly between measurement points. The helicopter must have the capacity to accommodate the pilot, co-pilot, winch operator, current meter, buoys, cables, and anchor weight. Accommodations for a portable computer and system operator are also recommended. The system operator monitors the data stream to assure that the meter is collecting data throughout the sampling period, and the computer is also used as a redundant data storage device. If space is unavailable for the computer and operator, recorded data are stored within the current meter, but no assurance can be made that the meter operates continuously throughout the sampling period. The helicopter must have a side-mounted power winch with sufficient power and lift capability to raise and lower the meter and its anchor weight. The fuel capacity of the aircraft and the payload weight establish the time limit between refueling. The number of points that can be sampled depends upon distance from the helipad to the study location and the distance between sampling points.

Current meters

Meters used for measuring currents are categorized by their sensing mode. Mechanical propeller or rotor type current meters have a long history of use in deepwater applications (Mimura 1988). The rotor or propeller is rotated by the flow of water, and the rate of rotation or number of revolutions per unit time is calibrated to measure the current (or speed of the fluid). Direction is indicated by the position of the meter relative to a rotational axis, and this position is monitored by internal compass readings.

In the nearshore, breaking waves can suspend sand and entrain air bubbles in high concentration, and these factors can have strong impacts on both the current meter and the supporting mount. Meters used under these circumstances must possess characteristics of solidity, ease of handling, and resistance to suspended sand and air. Electromagnetic and ultrasonic current meters physically satisfy these requirements, but the return of the ultrasonic acoustic signal is affected by high concentration of entrained particles or air bubbles.

The use of ultrasonic acoustic current meters has generally been offshore, but a few have been used in the nearshore area. Size, fragility, and acoustic properties of ultrasonic current meters have limited their use in the surf zone. The ultrasonic current meter uses pairs of piezoelectric transducers to emit and receive ultrasonic waves. Two or three pairs of transducers are employed to measure two- and three-dimensional components of current velocity, respectively. Current vector components are resolved from the time required for

ultrasonic wave pulses to propagate the distance between the pairs of transducers (Mimura 1988). The meter assumes the signal travels through a homogeneous medium with a constant speed of sound. High concentrations of entrained particles and air bubbles reduce the quality and the speed of the acoustic return signal.

Electromagnetic current meters are the principal current-measuring instrument used in field observations in the nearshore. The meter operates on the principle of Faraday's law of induction; electric current is generated in a conductive material by a change in magnetic flux. In the shell of the instrument, two excitation coils are set to radiate a magnetic field directed from the center to the circumference of the sensor, and two pairs of electrodes oriented at right angles are placed on the surface. The flow of seawater around the meter results in a change in magnetic flux of the water and the coil, causing a change in voltage. This voltage is proportional to the speed of the water flow. Component vectors from the perpendicular electrode pairs are resolved into a resultant current vector (Mimura 1988).

An electromagnetic current meter was selected for use because it has no moving parts to foul, it is compact in size, and it can store data internally and/or transmit data to a remote computer (Figure 11). The InterOcean S-4 was selected because it is a multi-parameter meter capable of measuring both submergence and current velocity, and has an onboard magnetic compass and tilt sensors which determine and compensate for meter orientation. The current meter's range of velocity magnitude is 0 to 3.5 m/s (0 to 11.5 ft/s) with 0.002 m/s (0.007 ft/s) resolution, and an accuracy rating of ± 1.0 cm/s (± 0.4 in./s), and can accommodate up to 45 deg (0.79 rad) of tilt. The pressure sensor used for measuring the depth has a 70-m (229.6-ft) range with 4-mm (0.16-in.) resolution. Compass resolution is 0.1 deg (0.0017 rad). The precision of the meter is well within the uncertainties of a flexible mount. The components are housed in a plastic sphere 25 cm in diameter with a titanium rod passing vertically through its center. The sphere serves as the electronics housing, battery compartment, and mounting platform for the current meter probes. The titanium rod has locations at each end for use as mooring points and is intended to be a load-bearing member in a buoy/anchor system such as this system. There are no protruding sensors and, except for the electrical connector, the instrument is compact, smooth, and rugged (InterOcean Systems, Inc. 1987).

Prior to each study the meters were serviced and calibrated by the manufacturer so no corrections to the data were required and reasonable confidence could be placed in the results.

The current meter assembly consists of the current meter, anchor, and a subsurface buoy as shown in Figure 12. The current meter is connected to an anchor comprised of four lead balls weighing a total of 890 N. The anchor is attached to the lower end of the instrument approximately 1 m below the instrument housing. A subsurface buoy providing 130 N of lift is attached approximately 1 m (3.3 ft) above the instrument to keep the meter suspended

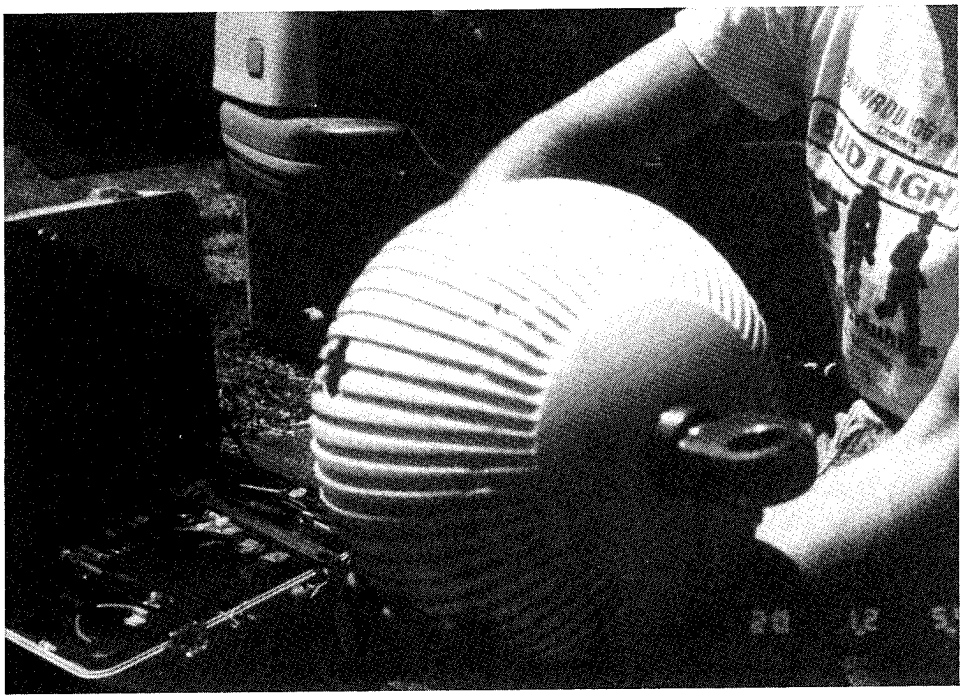

Figure 11. InterOcean S-4 current meter

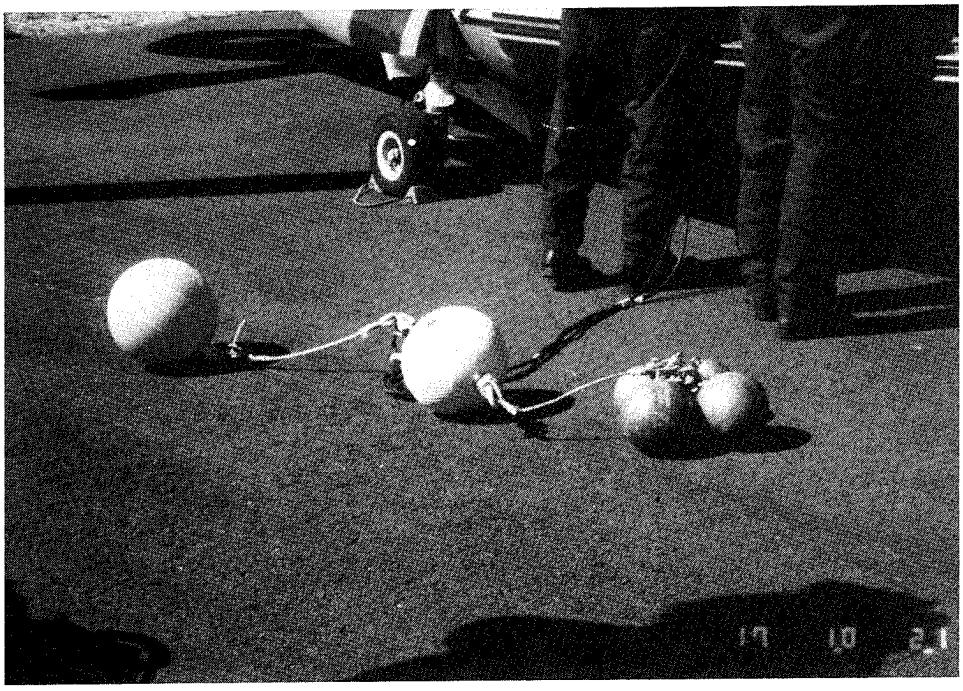

Figure 12. Photograph of current meter assembly consisting of (from left to right) current meter, anchor, and subsurface buoy

vertically in the water column. The four lead balls together create a footprint that is not easily rolled or moved on the seabed. The 1-m (3.3-ft) distance between components is needed to minimize flow interference with the current

meter instrument operation. A copper wire weighted with a 20-N weight secured at its lower end is attached to the bottom of the current meter assembly to dissipate the static charge developed by the helicopter. The meter assembly is shackled to the helicopter's winch so it can be brought alongside the aircraft for traveling to and from the site and for raising and lowering to the seafloor for measurements (Figure 13).

Electrical and computer system

A separate electrical umbilical 50 m (164 ft) in length is married with a support line to connect the instrument through an RS232 interface to a laptop computer onboard the aircraft. The computer is powered by a 12-V battery. This umbilical consists of a four-conductor electrical cable that is taped to a 3/8-in.-diam (0.95-cm-diam) rope for mechanical support. This line is not intended to support the weight of the instrument string, and this line is tended by hand as the instrument is lifted in and out of the water. Figure 14 shows the current meter and computer assembly. If the helicopter is equipped with an oceanographic winch and electromechanical cable, the electrical umbilical can be eliminated, reducing the workload of the crew and the possibility of fouling the lines. Figure 15 illustrates the meter assembly as it would appear attached to the helicopter and in use at the seafloor.

Figure 13. Current meter assembly shackled to helicopter's winch

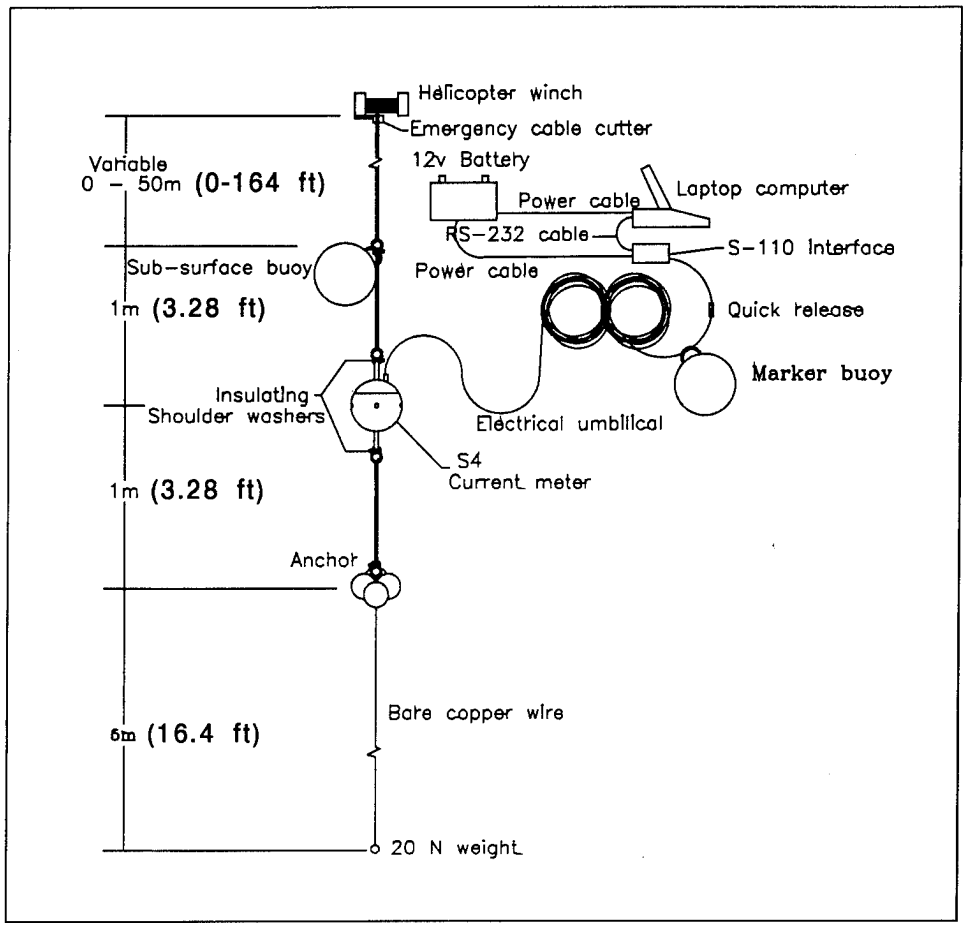

Figure 14. Current meter and computer assembly

The computer used for the study at Siuslaw River was a Zenith laptop running the Kermit communications program. An InterOcean S-110 interface connected the computer to the instrument via the electrical umbilical. The current meter was configured to record data internally as well as send it back through the umbilical where it was recorded on the computer's internal disk. This was done for two reasons: First, the instrument was in danger of fouling on obstructions each time it was lowered. If only internal data storage was used, and loss of the instrument occurred late in the flight, all data from the flight would be lost. Second, the effects of static electricity generated by the helicopter were unpredictable; therefore, monitoring the data stream ensured that the instrument was still functioning and recording good-quality data. During the course of operation at Siuslaw River, both of these preventative measures were tested.

During flight, a helicopter develops substantial electric charge with respect to earth ground, which is dissipated by the first available conductive path to ground. Crew members who perform rescue work are well aware of the need to let any cable dangling from the aircraft touch ground first. On the first few flights, the current meter was adversely affected by this static charge. Teflon

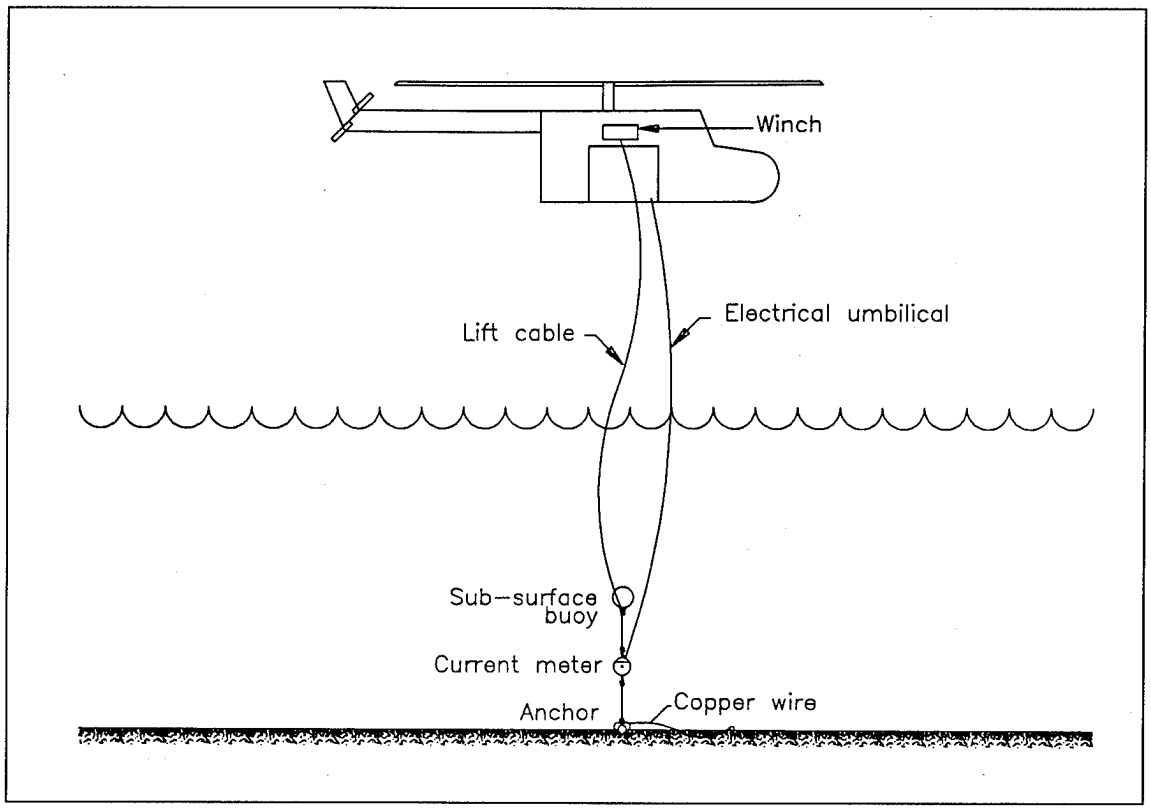

Figure 15. Meter assembly attached to the helicopter as it would appear in use at the seafloor

insulating shoulder washers installed in the mooring pads on the instrument's support rod prevented the charge from dissipating through the winch cable, leaving the instrument's umbilical as the primary current path. The static discharge caused the instrument to cease functioning each time it came in contact with the water, and a manual restart was required for every deployment. Removing the insulating washers allowed the charge to be dissipated by the anchor and lift cable, but breaking waves could still hit the gauge before it had completely discharged. Therefore, a weighted 5-m (16.4-ft) length of bare copper wire hanging below the anchor was installed to dissipate the charge under all wave conditions.

Safety releases

In the event that the equipment needed to be disengaged, all lines to the helicopter and computer were equipped with quick releases. The helicopter rescue winch contained an explosive cable cutter to sever the cable. Both the pilot and crew members had the ability to fire the cable cutter. Great care was taken to coil the electrical line in a fashion so that it could be jettisoned as a unit without endangering the aircraft or crew. The computer was secured to the helicopter and a waterproof connector in the electrical cable served as a weak link to disengage from the computer. A surface buoy attached to the end

of the electrical umbilical support line was used for relocation and recovery of the current meter string, should disengagement have been necessary.

In flight to and from the Siuslaw site, the instrument assembly was winched to the helicopter and secured to prevent it from falling accidentally. Once the helicopter was on station, the winch was energized and the current meter assembly was lowered into the water beneath the aircraft. During one instance while the meter assembly was underwater, the rescue hook became disconnected from the top end of the meter assembly. It was theorized that when floated, the surface buoy was able to twist and lift up on the safety latch of the rescue winch. With the weight of the meter assembly resting on the seabed and the cable slack, the rescue hook became free of the meter assembly, leaving the meter assembly at the seabed. To prevent reoccurrence of this problem, the assembly was attached to the rescue winch such that the subsurface buoy was located on the back side of the hook, and cable ties were secured through an eye of the hook and the safety latch to prevent the possibility of the latch being triggered. On one occasion, the anchor became fouled in the rocks of the jetty, and the aircraft was unable to free it. In this situation, the lift cable was cut, and the umbilical was disconnected from the computer and dropped with its attached marker buoy. The instrument was recovered in each instance, but ease of recovery could be improved by installing an acoustic release between the anchor and the meter. The acoustic release could be remotely detonated, allowing the meter to be separated from the anchor and float to the surface. This would allow the meter, subsurface buoy, and the electrical umbilical to be recovered easily with a small vessel, provided the meter was not fouled. The anchor would be abandoned on the seafloor and would need to be replaced.

Horizontal Positioning

Accurate horizontal position coordinates are achieved through the use of sighting prisms mounted on the helicopter (Figure 16) which served as a target for a total electronic positioning station located onshore (Figure 17). The electronic positioning station is an electronic theodolite that reflects a signal off the prisms, and then resolves the orientation of the theodolite head and the return time of the signal to establish the prism's location relative to the position of the theodolite.

In order to indicate the location of study sampling points, line of sight positioning by the pilot/crew to range markers on the beach and/or jetties is used for approximate positioning and to increase the speed of the maneuvering process. Buoys marking the intended point of sampling can also be used, but care must be taken to avoid fouling the buoy lines. Additionally, dye packets can be released to indicate surface currents for the pilot to follow, if this meets study needs.

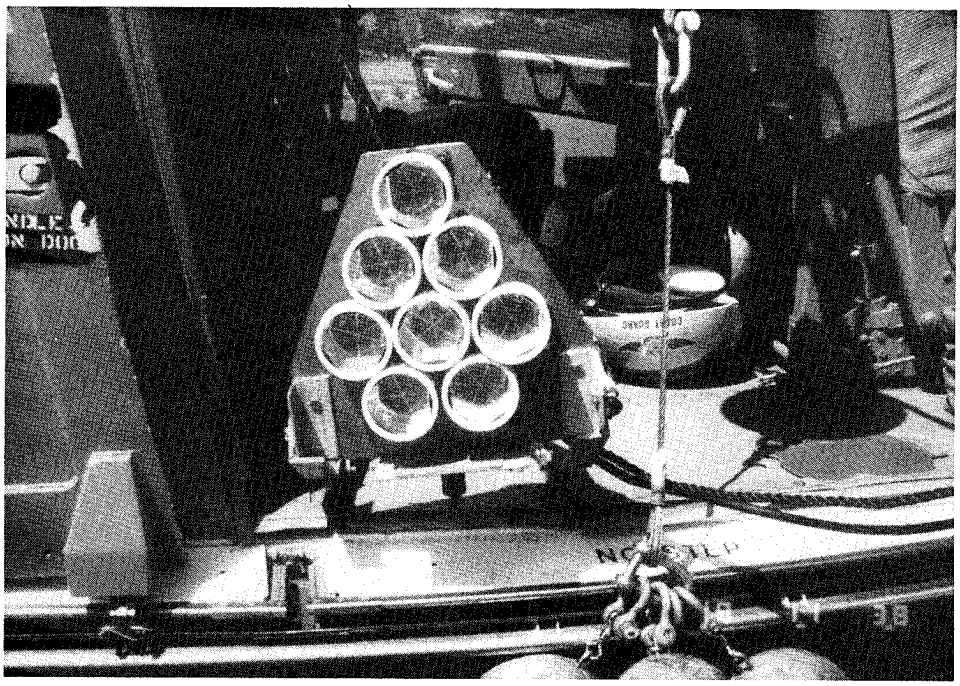

Figure 16. Accurate horizontal positioning coordinates are obtained through use of sighting prisms mounted in the helicopter doorway

Operating Procedure

During operation, the helicopter pilot aligns the aircraft with the range poles or follows a dye stream. Once in position, the current meter assembly is lowered until the anchor rests on the seafloor. The location of the helicopter is recorded using the total electronic positioning station at the instant the meter reaches the bottom and the meter support line goes slack. Horizontal positioning accuracy is estimated to be ±3 m (±9.8 ft). Timing and confirmation of position recording is assisted by radio communication between the helicopter and the shore crew. The helicopter hovers directly over the meter with slack line while current vector data and instrument depth are recorded. Sampling intervals vary with site and study objective. A second position is recorded at the end of the first sampling interval. After the second position is recorded, the helicopter lifts the meter assembly above the water, moves along a line of sight to the next measurement station, and repeats the procedure. Figure 18 illustrates this data acquisition sequence, and Figures 19-21 show the airborne current measurement system in operation near a structure.

Bathymetry, previous dye studies, tracer studies, photos, model study results, and any other available information concerning currents in the area are all considered in selecting the sampling locations. A grid pattern is useful for aligning the helicopter during the study and also for ensuring uniform coverage of sampling points in the study area.

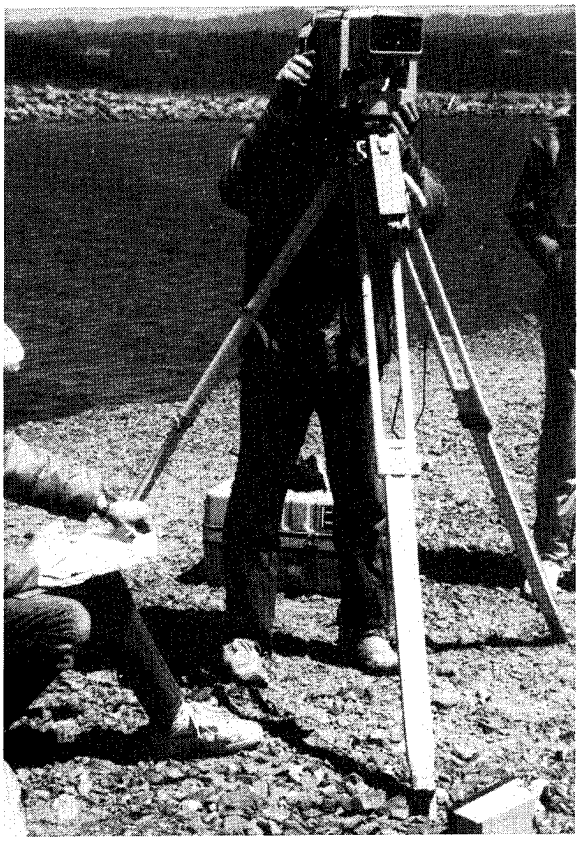

Figure 17. Total electronic positioning station located onshore

Selection of the sampling period at each point is different for each study. The physical parameters, the hypothesis being tested, and the equipment being used must all be considered. The length of the period selected involves balancing two conflicting needs: rapid sampling to increase spatial resolution, and measuring for a long enough period to obtain a representative steady current average value at each point.

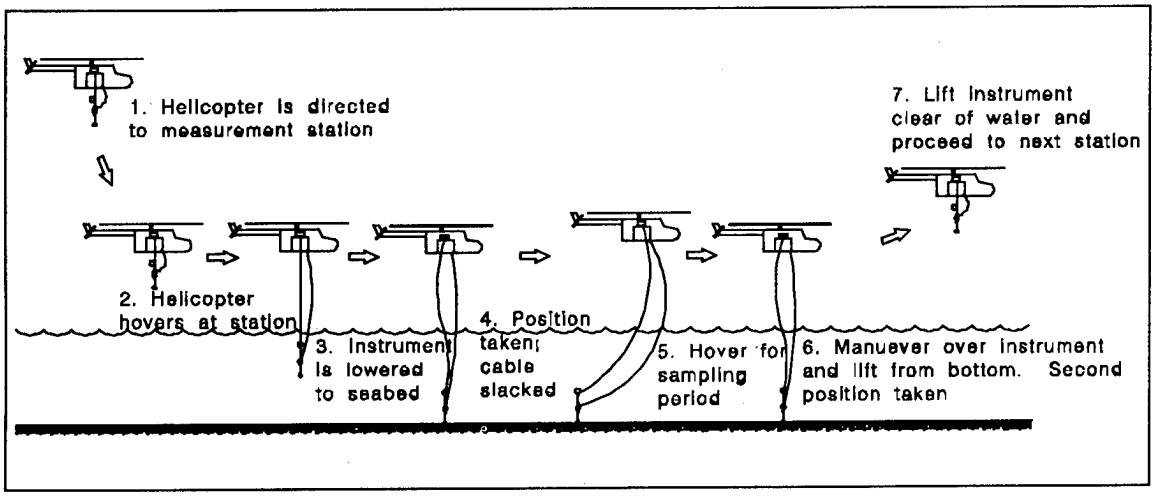

Figure 18. Sequence of helicopter positioning and data acquisition

Figure 19. Airborne Coastal Current Measurement System in operation near structure

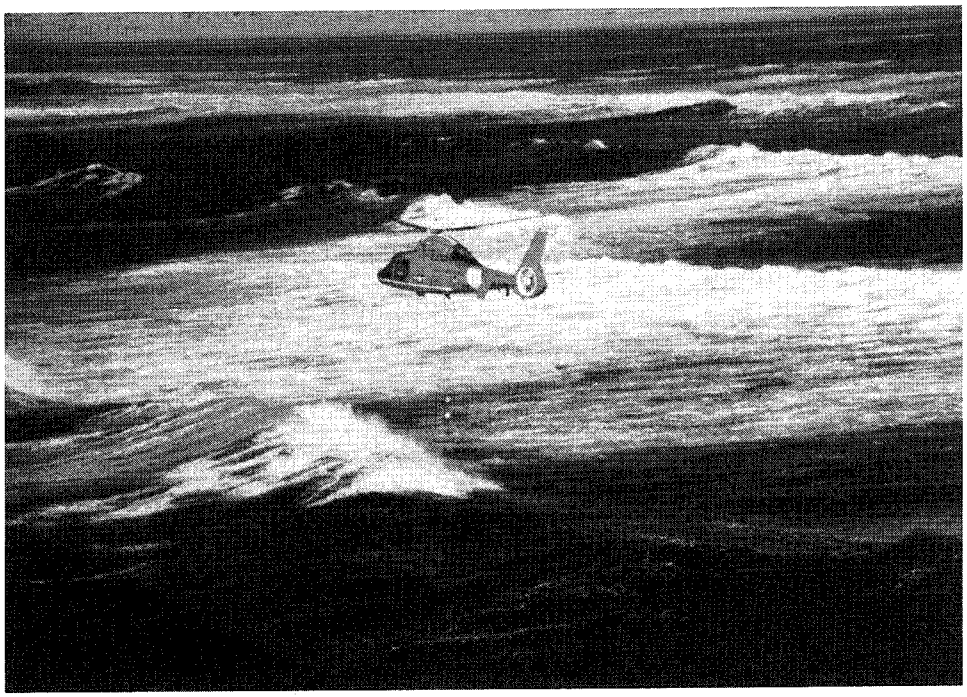

Figure 20. Airborne Coastal Current Measurement System operating in large waves

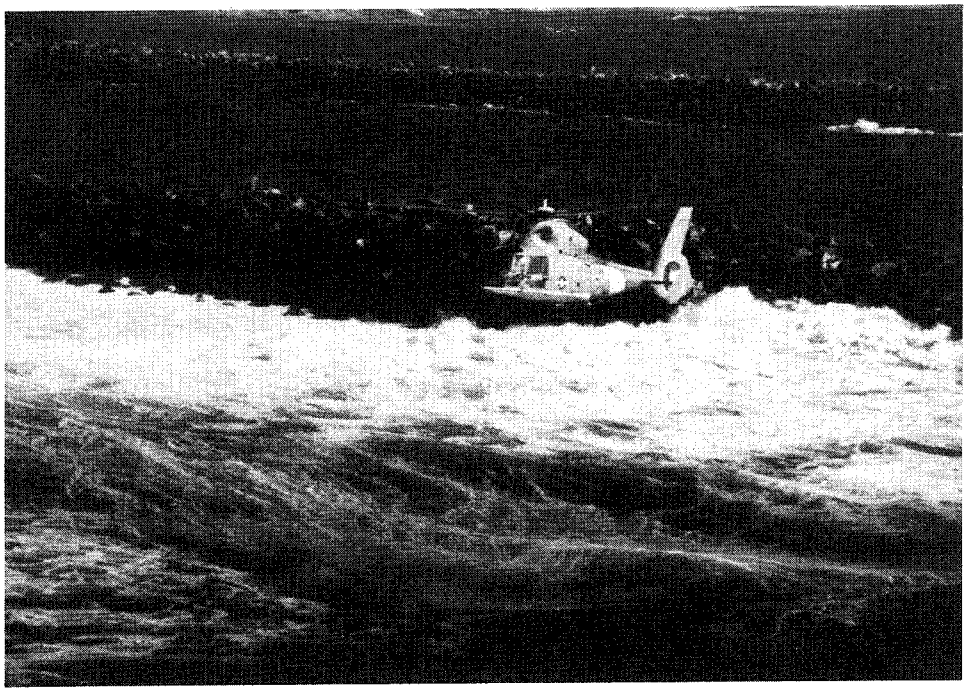

Figure 21. Airborne Coastal Current Measurement System operating near a structure in large waves

3 Data Collection, Analysis, and Presentation

Data Collection

Data are collected and stored internally within the current meter and stored externally in the attached computer. The computer provides backup data records in case the instrument becomes fouled and has to be released. Also, interruption of the data stream due to static electricity generated by the helicopter can be monitored. Continuous monitoring by computer informs the operator that the instrument is providing quality data.

The current meter records data continuously. The sampling interval can be adjusted to the study needs. The measured current data time series is related to the helicopter location by comparison with the position time series from the survey instrument. The period when the anchor is on the seabed is easily identified from the meter depth output. Figures 22-24 show samples of the current meter output for depth (Figure 22), northing (Figure 23) and easting (Figure 24) directions. The sampling frequency for this example is 2 Hz.

Data Analysis and Presentation

Time is used to correlate current data collection intervals with helicopter position. Unfiltered current data from one sampling period at one location are averaged into a single resultant current vector for each location and those vectors are displayed in mosaic form. Using Equation 1, the magnitude of the resultant vector (V_{avg})[1] is determined by calculating the current magnitude of each discrete current vector for each time-step and averaging the values from the sampling interval. Using Equations 2 through 6, the direction is determined by separately averaging the northing and easting components of the discrete vectors from the sampling interval and combining the averaged component vectors to yield a resultant vector direction. Typically the number of samples "n" will range from 15 to 25, but is a function of the study site and

[1] For convenience, symbols and abbreviations are listed in the notation (Appendix C).

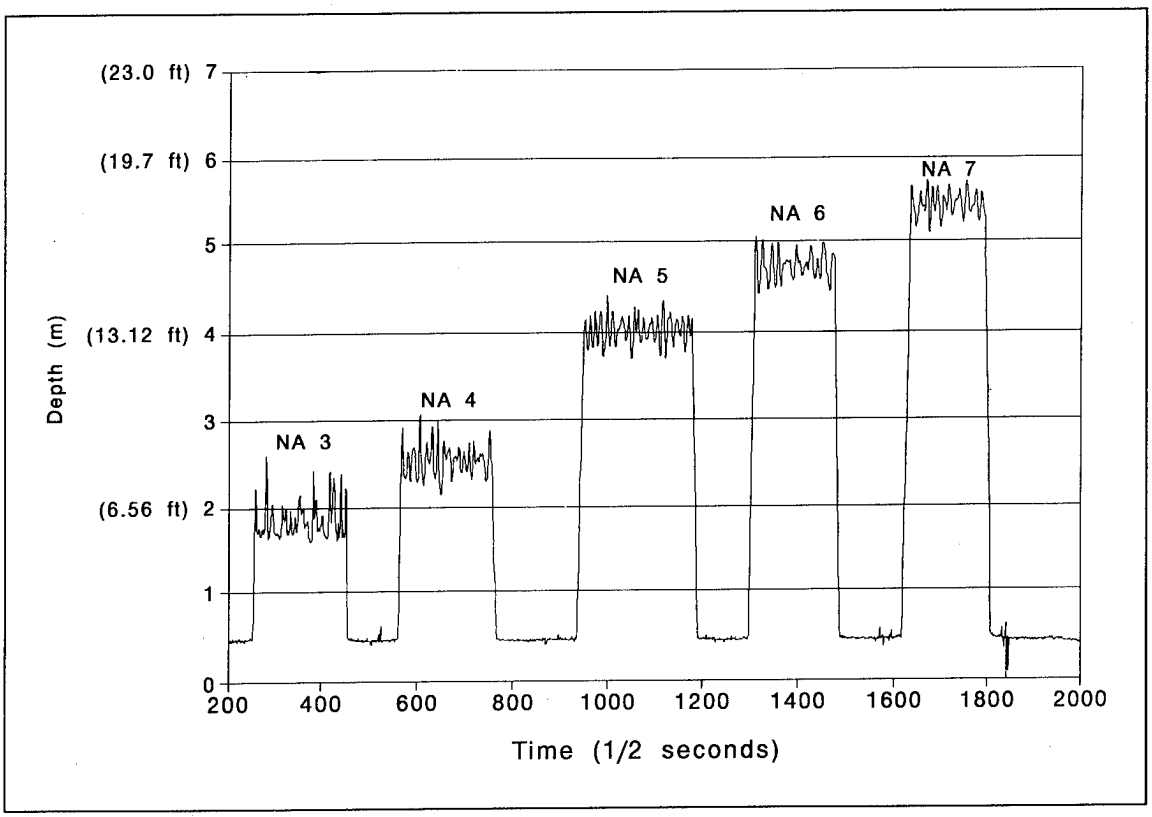

Figure 22. Example of meter output for time versus depth

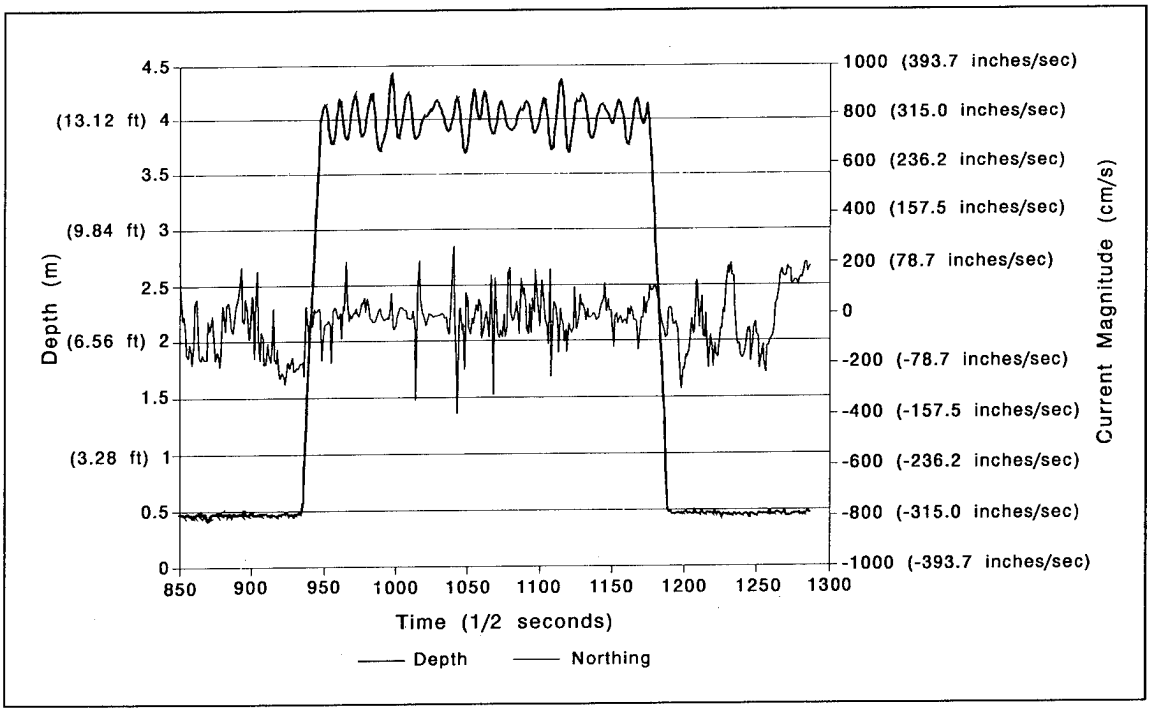

Figure 23. Example of meter output for time versus depth and the northing component of the current

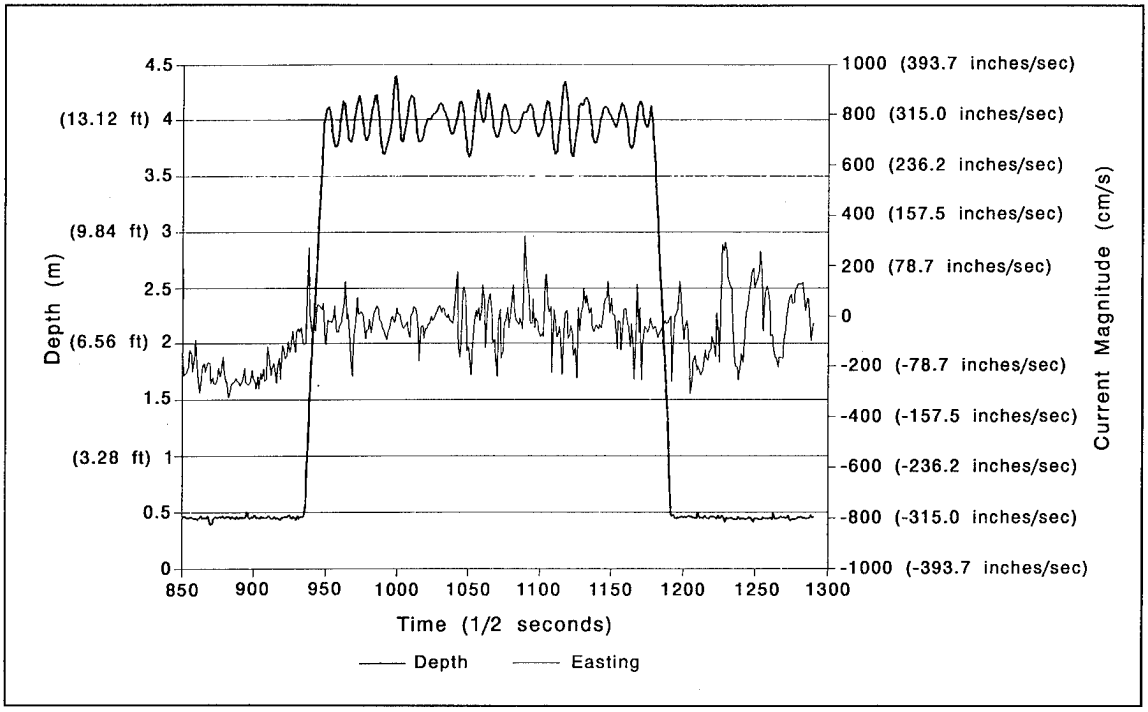

Figure 24. Example of meter output time versus depth and the easting component of the current

objectives. An adjustment to the vector direction is made for the angle of declination (the difference between true north and magnetic north). The adjustment specified by the U.S. Army Engineer District, Portland (NPP) (U.S. Army Engineer District, Portland 1986) indicates that true north is 19 deg east of magnetic north for the year 1984 and that the decrease in the angle is 6 min for each subsequent year. Therefore, in 1992 (8 years later), the decrease in the angle of declination is calculated as 48 min, yielding a correction of 18.2 deg (0.31 radians) to be added to the measured magnetic direction to correct the vector direction to true north.

In the mosaic, the origin of the vector coincides with the data collection location, and the length and heading of the vector indicate average magnitude and direction of the current at the time of sampling.

$$V_{avg} = \frac{\sum_{i=1}^{n}(N_i^2 + E_i^2)^{\frac{1}{2}}}{n} \qquad (1)$$

$$\theta_{init} = \tan^{-1}\left[\frac{\sum_{i=1}^{n}\frac{E_i}{n}}{\sum_{i=1}^{n}\frac{N_i}{n}}\right] \tag{2}$$

$$\theta_{degree} = \theta_{init}\left(\frac{180}{\pi}\right) \tag{3}$$

$$\begin{aligned} &\text{If} \quad \theta_{degree} > 0.0 \\ &\text{and} \quad \sum_{i=1}^{n}\frac{E_i}{n} > 0.0 \\ &\text{then} \quad \theta_{degree} = \theta_{degree} \end{aligned} \tag{4}$$

$$\begin{aligned} &\text{If} \quad \theta_{degree} < 0.0 \\ &\text{and} \quad \sum_{i=1}^{n}\frac{N_n}{n} > 0.0 \\ &\text{then} \quad \theta_{degree} = \theta_{degree} + 360.0 \end{aligned} \tag{5}$$

$$\begin{aligned} &\text{If} \quad \sum_{i=1}^{n}\frac{N_n}{n} < 0.0 \\ &\text{and} \quad \sum_{i=1}^{n}\frac{E_n}{n} < 0.0 \\ &\text{then} \quad \theta_{degree} = \theta_{degree} + 180.0 \end{aligned} \tag{6}$$

where

V_{avg} = magnitude of the resultant vector average

n = number of samples

i = sample number

N = northing component of the current vector

E = easting component of the current vector

θ_{ini} = resultant vector angle of the average vector components

θ_{degree} = resultant vector angle relative to magnetic north

A computer program that produces a spreadsheet is used to tabulate collected data and vector locations, magnitude, and directions. Table 1 is an example of the spreadsheet in which column 1 contains the label associated with the data collection location. The naming convention for the profiles is *N* for north of the jetties; A B C D are the respective profile lines (Figure 25). The numbers (#) are the consecutive count along each profile line. Other types of naming conventions were used for other sampling schemes. DYE $\#_1,\#_2$ was used to signify points when the helicopter was following dye patterns, $\#_1$ is for the specific dye study and $\#_2$ is for the consecutive point along that dye path. DREC # signifies locations of radio directions from shore by the project director, and # again is for consecutive points during the shore-directed sampling interval. For convenience, the points were renamed for plotting using consecutive numbers beginning with 1 for each sampling interval.

In columns 2 and 4, the start and end times (1/2 s) are actually counters for the data set that shows when the instrument string anchor was on the bottom and the instrument was collecting data. During helicopter operations, the instrument continuously collects data at 1/2-s intervals while in the air, during its descent into the water and down to the seabed, and during recovery and transport to the next location. Only data recorded while the instrument string is at rest on the seabed are of interest for this study. Start and stop times are used to bracket the interval of data used to calculate vector magnitudes and directions.

Clock times in columns 3 and 5 were calculated for each point by adding multiples of 1/2 s to the initiation time of the instrument for each sampling interval. In the example, Pacific Standard Time is used to identify the time at which the instrument is started, and start and end times are added to yield the sampling time interval. This information is used to correlate collected current data with sampling point locations and tidal flows.

Average depth, tabulated in column 6, is the average depth of the instrument sensor calculated from the sum of all depths throughout the sampling interval at individual points while the instrument string is resting on the seabed, divided by the number of depth entries. This is the average depth of the instrument; the seabed is 1 m (3.3 ft) deeper than the instrument.

In column 7, current magnitude is the vector magnitude, and is calculated using Equation 1 as described previously. Column 8 contains the direction of the current vector relative to true north, and is calculated as described previously. Thus, columns 7 and 8 describe an average resultant vector for each sampling point.

Columns 9 and 10 contain values of *N-Vector* (cm/s) and *E-Vector* (cm/s), which are the component vectors of the resultant vector described in columns 7 and 8. A data reduction program is used to calculate the values in columns 6 through 10 for each sampling interval, and the results are entered into the spreadsheet.

Table 1
Sample Vector Information

Point	Start Time		End Time		Current Meter Avg Depth, m	Current Mag, cm/s	Current Dir, deg	N-Vector, cm/s	E-Vector, cm/s	Start Point	
	1/2s	Clock	1/2s	Clock						X	Y
4 September 1991 Sampling Interval I											
1	966	10:47:13	1108	10:49:14	2.6	94.6	271.0	28.0	90.4	1042007	878364
2	3	10:51:01:5	120	10:52:00	3.0	132.7	238.7	100.9	86.1	1042007	878364
3	258	10:53:09	446	10:54:43	1.8	166.6	291.5	9.4	166.4	1042007	878364
4	566	10:55:43	754	10:57:17	2.5	78.3	219.8	72.8	28.8	1042007	878364
5	950	10:58:55	1174	11:00:47	4.0	86.3	249.4	54.1	67.2	1042007	878364
6	1309	11:01:54:5	1473	11:03:16:5	4.7	51.3	243.9	35.8	36.7	1042007	878364
7	1635	11:04:37:5	1785	11:05:52:5	5.4	43.5	374.4	43.4	2.9	1042007	878364
8	2578	11:12:29	2754	11:13:57	6.3	56.2	368.9	55.4	9.1	1042007	878364
9	2871	11:14:55:5	3026	11:16:13	3.8	87.4	332.8	61.4	62.2	1042007	878364
10	3136	11:17:08	3333	11:18:46:5	3.5	107.5	239.8	80.4	71.4	1042007	878364
11	3481	11:20:00:5	3649	11:21:24:5	5.8	80.6	349.8	70.9	38.3	1042007	878364
12	3772	11:22:26	3859	11:23:09:5	6.5	33.3	49.7	28.4	17.4	1042007	878364
13	4040	11:24:40	4182	11:25:51	6.6	42.6	322.5	24.0	35.2	1042007	878364
14	4648	11:29:44	4794	11:30:57	3.0	99.9	206.5	98.9	14.4	1042007	878364
15	4865	11:31:32:5	4995	11:32:37:5	3.2	78.3	262.7	33.7	70.7	1042007	878364

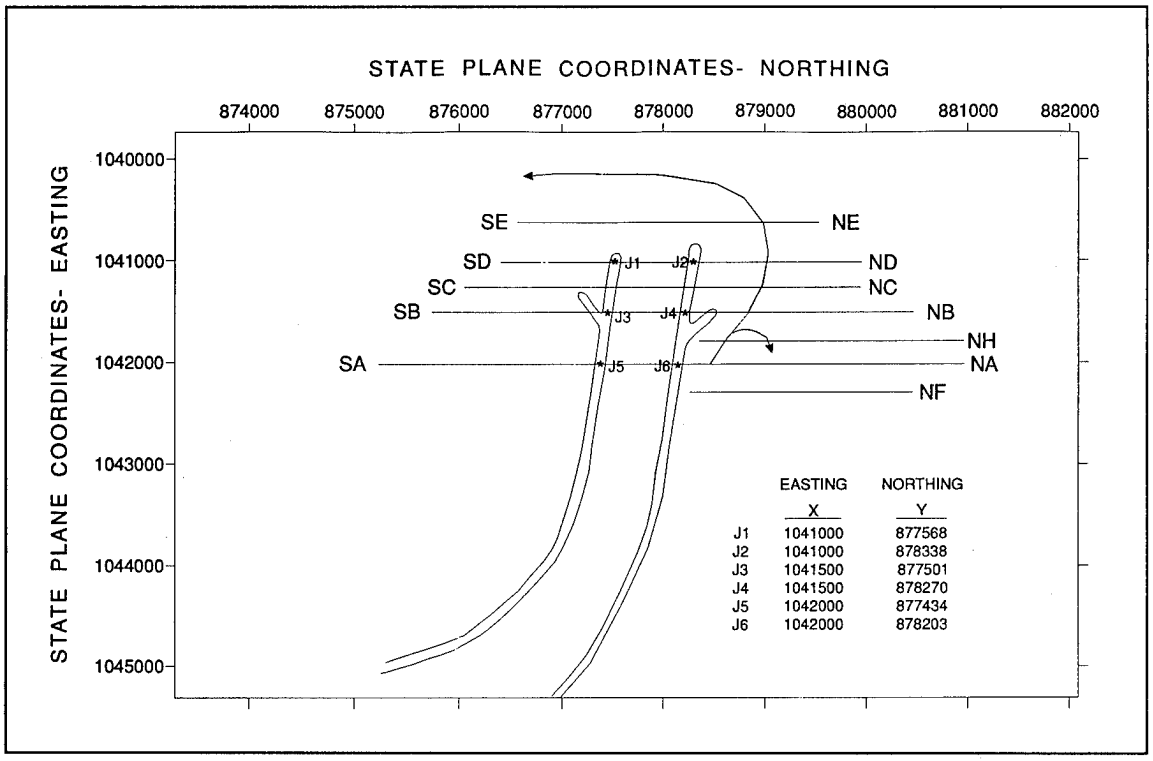

Figure 25. Current profiling lines and naming convention

Start points, columns 11 and 12, are state plane coordinates for the starting points of the Lagrangian motion of a water particle in the direction of the average resultant vector for a period of 1 min. Start points are plotted as the vector's tail in the mosaic format. The *XY* location of the start point is the horizontal location of the instrument during the sampling interval. This information is transferred directly from the survey notes to the spreadsheet. The end point *XY* is determined by calculating Equations 7 and 8.

$$Y_{endpoint} = 60(E\text{-}Vector) + Y_{endpoint} \quad (7)$$

$$X_{endpoint} = 60(N\text{-}Vector) + X_{startpoint} \quad (8)$$

The *N-vectors* and *E-vectors* are multiplied by 60 sec, and these values are added to the start point y and x values, respectively (Equations 7 and 8). Computer programs used for data analysis are included in Appendix A.

4 Airborne Coastal Current Measurement System Application at Siuslaw River, Florence, OR

The Airborne Coastal Current Measurement study was conducted in support of a study to evaluate the effectiveness of spur jetties in deflecting current-transported sediment away from the entrance channel, thus reducing shoaling in the channel. One task of the study was to establish whether the spur jetties did in fact induce a current circulation pattern off the spur tips and/or a current pattern that extends seaward of the jetty tips as was observed in physical model tests of the structures. Both current patterns have the potential to reduce shoaling in the entrance channel. Bottom-trailing drogues, dye studies, and aerial photographs were used to define current patterns in the area, but these tools were not adequate to delineate bottom currents in the area. The drogues only provided release and recovery locations and were relatively inconclusive for identifying any circulation patterns. The dye studies and aerial photos exhibited the circulation patterns of the surface currents but did not establish that the bottom currents were similar to the surface currents in this dynamic area which included the breaker zone and regions seaward of the breaker zone. To address this deficiency, the helicopter current measurement system was developed and employed to measure bottom currents and to establish bottom current patterns in the area.

Site Description and Location

The Siuslaw River enters the Pacific Ocean near the City of Florence, OR, approximately 240 km (149 miles) south of the Washington-Oregon state border (Figure 26). The project area extends from the entrance upstream to approximately river kilometer 26.4 near the community of Mapleton. The lower 42 km (26 miles) of the river are subject to tidal influences. The tidal range between mean lower low water (mllw) and mean higher high water (mhhw) is 2.0 m (6.6 ft) at the mouth, with an extreme range of about 3.4 m

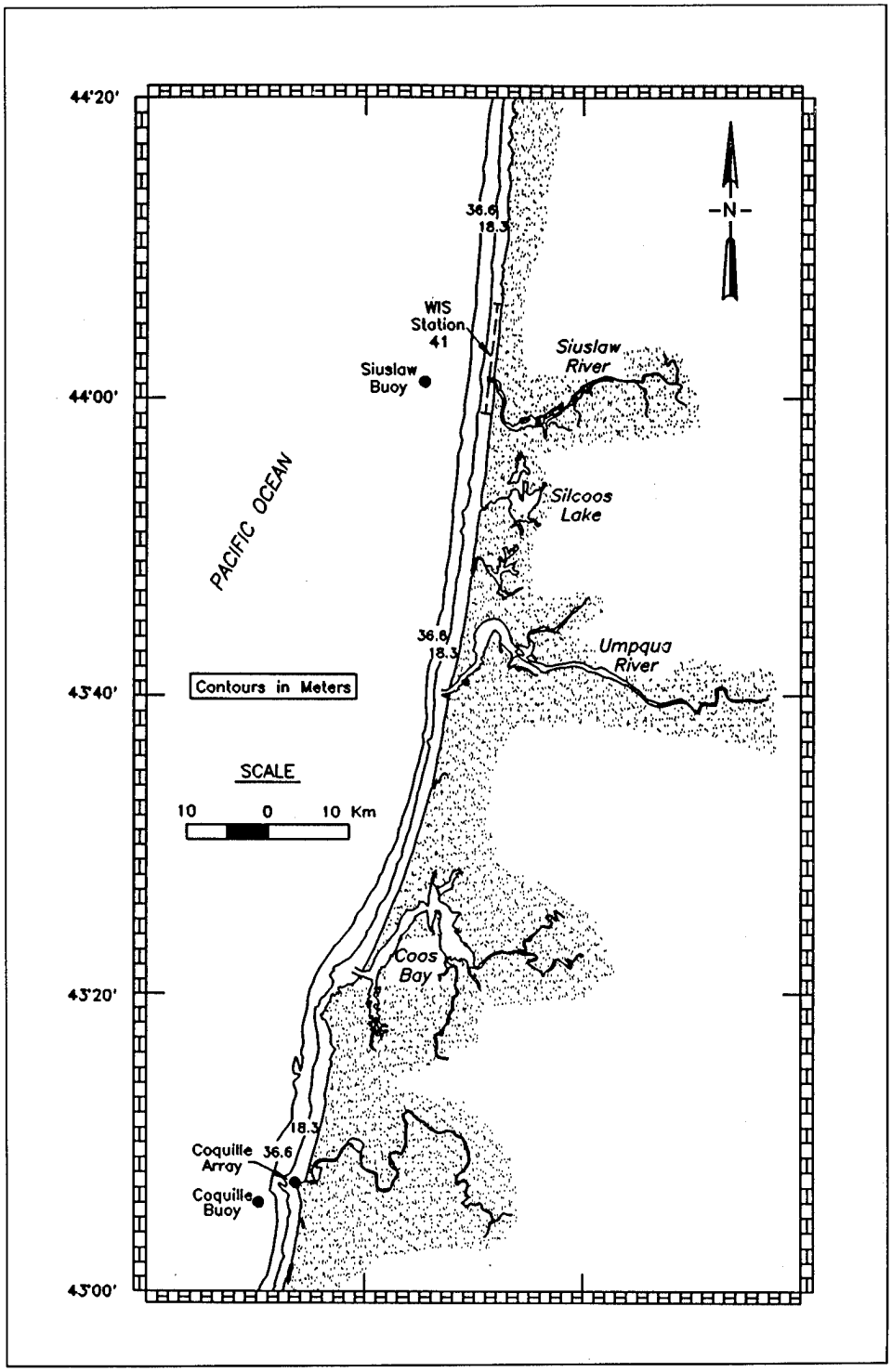

Figure 26. Location map of the Siuslaw River mouth along the Oregon coast

(11.2 ft). The Siuslaw Estuary covers approximately 9.1 km^2 (3.5 square miles) (Hartman 1977).

In 1985, the rubble-mound jetties at the entrance to the Siuslaw River were extended offshore to reduce sediment shoaling and dredging requirements in the navigation channel. Figures 27 and 28 show the jetties prior to and after the extension, respectively. The north jetty extension was 580 m (1,900 ft), and the south extension was 670 m (2,198 ft). In addition, on the ocean side of the jetties, one 122-m-long (400-ft-long) spur oriented 45 deg (0.8 rad) to the main structure was constructed 275 m (902 ft) shoreward of the seaward end of each of the twin jetties. The heads of the jetties were constructed to depths of 7 m (23 ft), and depending upon the wave conditions, the breaker zone may occur inside the spurs or may extend well seaward of the jetty tips.

The concept of the spurs arose as a result of physical model studies conducted at CERC for the Rogue River project on the southern Oregon coast (Bottin 1982). Model results with spur jetties indicated that sediment in the nearshore zone moved toward the jetties and into an eddy which tended to

Figure 27. Siuslaw jetties prior to 1985 extension

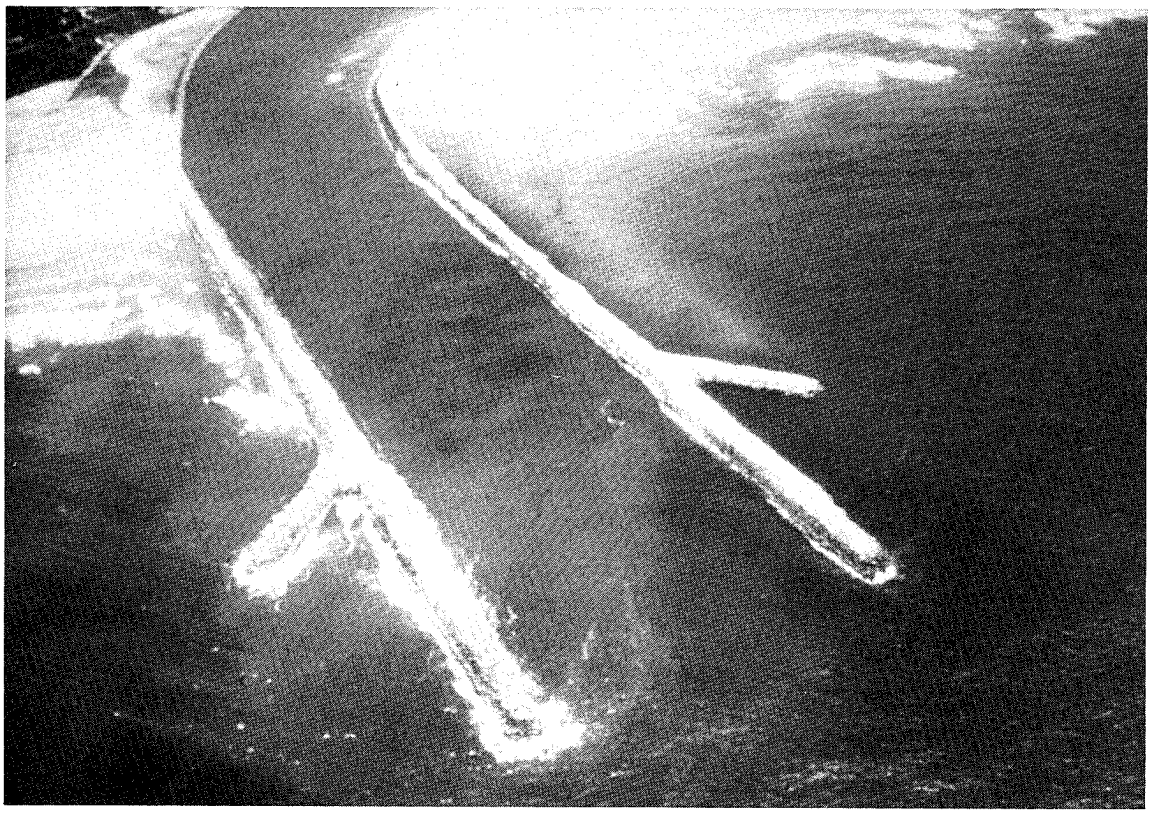

Figure 28. Jetties at Siuslaw River after 1985 extension

deflect material away from the structure. Sediment would flow back toward shore where it is either reintroduced into the littoral transport system or carried by a jet of water away from the jetty parallel to the spur. Under certain conditions, some material was carried around the end of the spurs and into the "V" formed by the spurs and the jetty trunk, and some material continued around the jetty head and into the entrance. Qualitative evaluations of the Siuslaw River jetty extensions were made using the Rogue River physical model (Bottin 1982). Overall, the model study indicated the spurs would alter the circulation pattern and potentially cause significant reduction of sediment shoaling in the navigation channel.

Airborne Coastal Current Measurement System Current Studies at Siuslaw River, Florence, OR

In July 1990 and September 1992, the Airborne Coastal Current Measurement System was successfully tested and deployed at the Siuslaw River Inlet structures to document current patterns around the north spur jetty. Mosaics of the current vectors around the jetty were used to identify circulation pattern trends in the prototype, and to compare qualitatively the current patterns with photographs of circulation patterns identified in a physical model sediment

tracer study performed by Bottin (1981, 1982). Appendix B lists each current vector's time, location, orientation, and magnitude for the studies.

Dauphin Rescue Helicopters supplied by the U.S. Coast Guard North Bend, Oregon, Air Station were used for the Siuslaw River Study. The helipad was located close to the study site, and this allowed the loaded helicopter to remain in the air between 1.5 and 1.75 hr before refueling. A fuel truck was contracted for the study periods to eliminate the need for the helicopter to travel 97 km (60.3 miles) to its home base for refueling. The survey crew and total electronic positioning station were positioned on the jetty trunk at the end of the vehicle access road. A 1-min sampling period (approximately 6 wave periods) with data recorded at a rate of 2 Hz was selected to yield the best balance between rapid sampling and length of sample. Sampling is considered qualitative because of the statistical uncertainty introduced by the short sampling interval. Allowing 1 min for sampling and 4 min for helicopter maneuvering, a new point could be sampled approximately every 5 min, averaging 18 points per 1.5-hr period. Range markers on the jetties and beach formed the line-of-sight grid for helicopter positioning. Figure 29 shows the jetty configuration, proposed measurement locations, and grid for the study. The grid pattern is divided into 150-m (492-ft) increments. During operation it was discovered that efficiency of helicopter maneuvering was best facilitated by eliminating the beach markers and using range markers to identify transects perpendicular to the jetties. The helicopter began sampling on the transect within 50 m (164 ft) of the jetties and collected data at several points along the transect as it moved away from the jetties. Length of the transect lines varied from transect to transect, but they were approximately 600 m (1,968 ft) in length near the shore and became shorter moving offshore.

A second sampling scheme was developed and employed during the study to better follow the dominant current flow patterns, and to test the theory that at this site, surface currents and bottom currents exhibited similar circulatory patterns in the dominant flow regions. Dye packets were dropped from the helicopter in what visually appeared to be the dominant flow. The helicopter sampled the path delineated by the dispersing dye. As dye intensity decreased to visually undetectable levels, another dye packet was dropped at the last sampling point and the helicopter followed the new dye packet flow pattern. Depths in the survey area ranged from 2 to 10 m (6.6 to 32.8 ft). Figures 30 and 31 are bathymetry maps of the local area for spring and fall of 1990. All maps use Oregon State Plane Coordinates and increments that divide the axis and contours are given in units of feet. Bathymetry was measured by NPP using a helicopter-borne bathymetry survey system (Pollock, in press). Tidal information was taken from National Oceanic and Atmospheric Administration (NOAA) tide tables for 1990 and 1992. Wave information was collected from a WaveRider buoy located offshore of the Coquille River approximately 97 km (60.3 miles) south of the Siuslaw River in 10 m (32.8 ft) of water (Scripps Institution of Oceanography 1990, 1992). Pollock et al. (in preparation) made a comparison of wave elevation and period between the Coquille buoy and a buoy located directly offshore of the Siuslaw River entrance. They found the difference between measured data at the two buoys was within the uncertainty

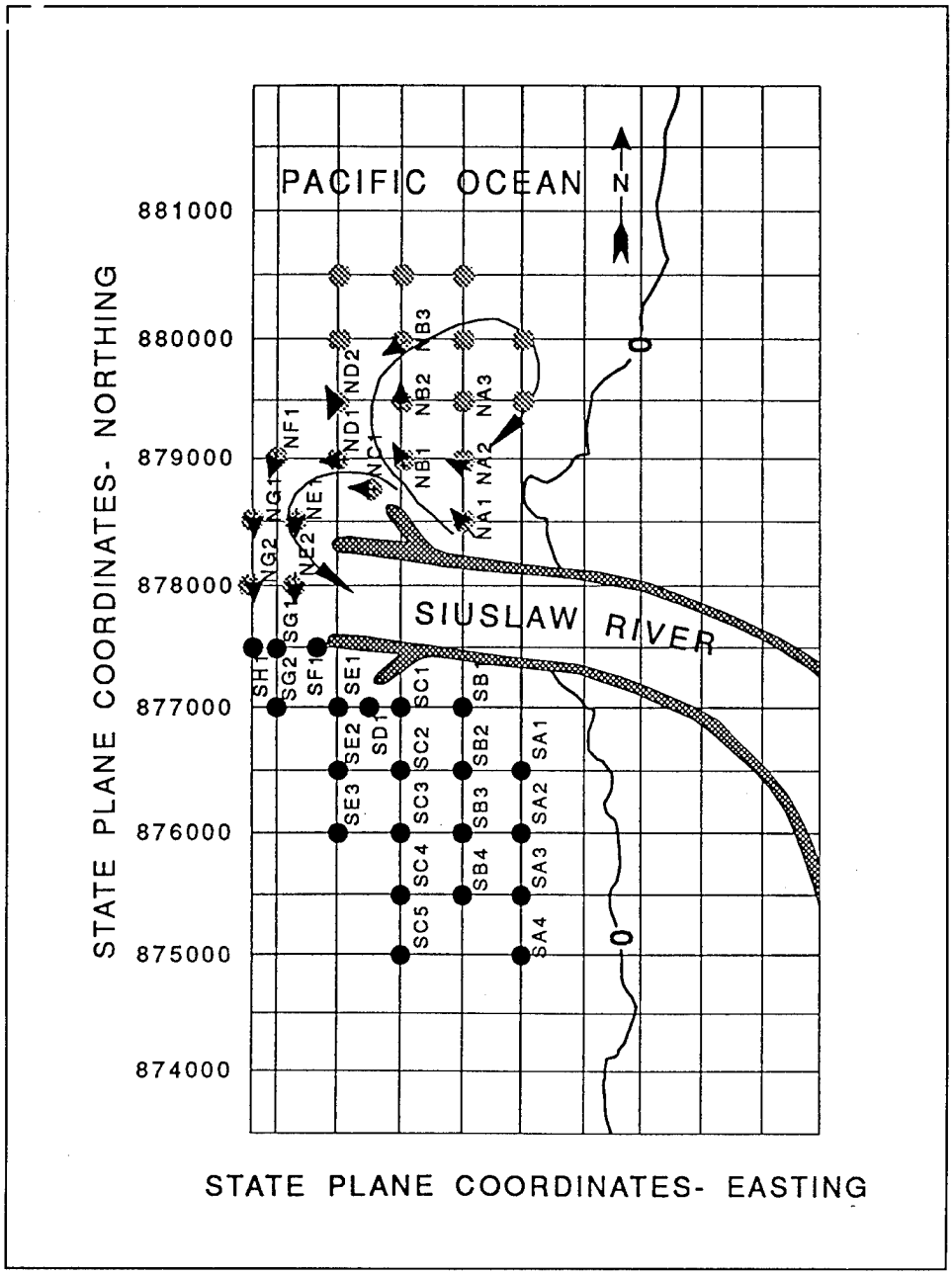

Figure 29. Jetty configuration, proposed measurement locations, and grid information for current studies

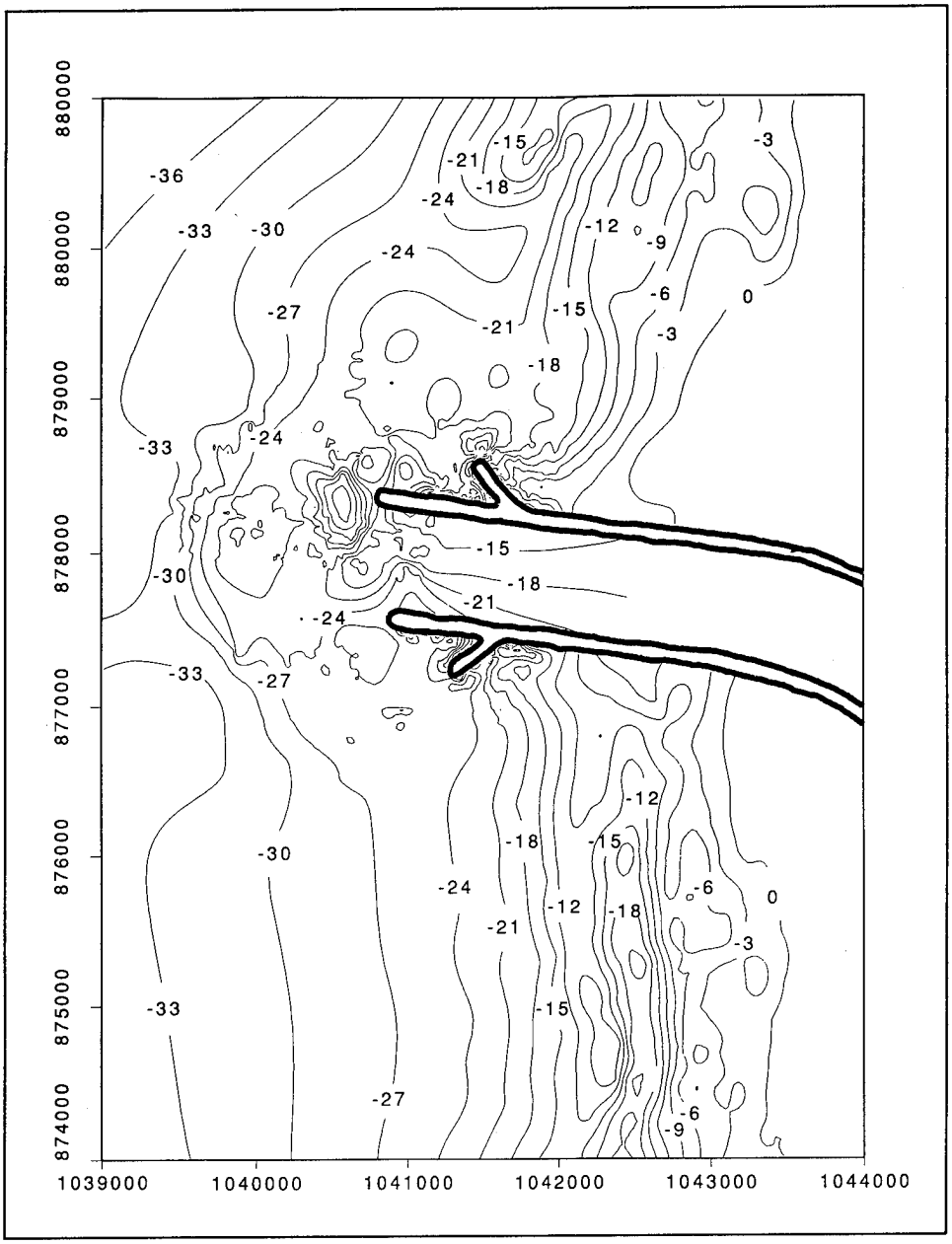

Figure 30. Bathymetry map of the Siuslaw area for spring 1990

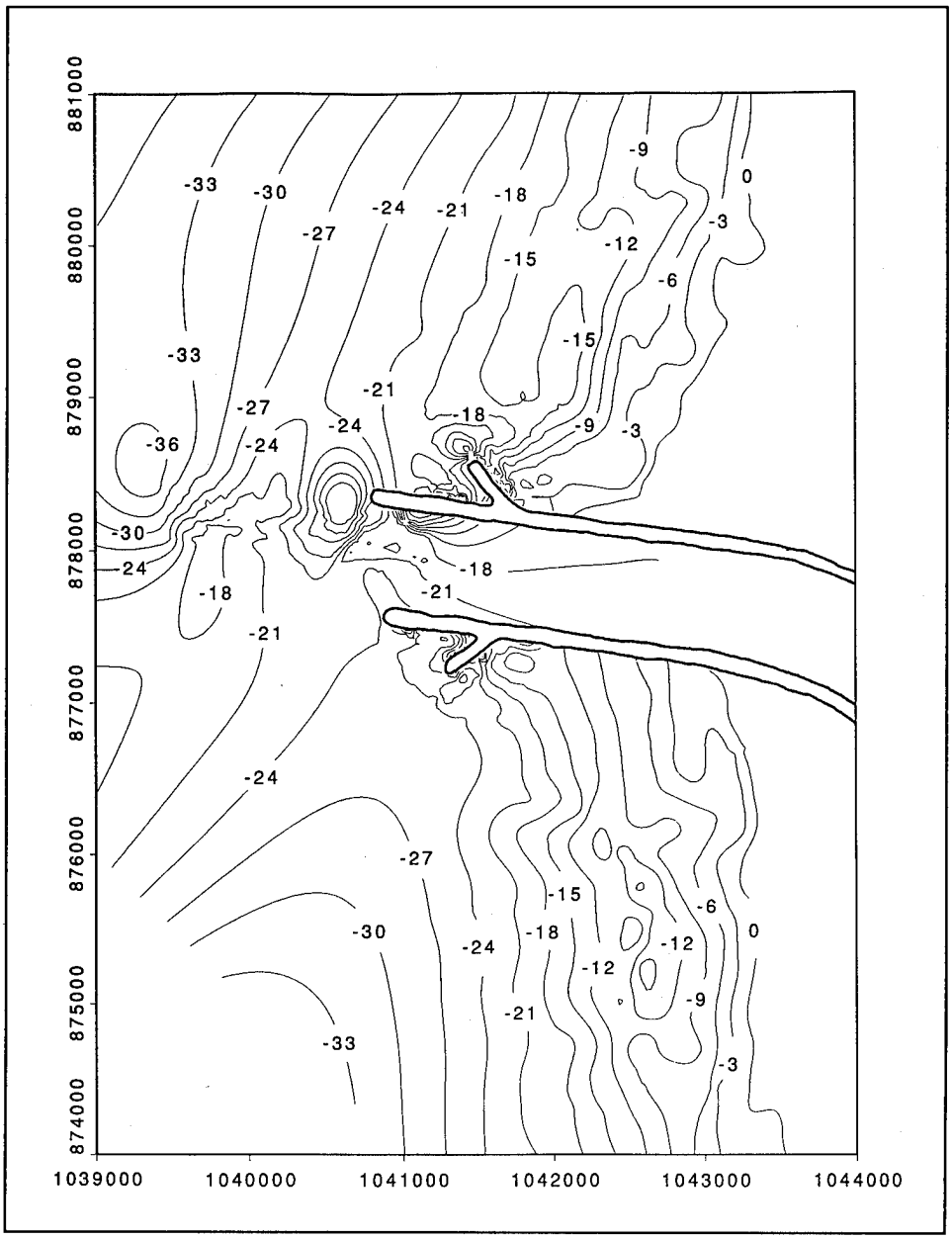

Figure 31. Bathymetry map of the Siuslaw area for fall 1990

of the individual measurements, and therefore wave climatology at both locations can be considered equivalent.

July 1990, Airborne Coastal Current Measurement Study at Siuslaw River, OR

18 July 1990, sampling interval I

Figure 32 is a mosaic presentation of current vectors at locations where measurements were made north of the Siuslaw jetties during a 1-hr sampling period on 18 July 1990. The sampling interval began at 9:53 a.m. and ended at 10:56 a.m. High tide was 1.43 m (4.7 ft) at 9:30 a.m. and a low tide of 0.98 m (3.2 ft) occurred at 2:00 p.m. Tides for the sampling interval were slack turning to ebb but water elevations only changed approximately 0.5 m (1.6 ft) over the entire ebb cycle. Deepwater wave heights were 2 m (6.6 ft) out of the north with a spectral peak period of 7 sec. Wind patterns throughout the study period were from due north and, at times, gusting to 74 km/hr (46 mph). Therefore, current patterns reflected wind-dominated currents for

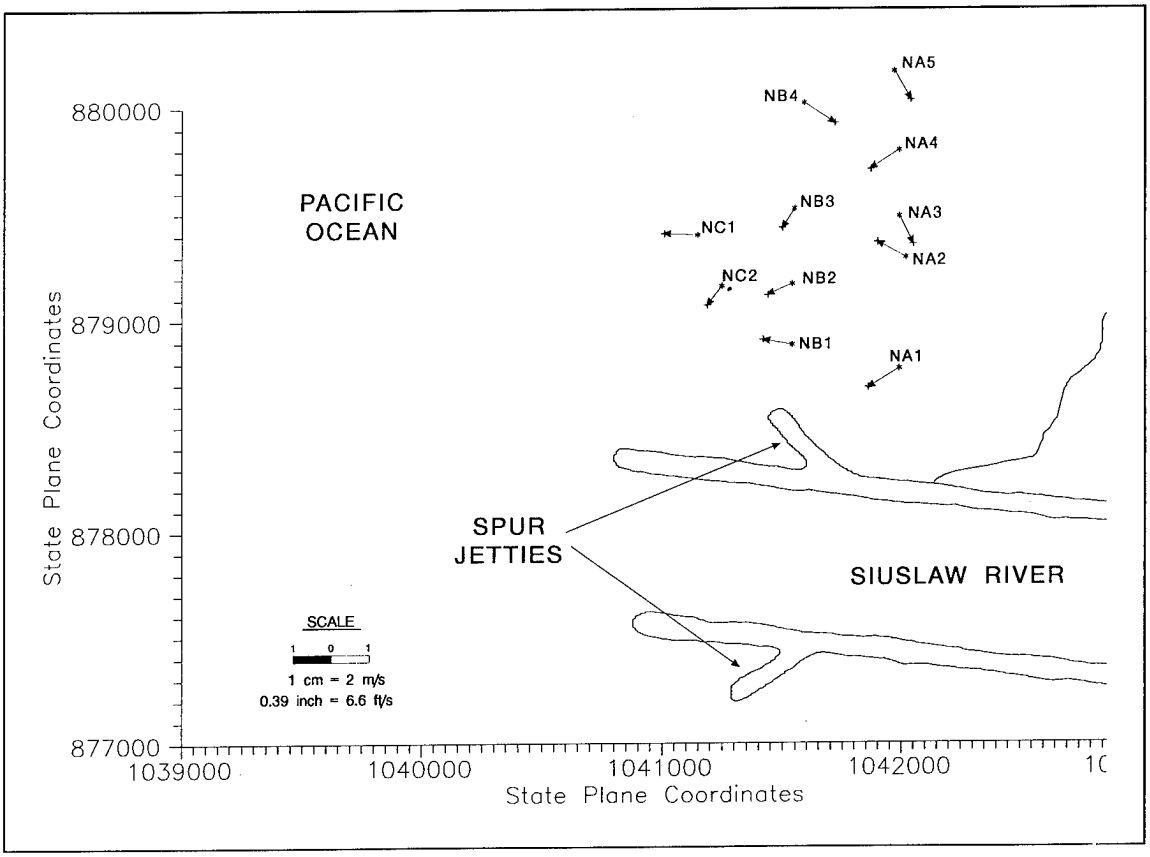

Figure 32. Mosaic presentation of current vectors for sampling interval I on 18 July 1990

the day. During this interval, vector patterns were difficult to describe but appeared to resemble a rip cell with inshore flow approximately 600 m (1,968 ft) north of the jetties and the offshore rip occurring just to the north of the jetty. The effect of the spurs appeared to be to displace the offshore jetty-parallel flow some distance from the jetty trunk.

18 July 1990, sampling interval II

Another sampling interval was conducted on the same day under similar wave and wind conditions. The interval began at 1:56 p.m. and ended at 3:00 p.m. The tide was low at 2:00 p.m. so the sampling interval was during the slack turning to flood tide. Twenty-two points were measured in the 1-hr sampling interval, and results are shown in Figure 33. Longshore currents flowed due south until they reached the jetty region where they turned due west and flowed offshore. Again the spurs appeared to affect the current by displacing the offshore jetty parallel flow away from the jetty trunk. Because prototype current patterns for the 18 July 1990 study were dominated by wind-driven currents directed from due north and tracer sediment movement in the physical model studies was the result of wave-induced currents with westerly components, a comparison was not made for these two sampling periods of the study.

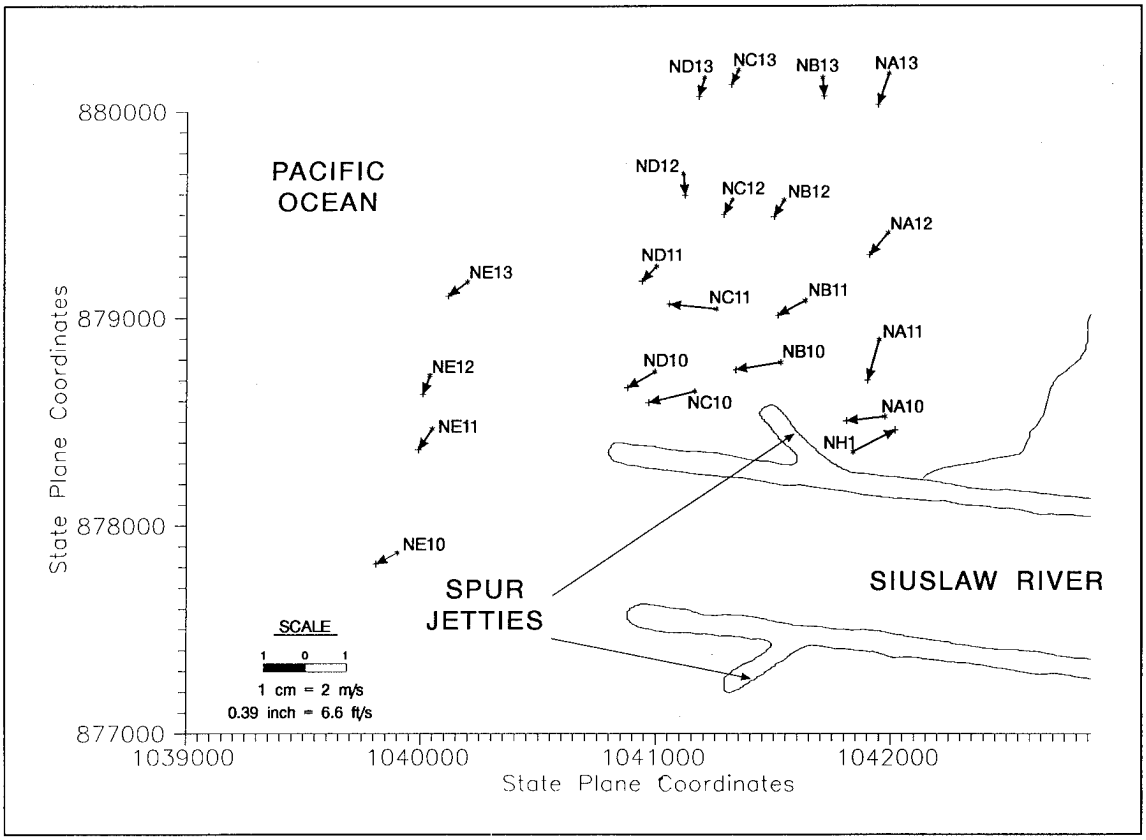

Figure 33. Mosaic presentation of current vectors for sampling interval II on 18 July 1990

19 July 1992, sampling interval III

During this sampling period conducted on a very calm day, the meter was placed too close to the jetty and became entangled in the jetty stone. Consequently, only 10 points covering one profile line were sampled on that day (Figure 34). The limited data suggest that a circulation pattern may have existed for the sampling period, but the sampling interval was discontinued when the meter became fouled at point NB1.

September 1992, Airborne Coastal Current Measurement Study at Siuslaw River, OR

A second study at Siuslaw River, OR, was conducted in September of 1992. Dense fog prevented operation for all but 2 days (September 3 and 9) during the 2-week period.

3 September 1992, sampling interval I

On the first operating day, 3 September 1992, only one sampling period could be completed before discontinuation of sampling due to fog. Waves and

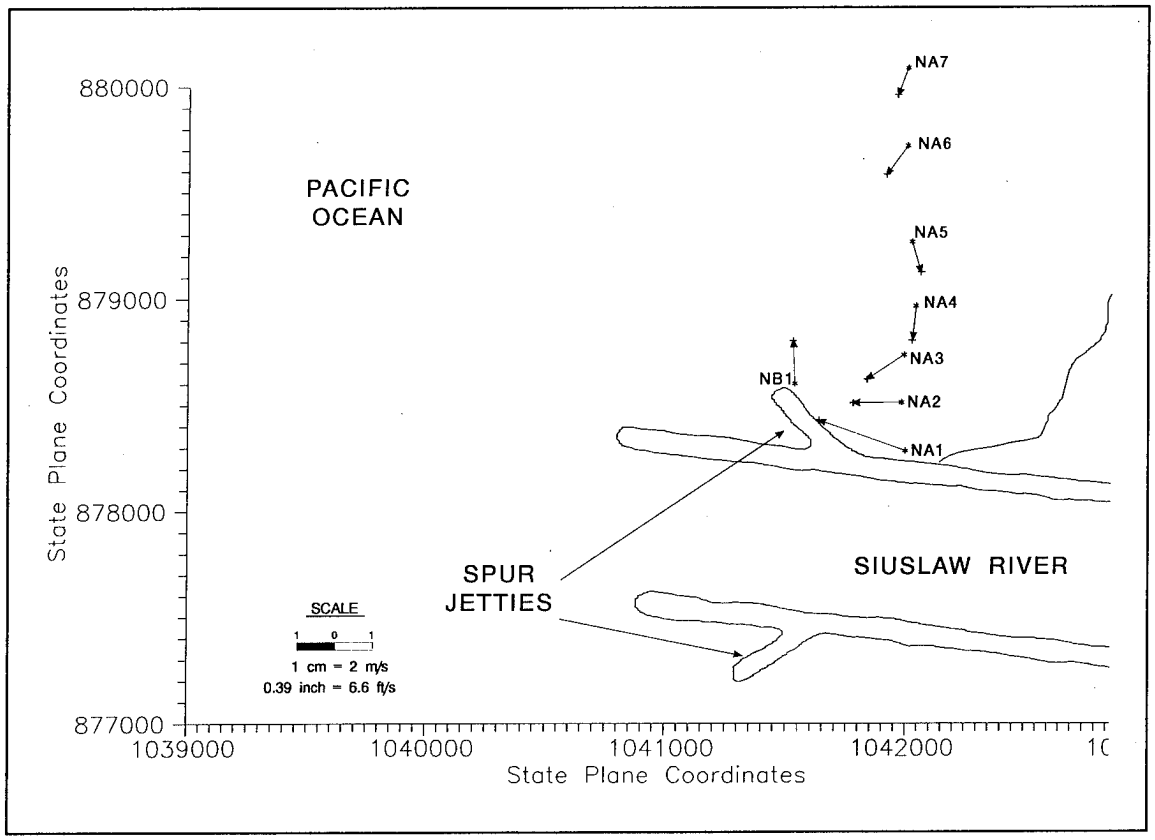

Figure 34. Mosaic presentation of current vectors for sampling interval III on 19 July 1990

winds were out of the northwest the entire day. The daily tidal low of 0.91 m (2.98 ft) and high tide of 2.04 m (6.69 ft) occurred at 11:20 a.m., and at 5:32 p.m., respectively.

Sampling Interval I began at 10:47 a.m. and ended at 11:43 a.m. and included 21 points in the 56-min sampling period. Figure 35 is a mosaic of the current vectors for the 3 September 1992 sampling period. Significant wave heights and periods measured at the Coquille wave array at 7:42 a.m. were 1.5 m (4.9 ft) and 7 sec, respectively; and at 2:11 p.m., waves measured 0.8 m (2.6 ft) in height with 7-sec periods. The Coquille buoy measured 0.6-m (2-ft) waves with periods of 5 sec. During this ebb-slack/turning to flood tidal period with relatively low wave heights, currents were directed offshore and increased in magnitude as they neared the jetties. As the currents passed the spur, they tended to be deflected slightly to the northwest. In the area approximately 100 m (328 ft) northwest of the spur tip, the current appears to become confused and then splits into two paths. While standing on the tip of the spur, this confused pattern was observed, and the helicopter was directed to make several samplings in the area. Vectors 9, 10, 17, and 18 are in the area of the described confusion. If vectors 8, 9, 19, 20, and 21 are tracked, then the current is observed to turn toward shore. Vectors 16 and 18 show offshore flow. Visual observation from a fixed-wing plane indicated that

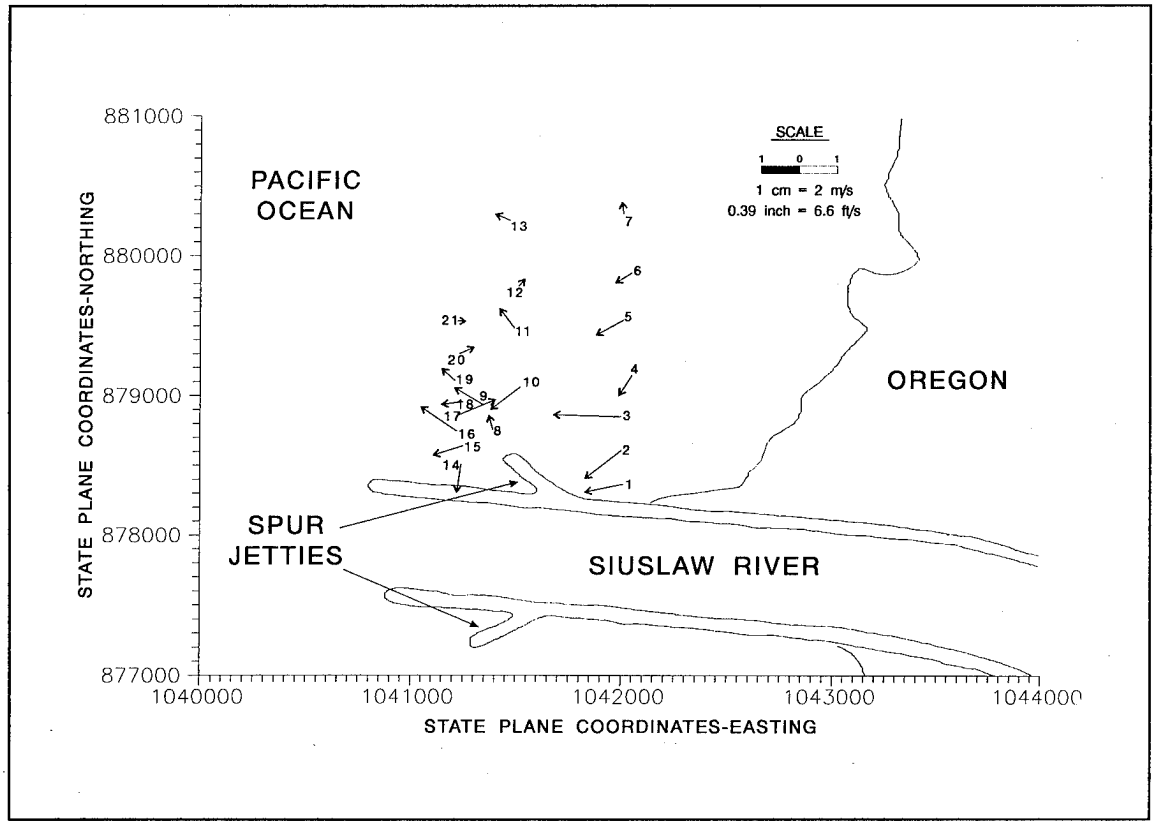

Figure 35. Mosaic presentation of current vectors for sampling interval I on 3 September 1992

flow patterns appeared to split, circulating back toward the shore and flowing offshore creating an eddy both seaward and shoreward of the spur tip. Figure 36 is a photograph taken during this sampling interval. Figure 37 is a photo of a dye study conducted previously that shows a similar split in current occurring on a calm day with relatively low wind and wave climate, and Figure 38 is an interpretation of the flow patterns observed from the fixed-wing plane and from the spur jetty. Additionally, shedding of gyres or vortices from the edges of the swift current paths was observed in the surface currents and could explain the vectors that appear to be misdirected. Vortices being shed from the head of a groin has also been noted in Australia (Smith 1989). Deep scour holes and shoals off the tip of the spurs may also account for the unpredictability of some of the vector directions. A rip current located to the north of the circulation was observed from the fixed-wing plane. This rip current may be responsible for the directions of vectors 1 and 13.

9 September 1992, sampling interval II

On the second day of operation, 9 September 1992, three sampling periods were completed, one during the incoming tide and two during the outgoing tide. Vector information can be found in Appendix B. Tidal high of 1.74 m (5.7 ft) occurred at 11:52 a.m., tidal low of 0.82 m (2.69 ft) at 5:32 p.m., and a high again of 1.98 m (6.5 ft) at 11:25 p.m. Waves and winds were out of the northwest the entire day and the surf zone extended past the jetty entrance tips.

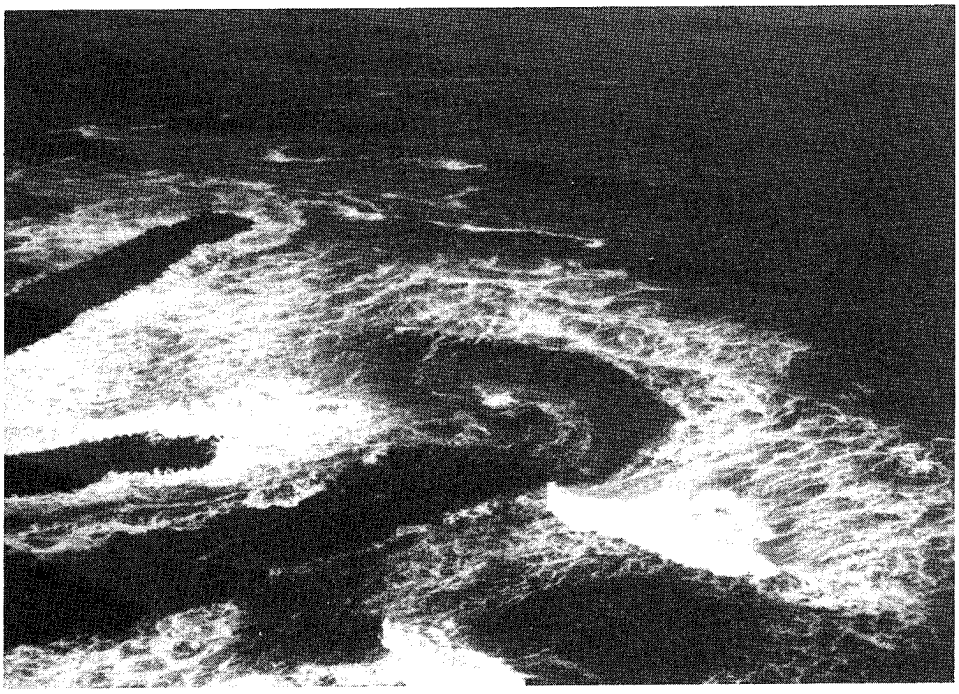

Figure 36. Aerial photo taken during sampling interval I, 3 September 1992

Figure 37. Aerial photo of dye study at south jetty showing current splitting

The first sampling period began at 10:58 a.m., and ended at 11:53 a.m., and included 13 sampling points in the 55-min period. During this flood-to-slack tidal-period, significant wave height and peak period measured at the Coquille buoy were 1.8 m (5.9 ft), and 9 sec, respectively; and at the Coquille array waves measured 2.2 m (7.2 ft), 9 sec. Breaking waves in the study area neared 3 m (9.8 ft) in height. This was the first time the sampling pattern followed dye flows. The added task of handling the dye packets reduced the number of points that were sampled.

Figure 39 is the current vector mosaic for this sampling period. Current vectors during this relatively high wave condition and flood to slack tide displayed a distinct circulation pattern induced by the spur. By tracing the vectors in Figure 39, it can be clearly seen that currents were deflected to the north and, in combination with the wave and tide approach, currents were directed into a spiral and flowed toward the shoreline. Visual observations from a fixed-wing plane indicated surface currents flowing in the same pattern. The photographs in Figures 40a and 40b show this eddy development. Figure 40c is a photograph of the sediment plume during an incoming tide.

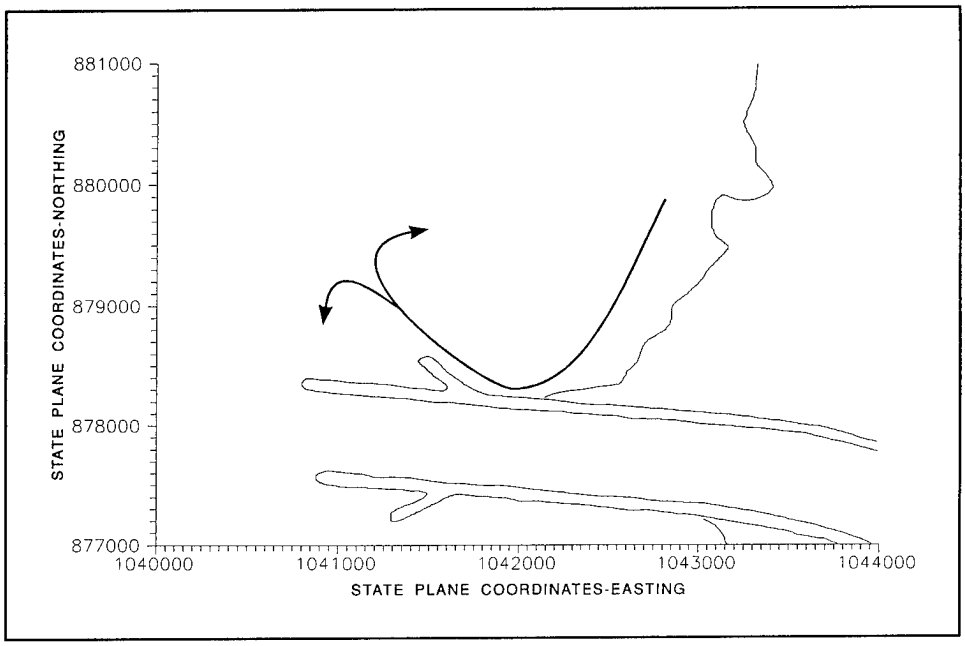

Figure 38. Interpretation of current flow patterns during 3 September 1992 sampling interval I

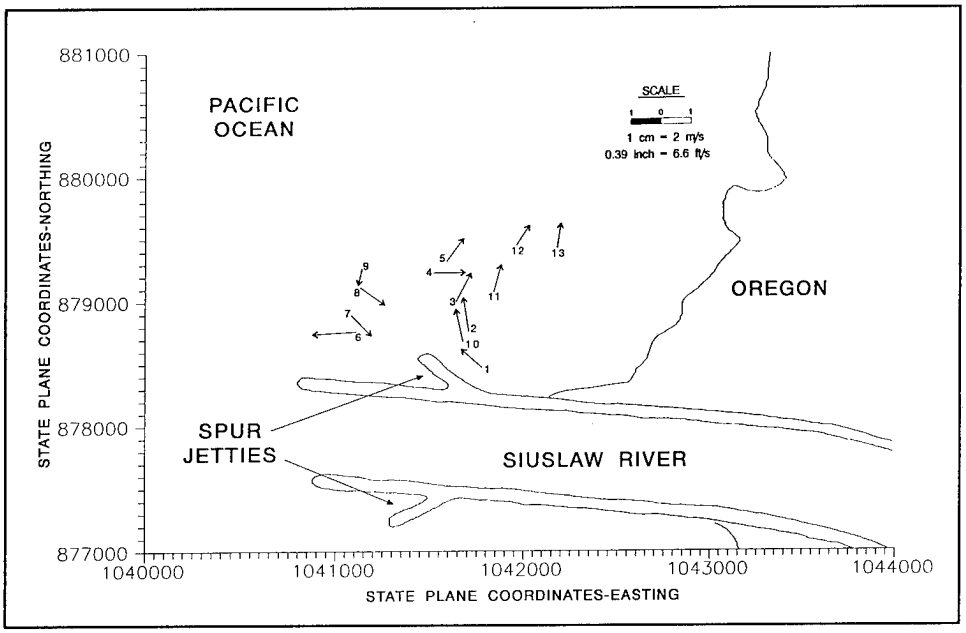

Figure 39. Current vector mosaic for sampling interval II on 9 September 1992

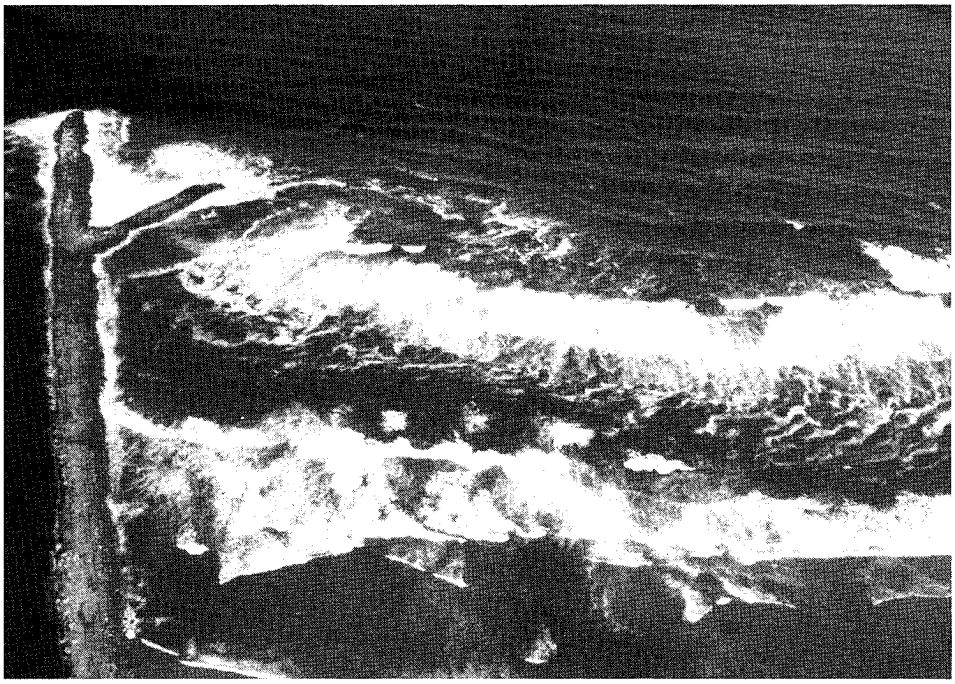

a. Early flood tide

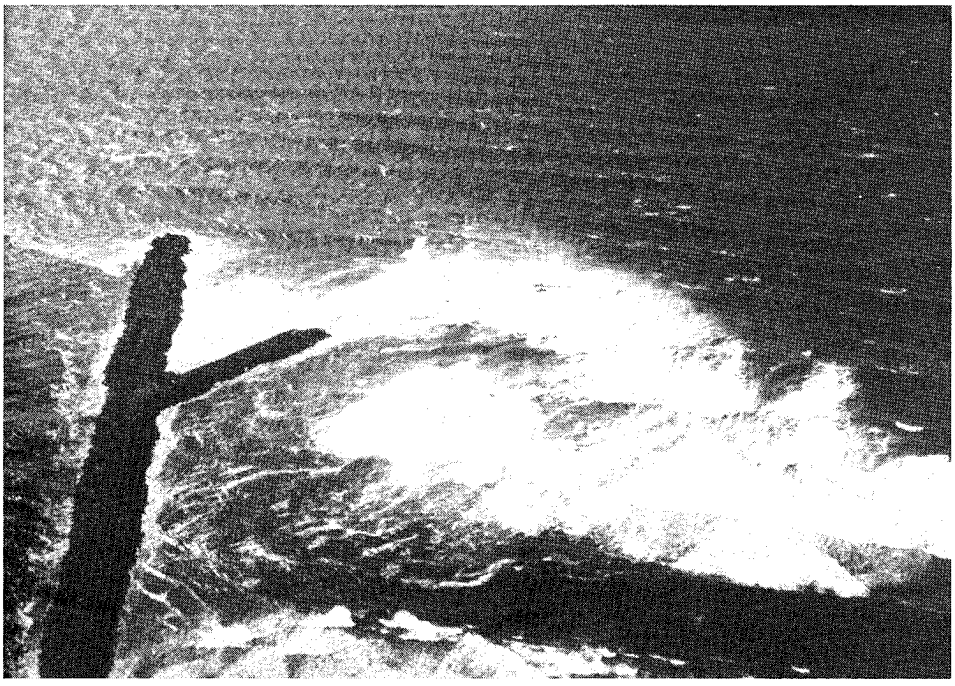

b. Middle flood tide

Figure 40. Aerial photos of clockwise rotation of current (Continued)

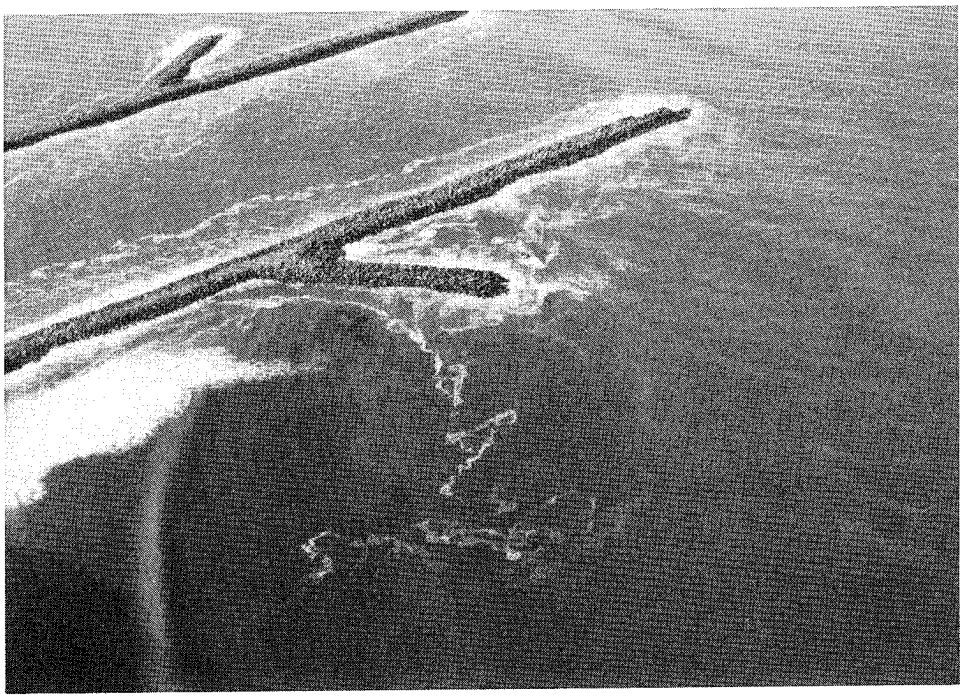

c. Sediment plume during incoming tide

Figure 40. (Concluded)

Figure 41 is an illustration of the visual observations made from the jetties and the fixed-wing plane.

9 September 1992, sampling interval III

The second sampling period on 9 September 1992 began at 1:21 p.m. and ended at 2:18 p.m., including 18 sampling points in the 57-min period. Waves for this time period were measured at the Coquille buoy as 1.8-m (5.9-ft) significant wave height, and 8-sec peak period. At the array, these values were 2.2 m (7.2 ft) and 8 sec, respectively. During this sampling period dye packets were dropped, and the sampling pattern followed the dye flow pattern. Figure 42 shows the current vector mosaic for this sampling period. During this high wave condition and outgoing tide, current vectors indicated the flow converged into a tightly constricted jet of water which extended past the spur approximately 500 m (1,640 ft) to the northwest of the spur tip. Vector magnitudes were greater for this period than for previous sampling periods. Current vector magnitudes appeared to increase as wave heights increased and as the tide neared the peak flow of the outgoing cycle. Again observations from the fixed-wing plane parallel the vector indications. In addition, a sediment plume was detected past the observed water current patterns. The sediment plume turned south and flowed past the jetty tips leaving approximately 100 m (328 ft) of blue water untainted by the sediment plume seaward of the jetty tips. Vortices were also observed spinning off seaward and shoreward of

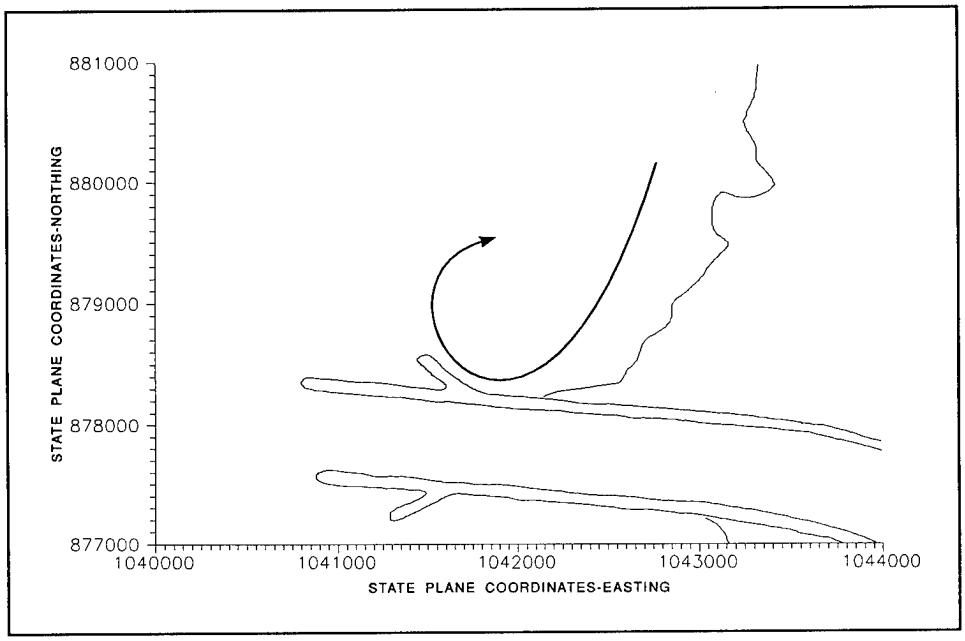

Figure 41. Interpretation of current pattern during sampling interval II, 9 September 1992

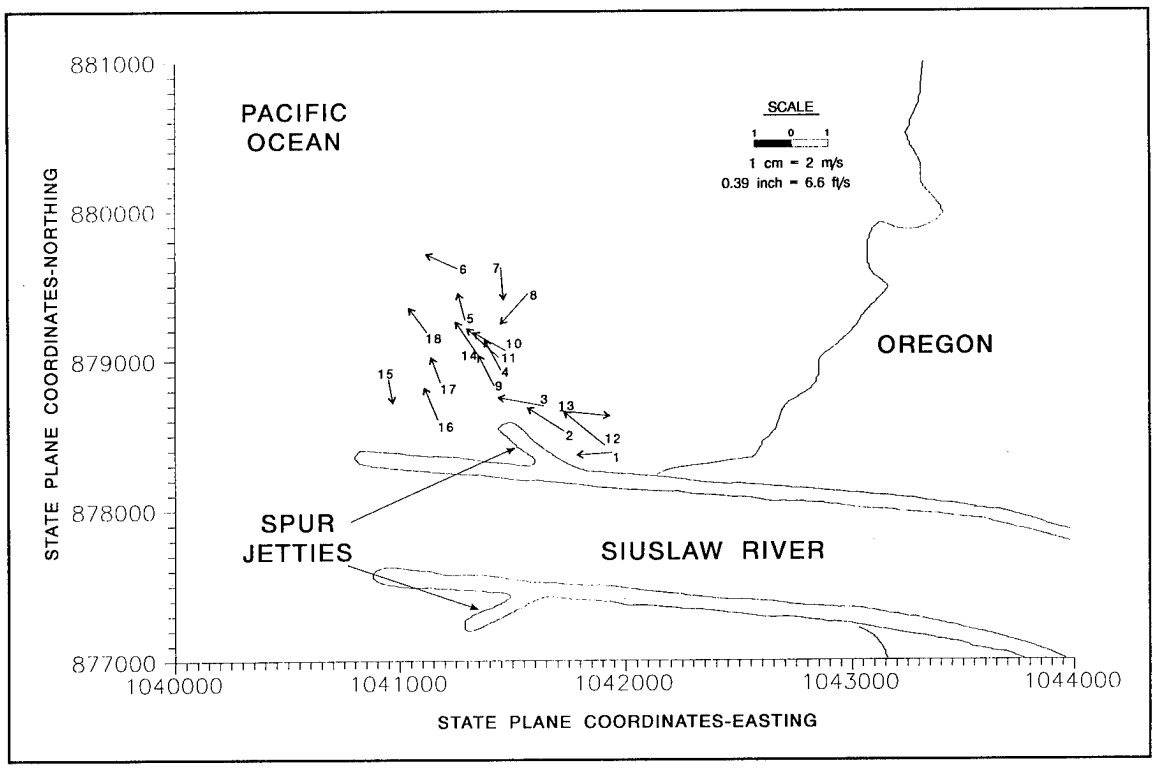

Figure 42. Current vector mosaic for sampling interval III on 9 September 1992

the jet flow. Photographs taken from a fixed-wing plane during this sampling period show the jet identified by the vector mosaic (Figure 43). Figure 44 is a photograph taken at another time that shows the described sediment plume flow pattern typical during outgoing tides. Figure 45 is an illustration of the flow patterns observed from the jetties and the fixed-wing plane. In the visually observed pattern, the flow pattern resembled a tight radius "S" curve of a racetrack with the jetty initiating the westwardly turn and the spur and the current magnitude dictating the radius and location of both the initial curve and the reverse curve.

9 September 1992, sampling interval IV

The third sampling period on 9 September 1992 began at 3:44 p.m. and ended at 4:25 p.m., and included 19 sampling points in the 41-min period. Range lines perpendicular to the jetty trunks were again used for the sampling pattern for this period. Visual observations immediately prior to the sampling interval showed the flow patterns to be broad, not exhibiting the constricted flow jet of the previous interval. Therefore it was expected that a grid sampling pattern would better serve in documenting the flows. Figure 46 shows the vector mosaic for this time period. During this high wave condition and mid-ebb tide flow, the spurs caused a less significant northwest flow that combined with the westerly or offshore current flow directed by the jetty trunk. The merging of the currents of the spur tip formed a wider jet of lesser intensity than that of sampling interval III. Vector magnitudes continued to

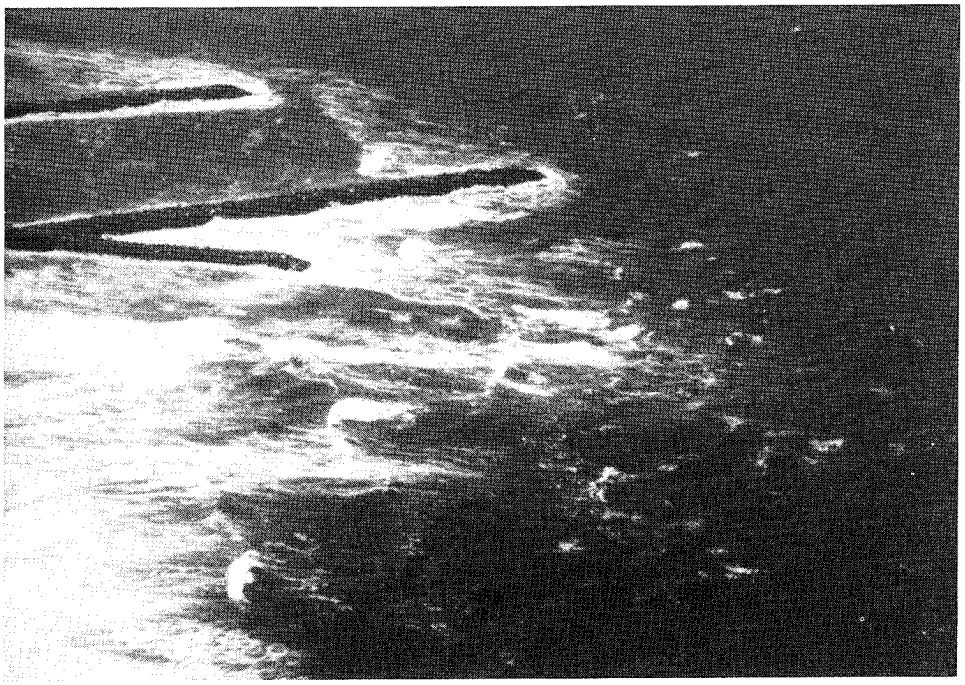

Figure 43. Aerial photo of current flow pattern during sampling interval III, 9 September 1992

Figure 44. Aerial photo of sediment plume flow pattern for outgoing tides

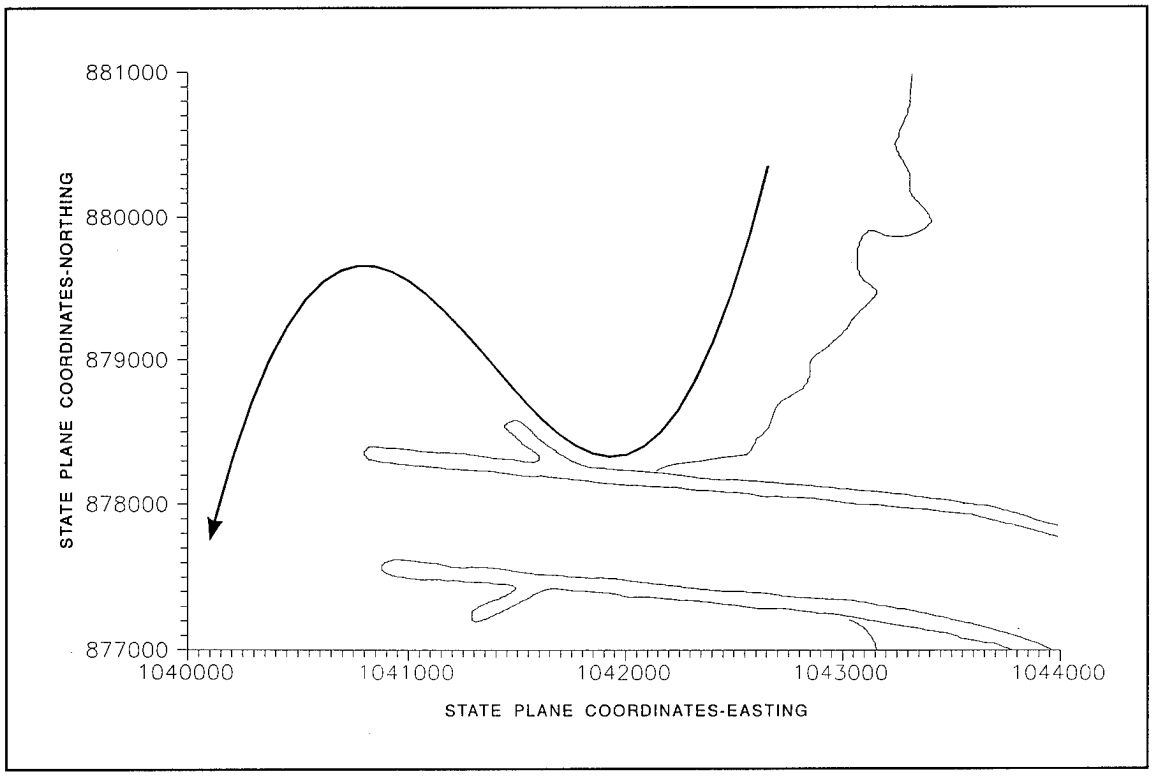

Figure 45. Interpretation of current flow pattern during sampling interval III, 9 September 1992

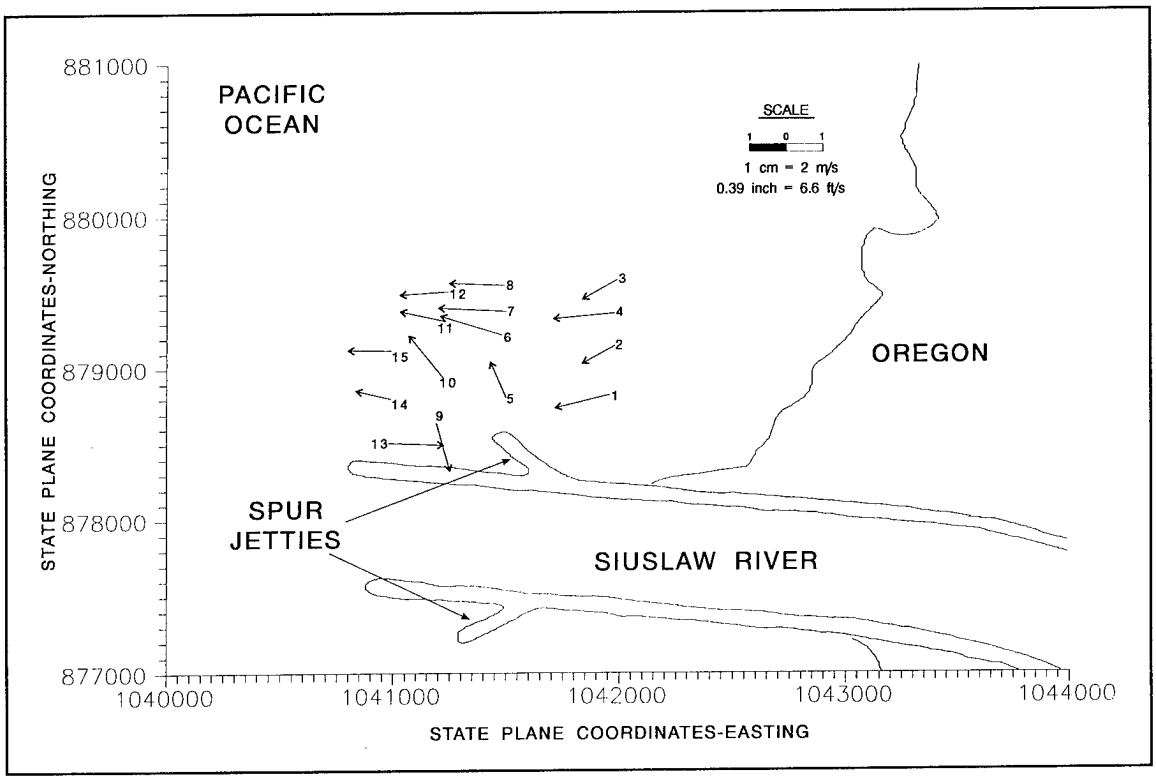

Figure 46. Current vector mosaic for sampling interval IV on 9 September 1992

increase to values greater than that of earlier sampling periods. Figure 47 is an illustration of visually observed surface flow patterns during sampling interval IV. The "S" curve described for sampling interval III is still present, but the radius of curvature is much larger and is made up of 130-deg (2.3-rad) arcs as opposed to the 180-deg (2.3-rad) arcs of the previous period. Additionally, the intersection of the two arcs parallels the jetty trunk for sampling interval IV, whereas for sampling interval III, it parallels the spur.

Summary of Current Patterns

Both the July 1990 and the September 1992 study periods established the capabilities of the helicopter-borne current measurement system and documented current flow patterns that occur near the structured entrance to the Siuslaw River. Both studies were conducted on the north side of the jetties during wind and wave conditions from the north. The opportunity to test the southern condition did not occur, nor did time allow for measurements on the south side of the jetties during a northern wind and wave condition. The July 1990 study documented wind-dominated current flows from due north. Sampling during the September 1992 study documented regimes dominated by waves from north-northwest. Tides also appeared to influence the current patterns.

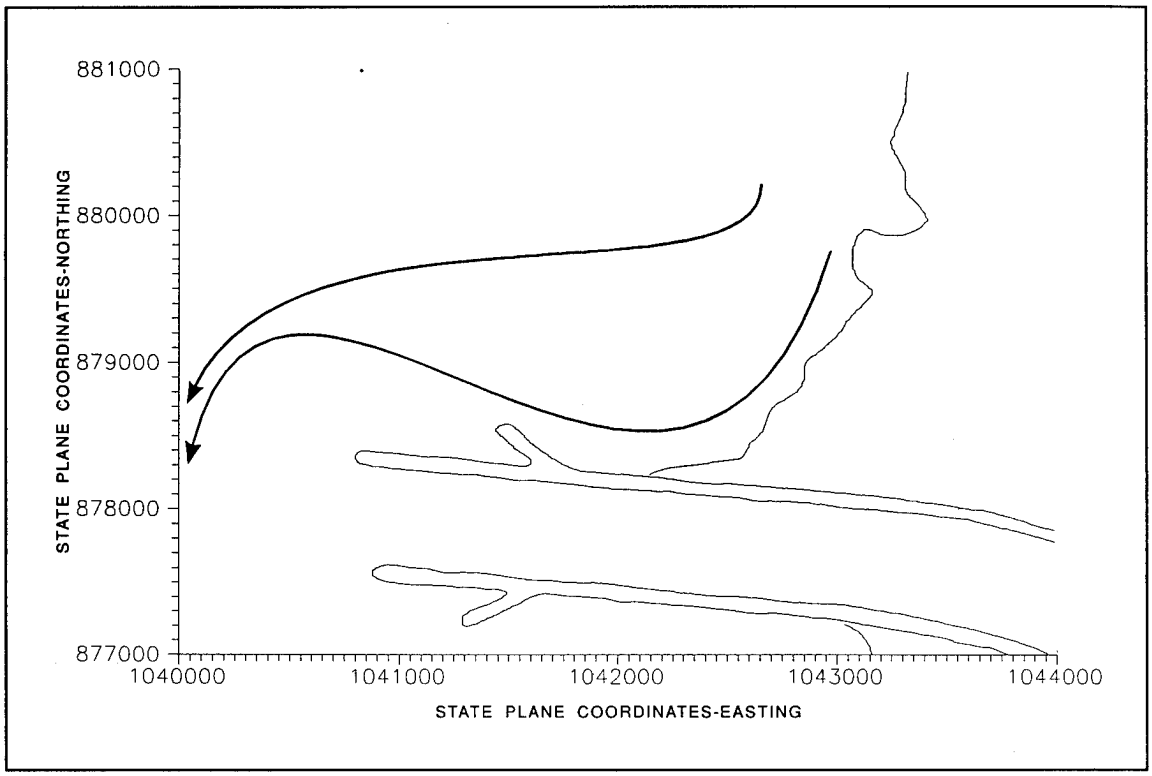

Figure 47. Interpretation of the current flow patterns during sampling interval IV, 9 September 1992

Mosaic presentations of current vectors from several sampling intervals served to identify current patterns for various wave, wind, and tidal combinations. Aerial photos and illustrations of visual observations enhanced the study findings. Comparison of photographs and visual observations during the 1992 study with vector mosaics from that study indicated that surface current patterns are indicative of bottom current patterns for this study area during tidal and wave-dominated flow regimes. Aerial photographs were not taken during the 1990 study.

For strong winds and large waves directly out of the north with either incoming or outgoing tide, the longshore current made no circular patterns as a result of the spurs. The spur may have been effective at displacing dominant jetty-parallel flows away from the jetty trunk, thereby reducing the potential for eddy formation at the jetty head on the inner channel side of the jetty trunk.

Waves and winds set up a longshore current that interacts with the jetty system to develop the localized current patterns. Arranging and comparing vector mosaics by tidal sequence, it appears that the current patterns that develop may also be tidal related when the tidal flows are strong. Figure 48 shows a sequential interpretation of the current patterns through a tidal cycle based on the results presented in this chapter. The onshore flow may assist in

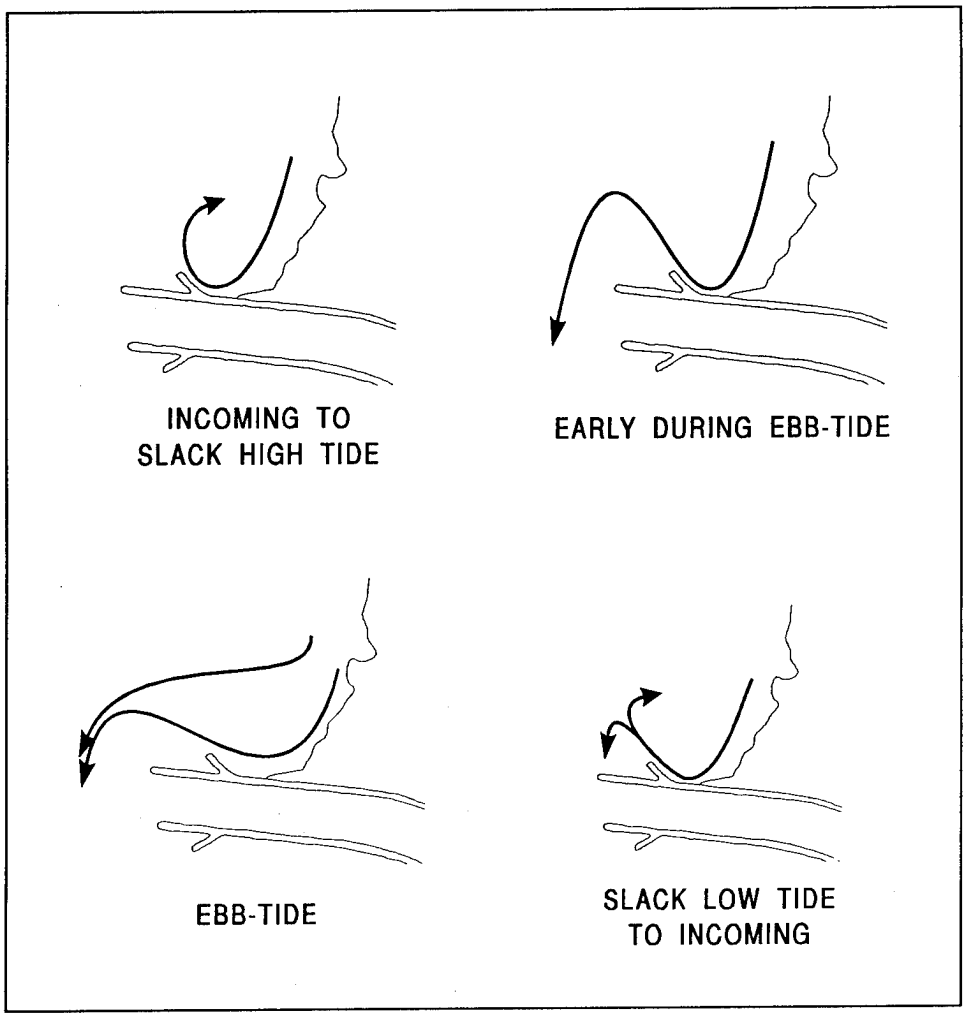

Figure 48. Sequential interpretation of the current patterns through a tidal cycle

forming the circulation eddy that directs the flow back toward shore, and the offshore flow may assist the flow jet in traveling offshore and around the jetty tips. Additionally, it may be hypothesized that both the alongshore component and the onshore/offshore component of the tides influence the localized current pattern when the tides are strong. Figure 49 was created from NOAA tide tables (National Oceanic and Atmospheric Administration 1992) and shows the time lag of the high and low phase of the tide along the Pacific coast and the directional tilt of the water surface indicating the alongshore directional component of the tidal flow. From this figure, the alongshore component of the tide flows south during an ebbing tide. During the flood tide the current flows north. On a tidal scale, the jetties initiate edge effects. The eddies that develop may be influenced by the interruption in tidal current flow by the jetty system. On a localized scale, the spurs may shape the form that the eddy takes. Hence, when tidal flows are strong and the longshore current is additive, a flooding tide may form an eddy north of the jetties and an ebbing tide

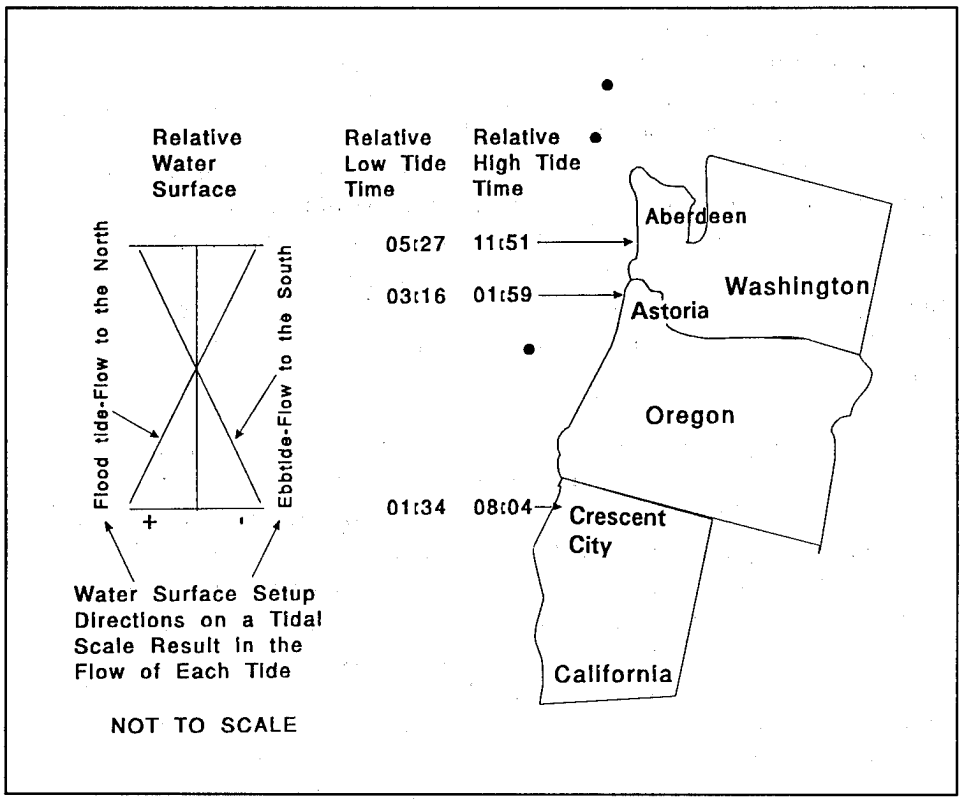

Figure 49. Time lag of high and low tide phases along the Pacific coast and directional tilt of the water surface

may form an eddy south of the jetties. Aerial photographs taken previous to these current studies document eddy formation on the south side of the jetties.

Comparison of Airborne Coastal Current Measurement System and Bottom-Mounted In Situ Current Measurement Systems

On 9 September 1992 ground truthing of the Airborne Coastal Current Measurement system was attempted. An in situ current meter was located approximately 1.6 km (0.99 miles) north of the north jetty tip in 14 m (46 ft) of water at latitude 44° 01.90' N, longitude 124° 08.50' E. The in situ meter was deployed from a U.S. Coast Guard vessel the night before, and its internal clock was set to collect wave and current data for 0.5-hr intervals twice during the day (10:00 a.m. and 2:00 p.m.). A meter assembly was arranged in the same fashion as the one used by the helicopter, except the anchor weight was composed of three cannonball weights totaling 667 N. A highly visible surface buoy anchored by a 356-N weight was connected to the current meter assembly by a 33-m (108.2-ft) line laid perpendicular to shore.

Using the location coordinates collected by the Coast Guard boat, the helicopter flew to the same Loran "C" location and spotted the surface buoy. Understanding the orientation of the in situ meter to the marker buoy, the pilot lowered the meter assembly attached to the helicopter to the seabed as close to the in situ meter as could be estimated. The helicopter hovered while the instrument collected wave and current data for a 0.5-hr interval (Figure 50). It was not possible to determine the exact relative arrangement of the two meters. It was intended to have the helicopter hover over the in situ meter for several minutes while the in situ meter collected data. Then the airborne meter was to be lowered to the seabed, and subsequently the meters were to collect data simultaneously.

Objectives of this portion of the investigation were to evaluate the effects the helicopter's rotor may have on waves and currents and to compare the system against an in situ meter. In the morning, fog prevented an early departure of the helicopter from the helipad. Although the helicopter did hover over the in situ meter for several minutes, the mobile meter was lowered to the seabed as the 0.5-hr data collection interval of the in situ meter was ending. Figure 51 shows an excerpt of the data collection record from the pressure sensors for both the in situ and the mobile meter. As can be seen, there is no overlap of data collection and no notable impacts from the helicopter rotor in the water depth or wave measurements. Figure 52 shows the current records for both meters. Assuming the meters were relatively close and currents and waves did not change dramatically between the two 0.5-hr intervals, a comparison of the time-averaged currents from the two meters reveals only a

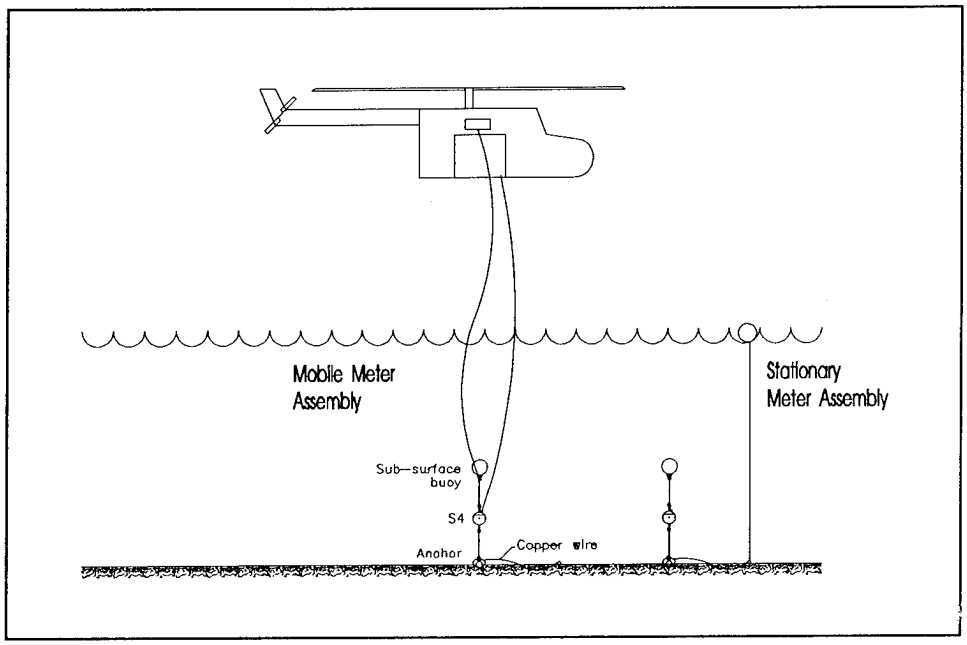

Figure 50. Ground truthing of Airborne Coastal Current Measurement System on 9 September 1992

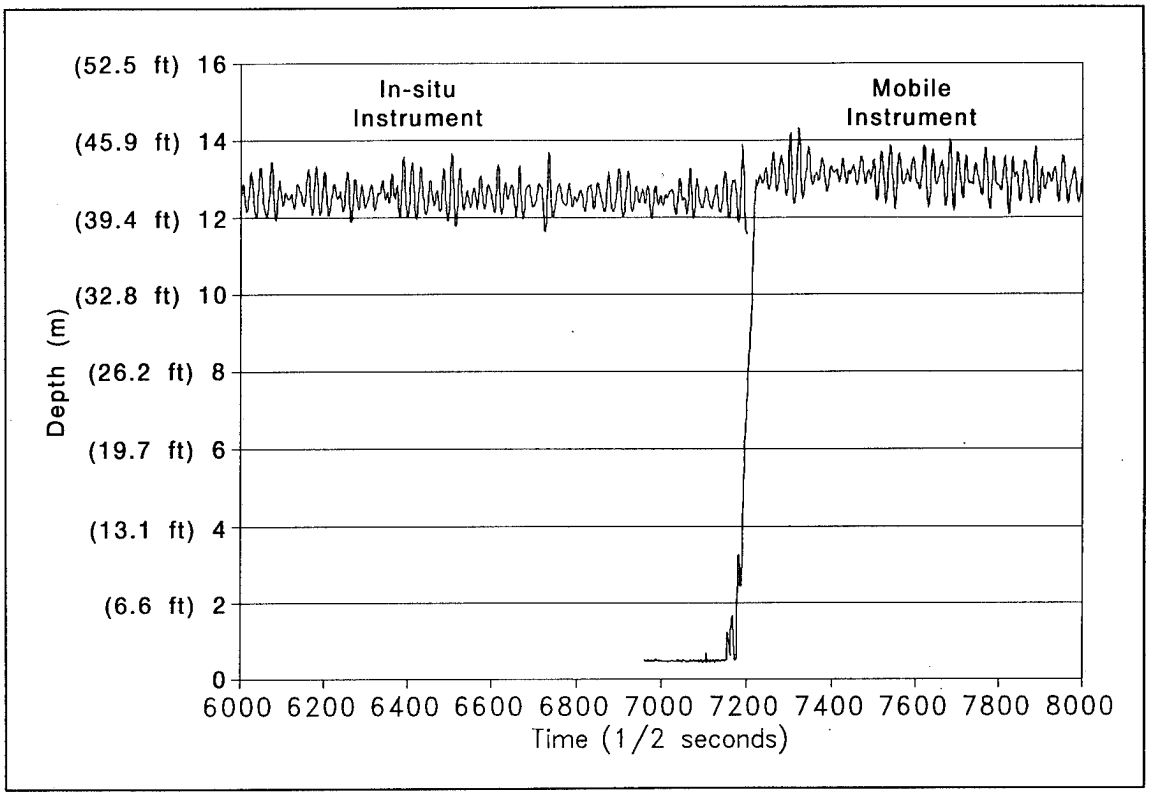

Figure 51. Pressure sensor data for both in situ and mobile meter

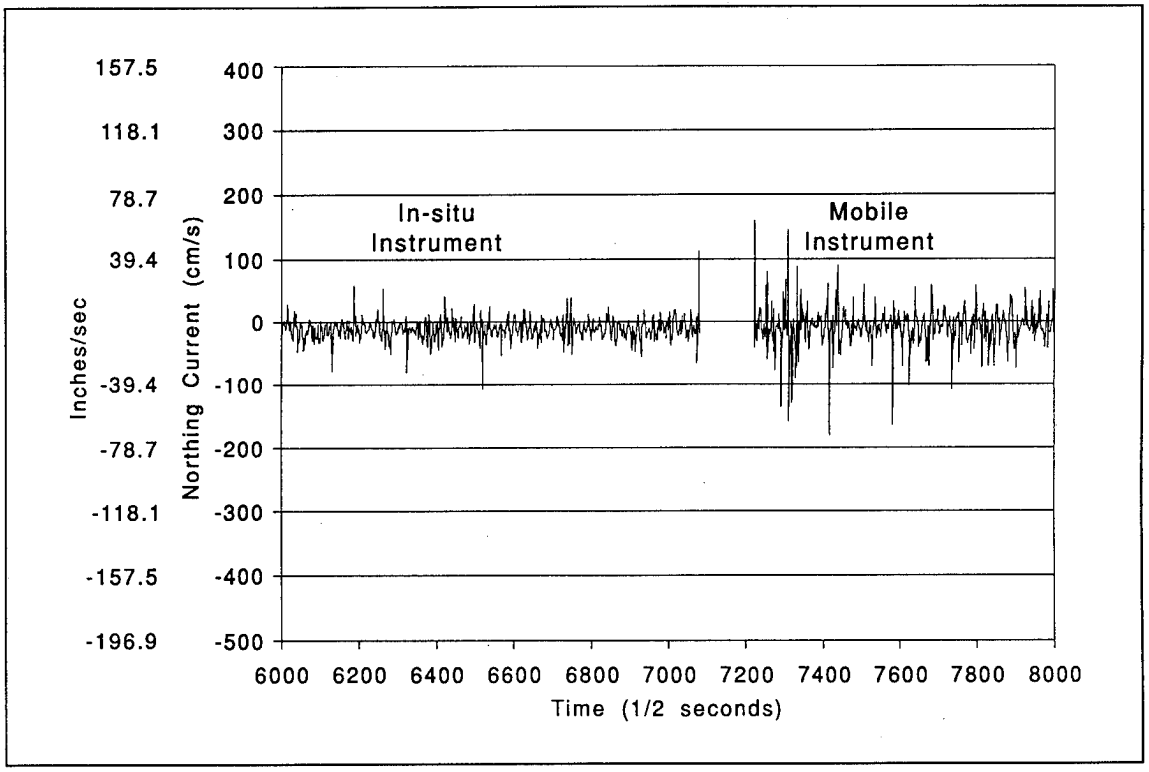

Figure 52. Current data for both in situ and mobile meter

2 cm/s (0.70 in./s) difference in magnitude and 1 deg (0.017 rad) in direction. As also shown in Figure 51, wave heights are similar. Although recorded depths vary slightly, this could be due to the meters actually being located at slightly different depths. The similar wave heights and currents support the assumption that the meters are located relatively close to one another. Based on the similarities in the recorded data of the two instruments and the lack of detectable effects of the helicopter on the data collection string, it is concluded that the Airborne Coastal Current Measurement System is capable of accurately measuring bottom currents.

5 Qualitative Comparison of Prototype Field Study Results With Physical Model Study Results

Mosaics of the current patterns around the jetty obtained from the Siuslaw River Airborne Coastal Current Measurement study are used to identify circulation pattern trends in the prototype, and are qualitatively compared with photographs of circulation patterns identified in a physical model sediment tracer study performed by Bottin (1981, 1982) for the Rogue and Siuslaw Rivers.

Physical Model Study of Spur Jetties

Bottin (1981, 1982) conducted tests involving proposed spur jetty modifications at the mouths of the Rogue and Siuslaw Rivers, OR, to qualitatively determine sediment movement and shoaling patterns at the river mouths for various test conditions and spur configurations. A tracer was used to identify sediment transport and depositional patterns. Due to limited funding and time, supplemental testing of spurs for the proposed jetty modifications at the Siuslaw River project were conducted using the existing model of the Rogue River, OR (Bottin 1982). Results from both studies influenced the prototype design for the Siuslaw jetties. Therefore, results from both studies will be used in this comparison.

The physical model (Bottin 1982) was constructed on a undistorted linear scale of 1:100, model-to-prototype to ensure accurate reproduction of short-period wave and current patterns. A fixed-bed model with a tracer was selected to identify sediment transport patterns. The model reproduced the lower 2,043 m (6,703 ft) of the Rogue River, approximately 2,134 m (7,001 ft) of the shoreline on each side of the river mouth, and underwater topography in the Pacific Ocean to an offshore depth of 20 m (65.6 ft). Vertical control for model construction was based on mllw datum.

Siuslaw River Physical Model Tests

The Siuslaw River (Bottin 1981) proposed jetty extensions were installed on the Rogue River model contours (Figure 53) and still-water levels (swl) were adjusted so that depths in the model were comparable to those at the proposed Siuslaw jetty heads and spur locations. Tests for the Siuslaw River were conducted on seven jetty improvement plans for representative test waves approaching from approximately azimuths of 340 deg (5.9 rad) and 220 deg (3.8 rad) with swl of 0.0 m (0.0 ft) mllw and/or +2.0 m (+6.6 ft) mhhw. Plans 4 and 6 correlate with actual prototype jetty construction.

Tracer material was introduced into the model north of the river entrance to represent sediment from the north shoreline, and tests were conducted for waves from 340 deg. Test results for the spur configuration in Plan 4 revealed that, for swl of +2.0 m (+6.6 ft), the 9-sec, 8.2-m (26.9-ft) wave (Figure 54), and the 11-sec, 3.7-m (12.1-ft) wave (Figure 55) both from the NNW, material was moved around the spur and formed an eddy that rotated in a counterclockwise movement. Tracer material was deposited in the V-shaped area between

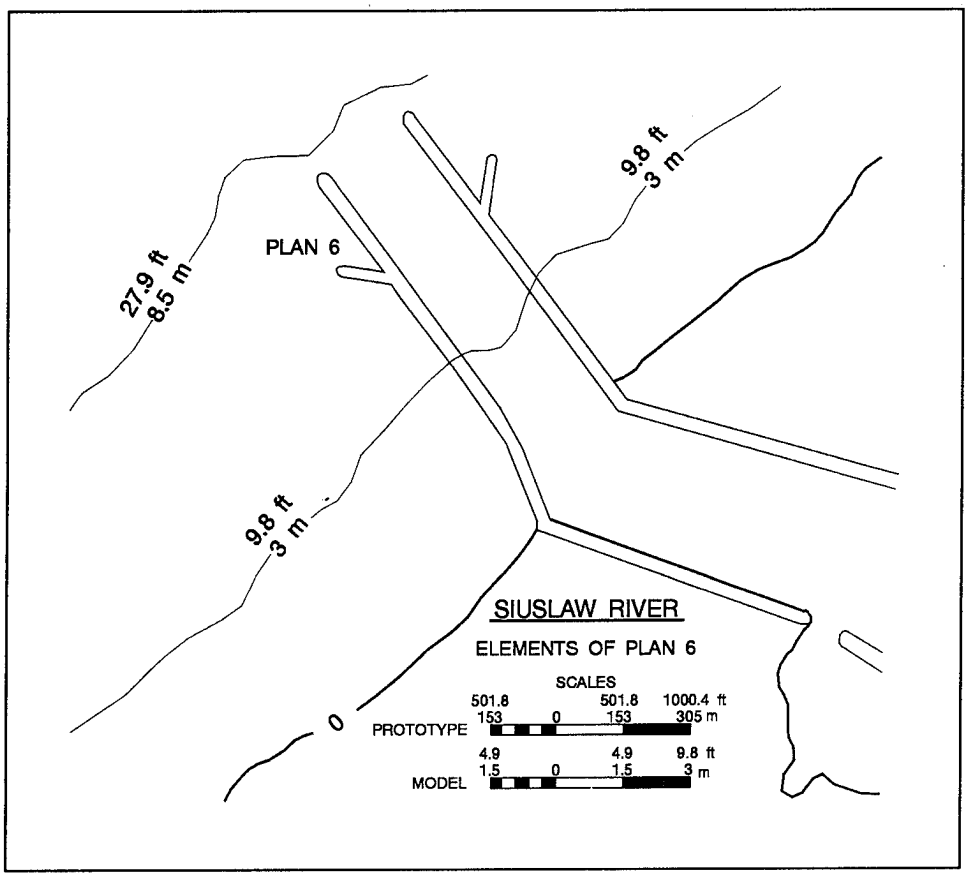

Figure 53. Siuslaw River, OR, jetties installed on the Rogue River model contours

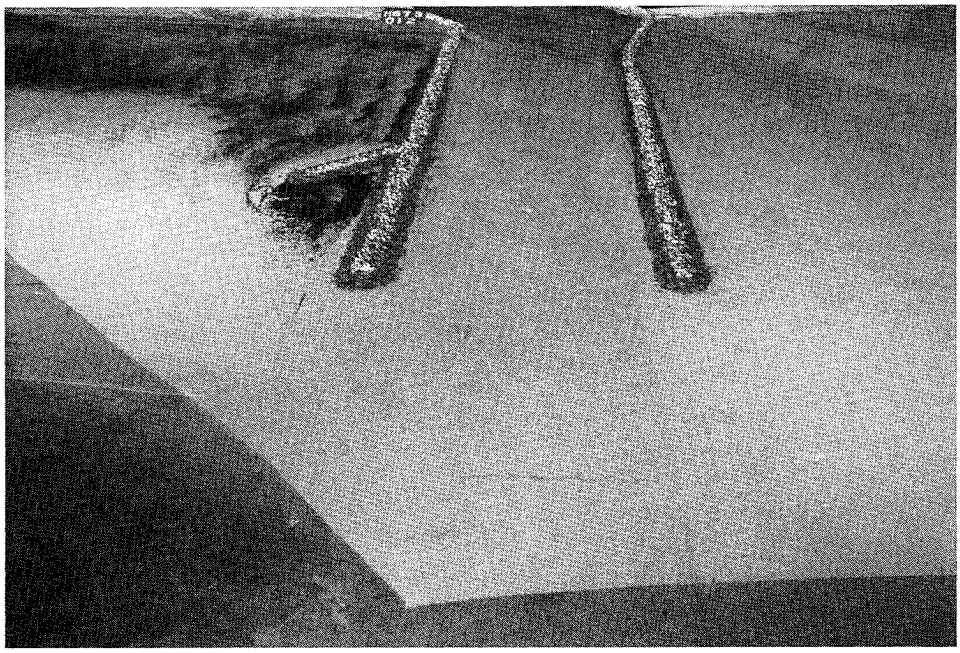

Figure 54. General movement and tracer material deposits resulting from 9-sec, 8.2-m (26.9-ft) wave from NNW for Plan 4 Siuslaw River; swl = +2.0 m (+6.6 ft)

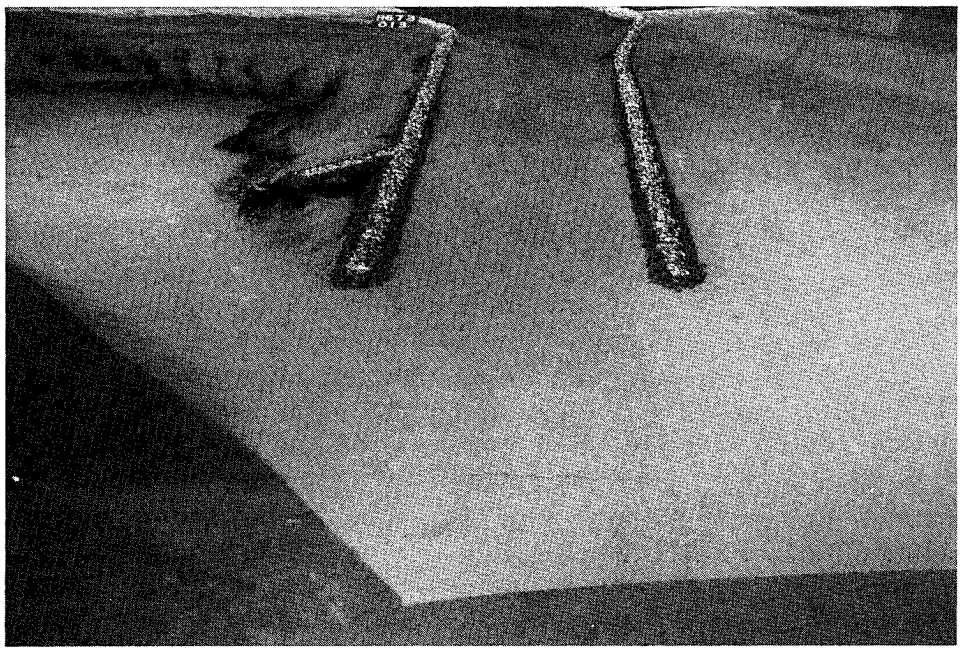

Figure 55. General movement and tracer material deposits resulting from 11-sec, 3.7-m (12.1-ft) wave from NNW for Plan 4 Siuslaw River; swl = +2.0 m (+6.6 ft)

the spur and jetty. Testing did not show what would happen when the V-shaped compartment became saturated with tracer. Additionally, there appeared to be a potential for deposition inshore of the spur slightly to the north, possibly resulting from a clockwise circulation near the spur tip. These deposition patterns resemble the September 1994 sampling intervals I and II. The 13-sec, 2.1-m (6.9-ft) wave at swl of +2.0 m (+6.6 ft) (Figure 56) displayed movement and deposition of the tracer material in a jet directed toward the northwest parallel to the jetty spur and extending approximately three times the length of the spur. This deposition pattern and relative length of the water jet correlate with September 1994 sampling intervals III and IV.

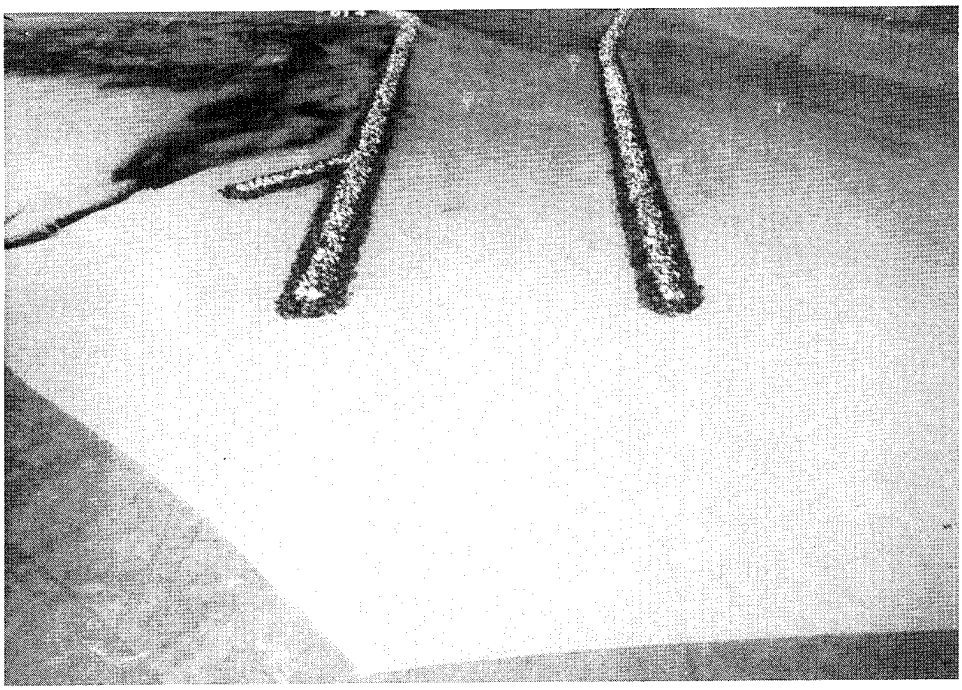

Figure 56. General movement and tracer material deposits resulting from 13-sec, 2.1-m (6.9-ft) wave from NNW for Plan 4 Siuslaw River; swl = +2.0 m (+6.6 ft)

Tracer material introduced south of the river entrance represented sediment from the south shoreline, and tests were conducted for representative waves from 220 deg (3.8 rad). General movement of the tracers for waves from the south in Plan 6 mirrored that of tracer movement for waves out of the north in Plan 4.

Rogue River Physical Model Study

Base tests for the Rogue River (Bottin 1982) were conducted on 58 variations of the design elements' three basic remedial improvement plans. Of these, spur jetties were included in the grouping of jetty extensions. The

trunks of the jetties at the Rogue River are angled slightly to the south relative to the shore, and the trunks of the jetties at Siuslaw River are angled slightly to the north. Waves approaching from the north for the Rogue River are subjected to an obtuse angle between the jetties and the shore. For the Siuslaw River, the angle is acute. Because of the orientation of the Rogue River jetties relative to the shoreline, the south jetty with a southern wave approach can be considered the reverse of the Siuslaw north jetty with a northern wave approach.

Plans 4 and 5 (Figure 57) involved spur jetties similar to the Siuslaw study with several versions of jetty and spur lengths for the north and south jetties, respectively. Plan 5 includes Plan 4d configuration for the north jetty. For the various wave conditions, variations in the jetty configuration result in similar depositional patterns. Figures 58-60 are photographs from the physical model study showing depositional patterns. Arrows placed on the photographs indicate possible flow patterns that create depositional patterns for waves from the north-northwest. The arrows were placed based on deposition patterns, not on observed flow patterns. Therefore, current flow patterns may vary slightly from the interpretation indicated by the arrows.

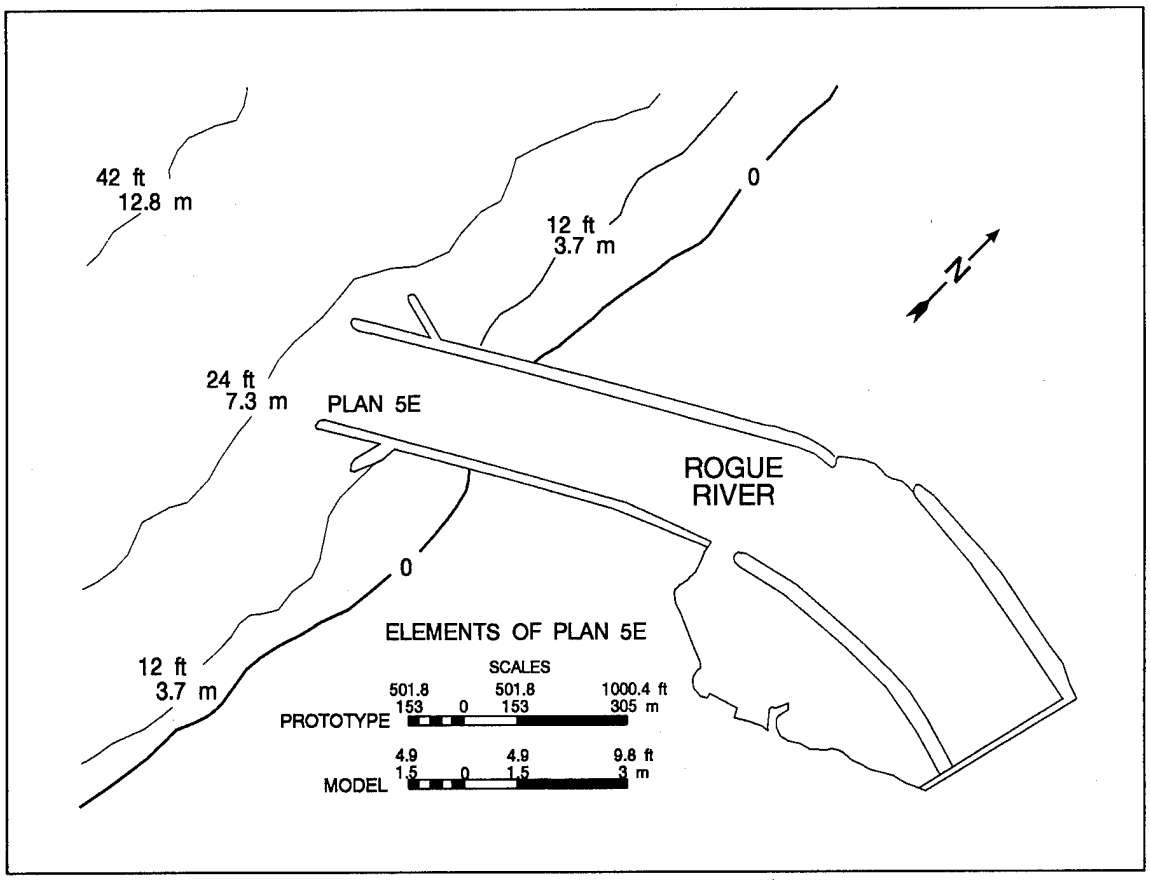

Figure 57. Rogue River, OR, jetty configurations, Plans 4 and 5

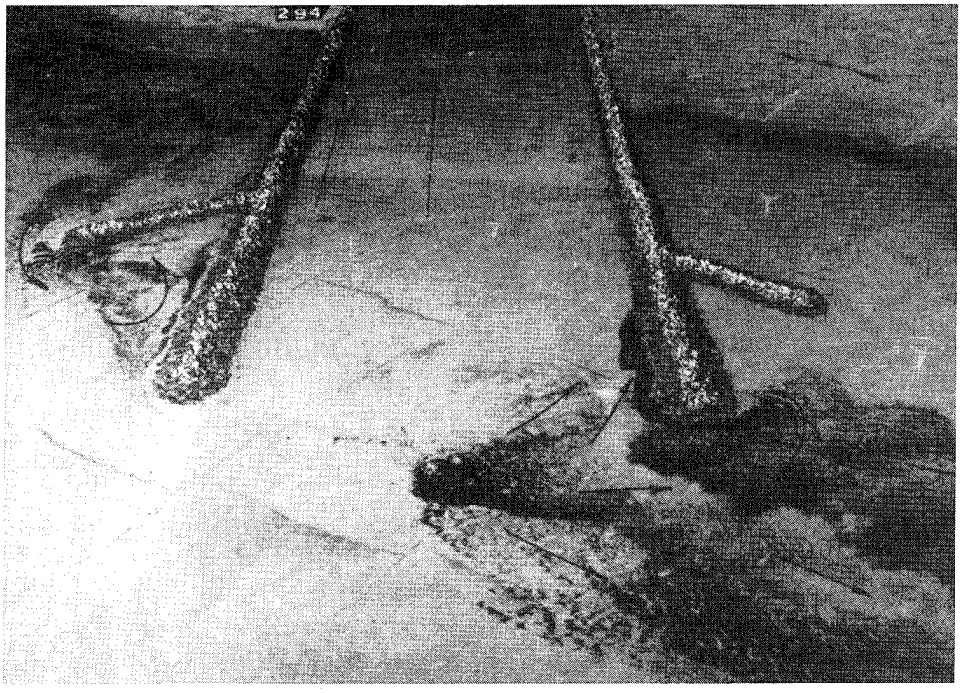

Figure 58. General movement and tracer material deposits resulting from 9-sec, 8.2-m (26.9-ft) wave from NNW for Plan 5 Rogue River; swl = +2.0 m (+6.6 ft)

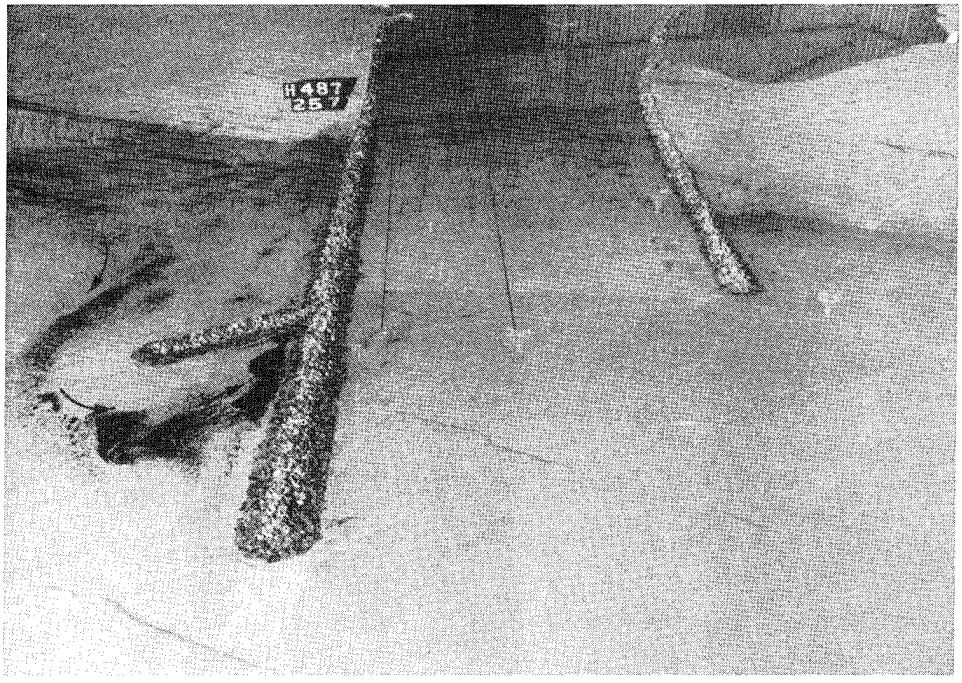

Figure 59. General movement and tracer material deposits resulting from 11-sec, 3.7-m (12.1-ft) wave from NNW for Plan 4 Rogue River; swl = +2.0 m (+6.6 ft)

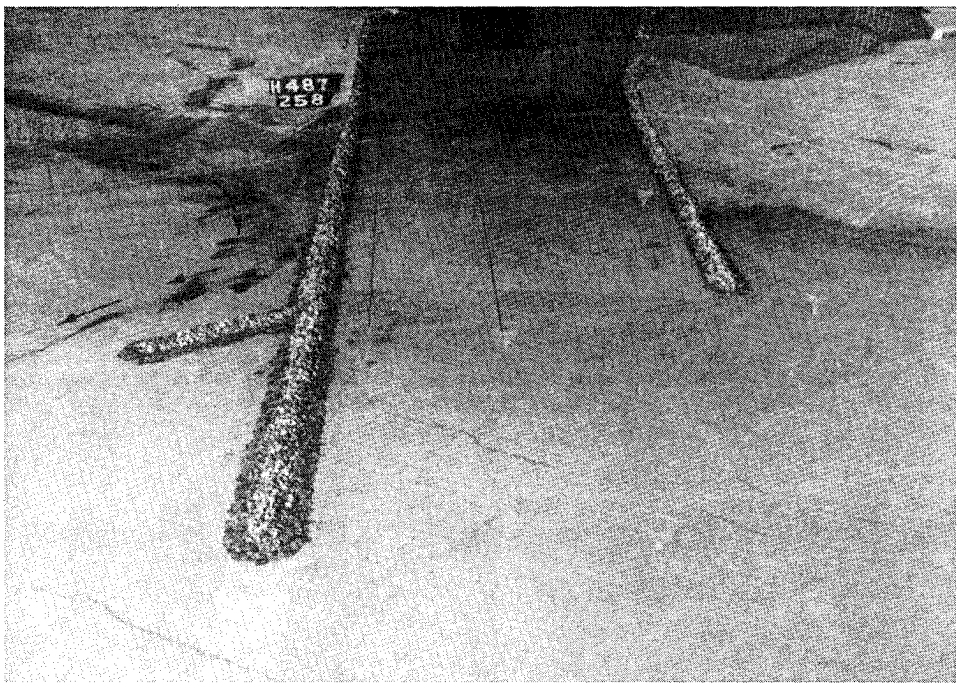

Figure 60. General movement and tracer material deposits resulting from 13-sec, 2.1-m (6.9-ft) wave from NNW for Plan 4 Rogue River; swl = +2.0 m (+6.6 ft)

Inspection of these figures indicates that, as the incident wave period increases (wave length increases, longshore current increases), the current patterns change from circular patterns depositing sediment in the jetty spur to the jetty system carrying sediment away from the jetty. Assuming the longer-period waves induce a stronger longshore current than waves of shorter period, this pattern progression is analogous to the evolution outlined previously for increasing current magnitude in the prototype.

For Plan 5E, Bottin (1982) presents photographs of the tracer study for four water levels (0.0, 0.5, 1.31, and 2.04 m (0, 1.5, 4.3, and 6.7 ft)), and a consistent wave condition of 11 sec, 3.66 m (12.0 ft) from the northwest (Figures 61-64). Tracer is introduced into the model from the north and at the channel entrance. Tracer initiated into the channel entrance is not tracer that flowed around the jetty tip. Incremental changing of the water level in the model effectively changes the jetty trunk length and the water depth at the structure. In the prototype, changes in water level are not incremental. The tide continuously changes the water level, and flow patterns are influenced by the tidal current. A fifth picture (Figure 65) is added to this photo essay showing deposition of the tracer for the 2.04-m (6.7-ft) water level and a longer period wave (13 sec) of less height (2.13 m (7.0 ft)). Changes in tracer deposition patterns can be seen for the various water levels, and can be compared with changes in water level in the prototype due to tide. Photographs from the physical model show that for the lower water levels, the spurs cause a clockwise and counterclockwise rotation off the spur tips. This correlates with

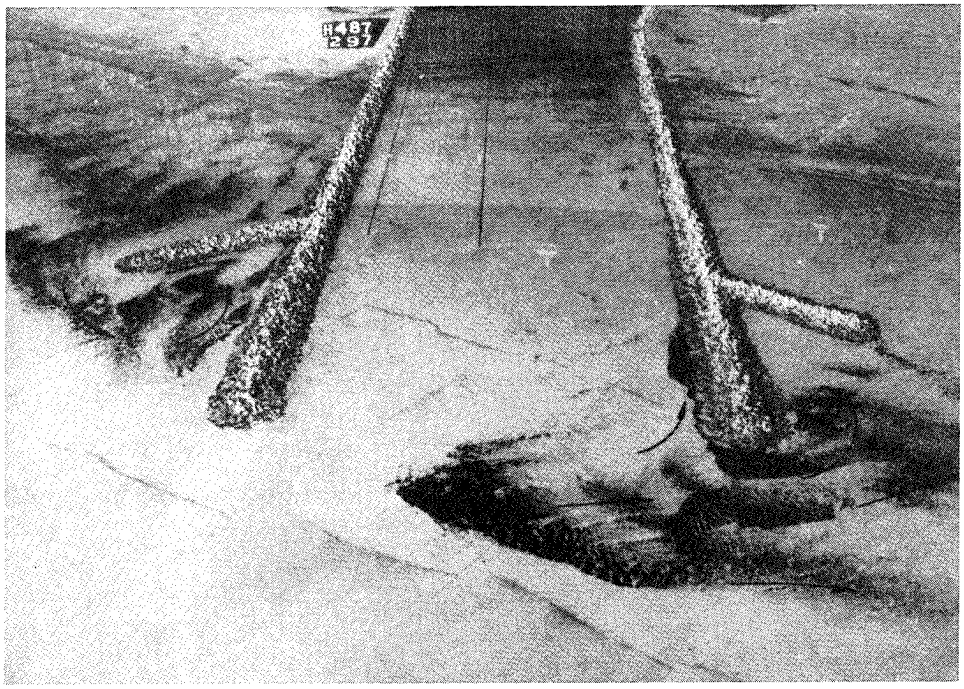

Figure 61. General movement and tracer material deposits resulting from 11-sec, 3.7-m (12.1-ft) wave from NNW for Plan 5 Rogue River; swl = 0.0 m (0.0 ft)

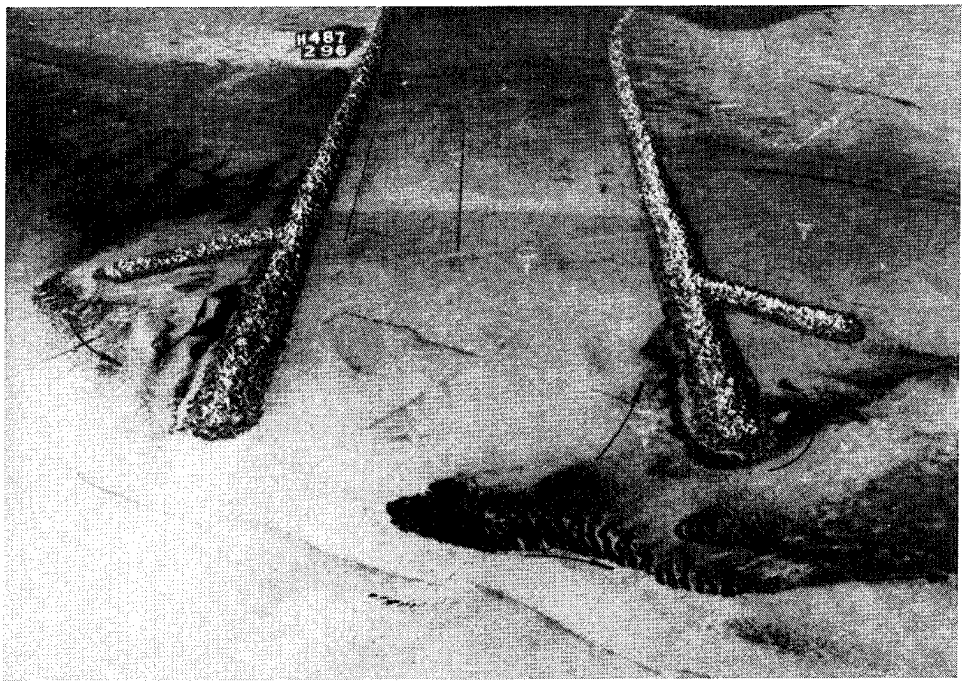

Figure 62. General movement and tracer material deposits resulting from 11-sec, 3.7-m (12.1-ft) wave from NNW for Plan 5 Rogue River; swl = +0.5 m (+1.6 ft)

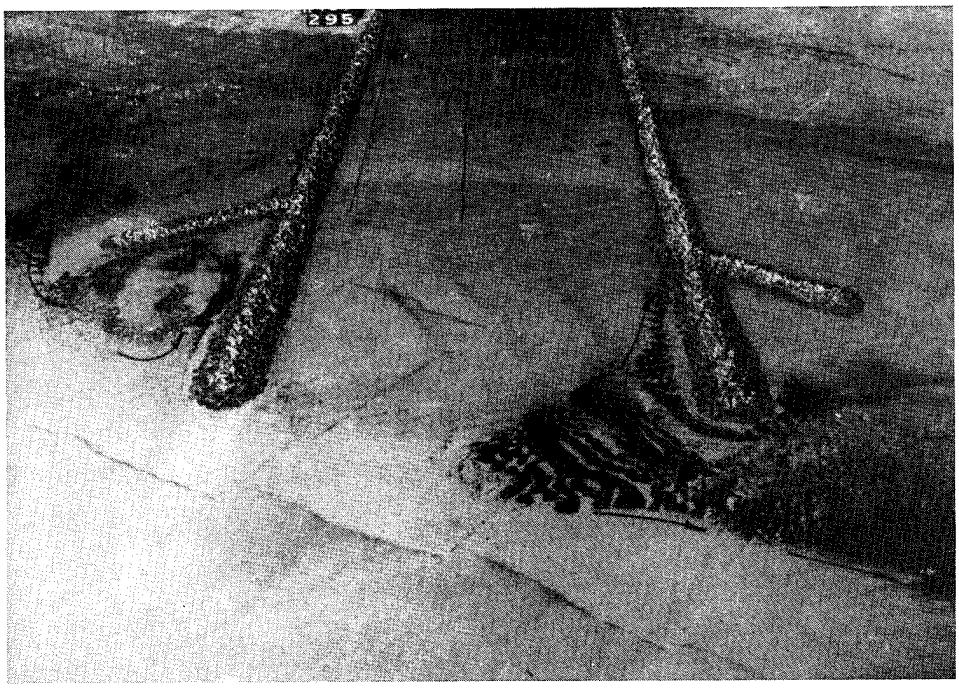

Figure 63. General movement and tracer material deposits resulting from 11-sec, 3.7-m (12.1-ft) wave from NNW for Plan 5 Rogue River; swl = +1.31 m (+4.3 ft)

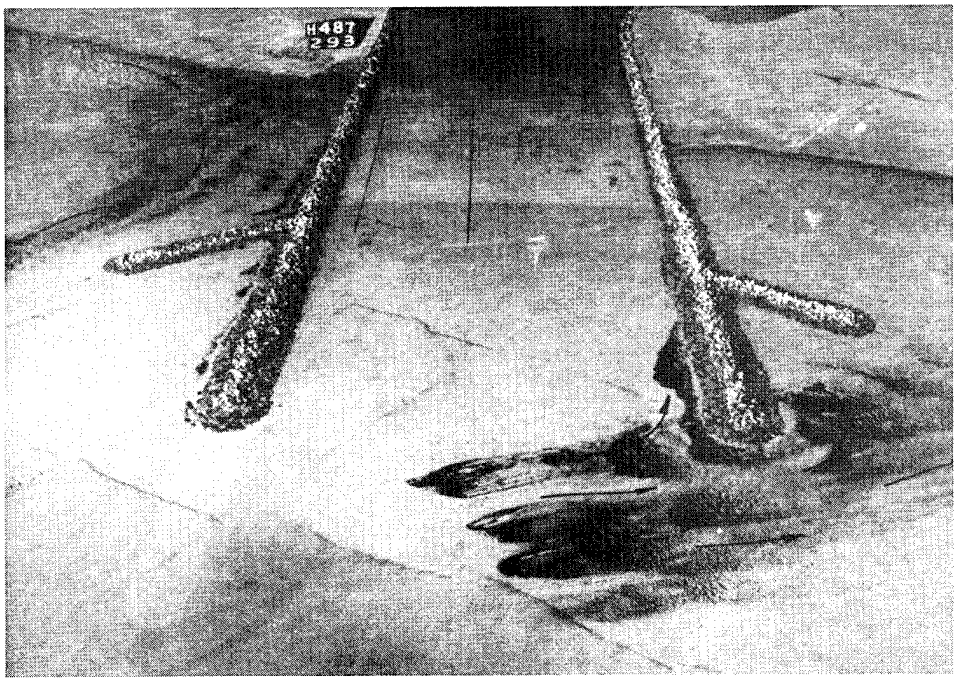

Figure 64. General movement and tracer material deposits resulting from 11-sec, 3.7-m (12.1-ft) wave from NNW for Plan 5 Rogue River; swl = +2.04 m (+6.6 ft)

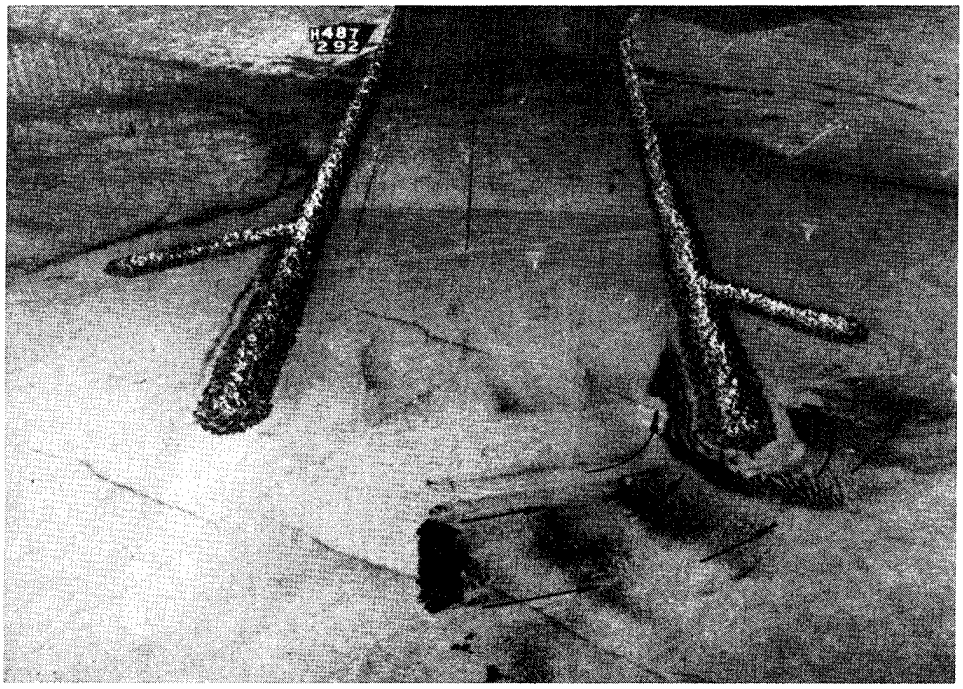

Figure 65. General movement and tracer material deposits resulting from 13-sec, 2.1-m (6.9-ft) wave from NNW for Plan 5 Rogue River; swl = +2.01 m (+6.6 ft)

prototype current patterns of September 1992 interval I low water slack tide. In the prototype, these rotations are more pronounced. This is possibly due to either the smaller angle between shore and the jetty, difference in water levels, difference in jetty trunk length, different wave conditions, or actual flows from the tides.

At the higher water levels, the spurs cause deposition in a line parallel to the spurs that is similar to the jet of water and flow patterns described for prototype September III and IV. A fifth picture added to the photo essay, with longer wave period, may be associated with an increase in current velocity over that of the 11-sec wave at the same water depth. This increase in current could be analogous with combining tidal and longshore currents in the prototype. The photograph shows a longer, more distinct jet of flow that parallels the spur, and is directed to the northwest. This depositional pattern is most like September interval III where the water level is higher than the water level during the September sampling interval I and tidal flows are offshore and to the south. Figure 66 also shows depositional patterns and plausible current patterns in the lee of the entire jetty system for waves out of the northwest. At the southern edge of the photographs on the downdrift side of the jetty system there is a deposit of sediment from a counterclockwise rotation. This rotation correlates with the hypothesis for the prototypes that the jetty system interrupts the flow and creates an edge effect that combines with the spurs to create a downdrift eddy.

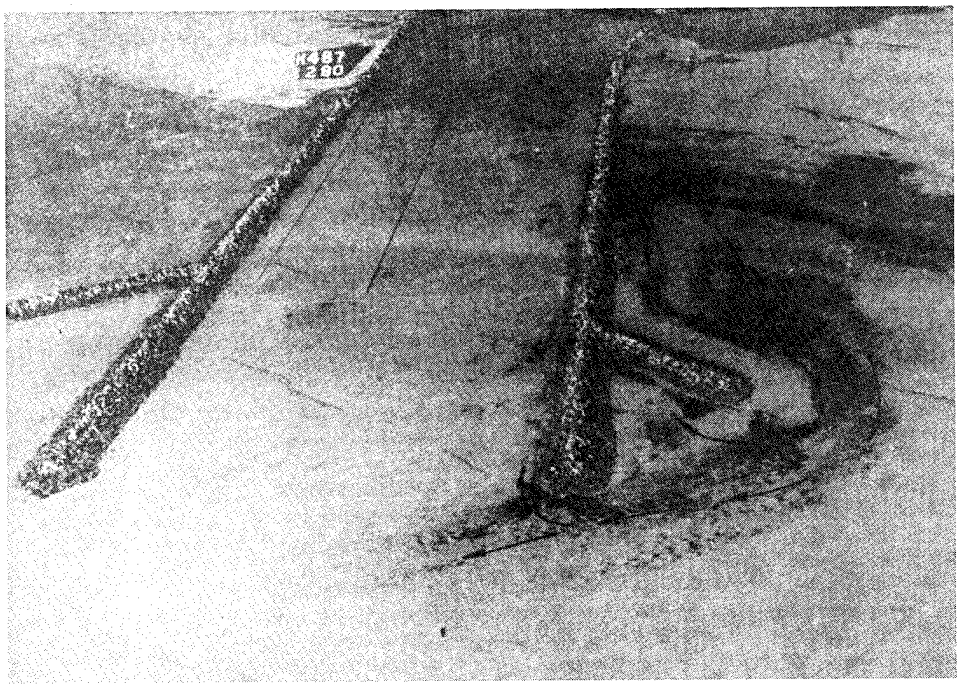

Figure 66. General movement and tracer material deposits resulting from 13-sec, 2.1-m (6.9-ft) wave from SSW for Plan 5 Rogue River; swl = +2.0 m (+6.6 ft)

For Plan 5, Figures 66 and 67 show samples of sediment deposition with arrows depicting plausible current patterns for various wave conditions from the south. Similar reverse image deposition patterns for southern wave approaches are evident for several different wave and water levels and jetty configurations in the physical model, as also were seen in the prototype for northern wave approach. These are the clockwise and counterclockwise rotations, the jets of water, and the "S" turns.

Inspection of all the photographs from the model tests suggests some physical parameters that influence the depositional trends. Longer spurs, deeper water, and acute angles between the shore and jetty make the development of these patterns more likely. It also appears that the water levels must be high enough, or the length of the jetty trunk must be long enough, to allow development of an offshore rip current that tightly hugs the jetty trunk (Perhaps this length is associated with the width of the breaker zone). Both the prototype and the model study suggest that the form the current takes past the spur tips appears to be a function of the current strength, and is associated directly with longer period waves and deeper water. As the current magnitude increases, the form evolves from a tight circular form to a jet pattern or large radius "S."

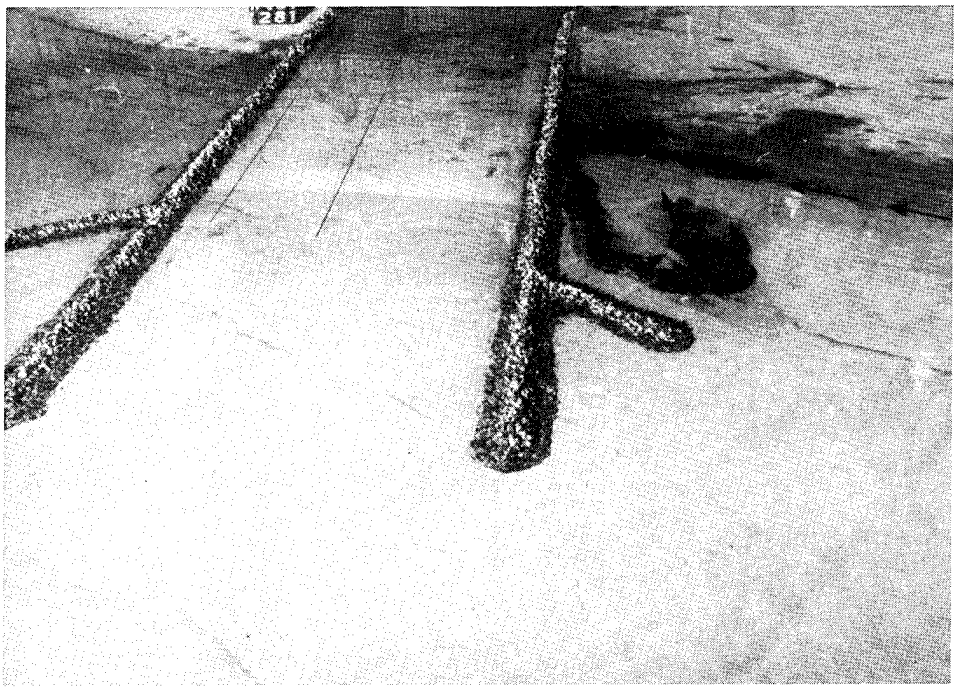

Figure 67. General movement and tracer material deposits resulting from 11-sec, 3.7-m (12.1-ft) wave from SSW for Plan 5 Rogue River; swl = +2.0 m (+6.6 ft)

Qualitative Comparison of Physical Model Test Results With Current Flow Patterns Identified in the Prototype

Prototype mosaics and physical model tracer studies for spur jetties exhibit strong correlations. The physical model tracer study repeatedly showed rotational and deflection patterns similar to those exhibited by the prototype. Those patterns can be related to relative changes in water levels, wave periods and heights, and tidal flows. Variances in the patterns are explained by differences in geometry and bathymetry, wave conditions, actual flowing tides in the prototype (both onshore/offshore and longshore components), and for the Rogue River model the angle between the jetty trunk and the shoreline is slightly different.

Figure 68 displays interpretations of flow patterns related to stages of the tide, or water levels for the physical model studies, and for the prototype current studies. Water levels for the physical model studies range from 0.0 m to 2.04 m (0.0 ft to 6.7 ft), and for the prototype range from 0.82 m to 1.74 m (2.7 ft to 5.7 ft). In the model study, the maximum water level and longest period wave is associated with the strongest current flow, and is aligned with the prototype test conducted during the strongest portion of the offshore tidal flow. Correlations can be seen in the results of the prototype and model as

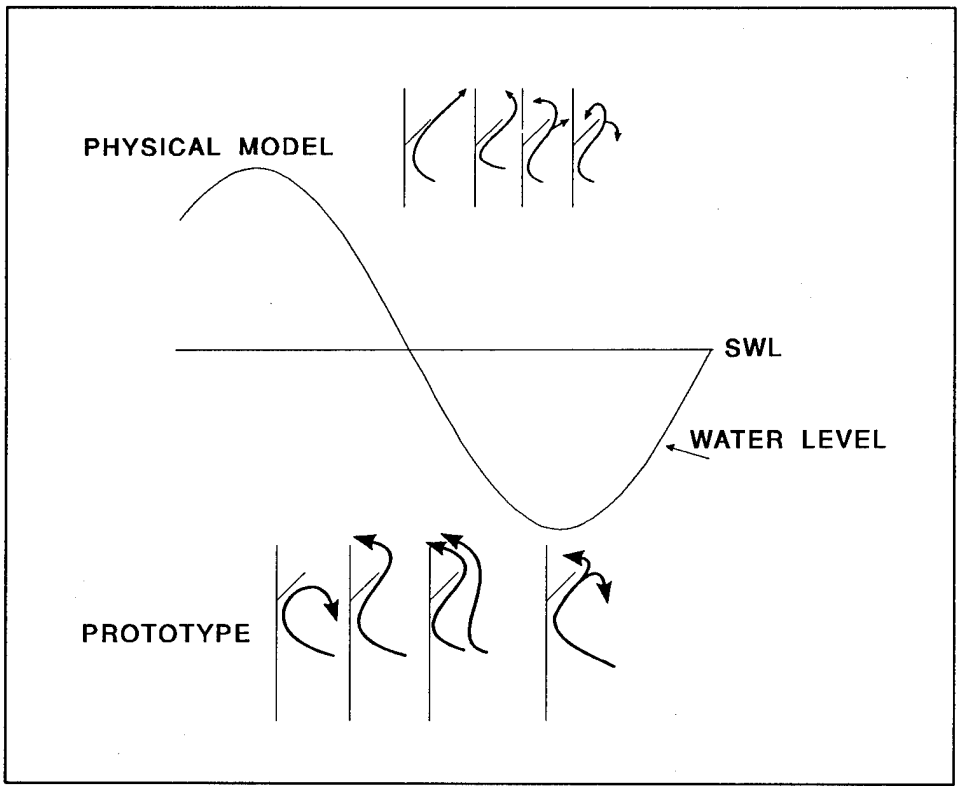

Figure 68. Flow patterns related to tide stages or water levels for the physical model and the prototype

current strengths increase. For all water levels the water flows strongly along the jetty trunk and turns tightly to parallel the spur until it reaches the spur tip where, for different conditions, the flow patterns differ. For the shallower water conditions the flow patterns for both studies are described by clockwise and counterclockwise rotational eddies. As water levels increase the flow pattern still hugs the jetty trunk and parallels the spur, but the clockwise rotation diminishes and the radius of the counterclockwise rotation increases until it extends around the jetty tip.

For the Siuslaw physical model study, the high-water, 11-sec waves showed the clockwise and counterclockwise rotation off the spurs. The 13-sec high-water condition resulted in the spur parallel flow jet deflecting water and sediment to the northwest. In the Rogue River model, both the 11- and 13-sec waves at high water created this flow pattern. For the more acute angle of the jetties and the longer wave period, the jet flow or "S" pattern is more likely to occur.

Factors that influence the deposition pattern include jetty geometry, water level (or, in effect, length of the jetty trunk), wave period and height, and tidal flow. In comparing prototype and model studies, some current and depositional pattern trends associated with physical parameters are apparent. For longer period waves, the spurs need to be longer to create the clockwise

rotation. The longer period waves induce stronger current flows and more defined current patterns. The acute angle between the jetty and the shore is more effective at deflecting the material away from the channel. Changes in longshore current strength initiate changes in current/depositional patterns. The longer period waves and longer spurs are more effective at inducing a longer midsection of the "S"-shaped current/depositional pattern, which deflects the sediment further from the jetty entrance. Both the longshore and the onshore/offshore component of the tides combine with the wave-induced currents to assist current pattern formation. During a flood tide, the onshore component aids in the clockwise rotation. The longshore component is to the north on a flood tide and this also assists in developing the clockwise rotation. Because the physical model had no tide, the clockwise rotation was not prevalent. In the prototype, during an ebb tide, the "S" pattern is assisted in carrying material offshore around the jetty tips. Additionally, the alongshore component flows to the south and aids in the development of the "S" pattern.

During calmer wave conditions in the prototype and in the physical model, currents and tracer flowed along the jetty trunk and spur, past the jetty tip, and directly into the channel. Therefore, for the spur jetty systems to be effective, the energy in the wave field must be high to create strong longshore currents.

Once the geometry is set, changes in the current/depositional patterns appear to be associated with the velocity of the longshore current and evolve from a circular to an "S" pattern. Current in the prototype is a combination of wave, wind, and tide. In the model, the current is due to waves only. Figure 69 illustrates (in order of increasing current velocity) a simplistic-qualitative interpretation of the current/depositional pattern evolution process for a jetty trunk oriented perpendicular to shore. It is assumed that the jetty trunk is sufficiently long to allow development of the rip current along the jetty trunk and spur.

Stage one is a result of the weakest of currents. The longshore current is turned offshore by the jetty trunk and spur and a rip develops that tightly hugs the jetty. The rip current is weak and is turned back toward shore, creating an eddy effect. The pattern is elliptic in shape. Curvature in the onshore/offshore direction a is constant and is a function of the geometry of the shore, trunk, and spur. The longshore dimension b is variable and is a function of current velocity. In this stage a is likely to be less than b.

In stages two and three, b increases as the current velocity and replaces a as the larger dimension. Eventually the current velocity reaches a magnitude at which b goes to infinity and the elliptical shape begins to uncoil. This is analogous to a tightly coiled hose. As the flow in the hose increases, the tight radius cannot be maintained and the hose unwraps. The unwrapping process begins with the end of the hose and progresses until the pressure is relieved or it conforms to a barrier. For the current pattern, the barrier is the spur jetty.

In the fourth stage, the current splits and an offshore component of flow develops with some radius of curvature r.

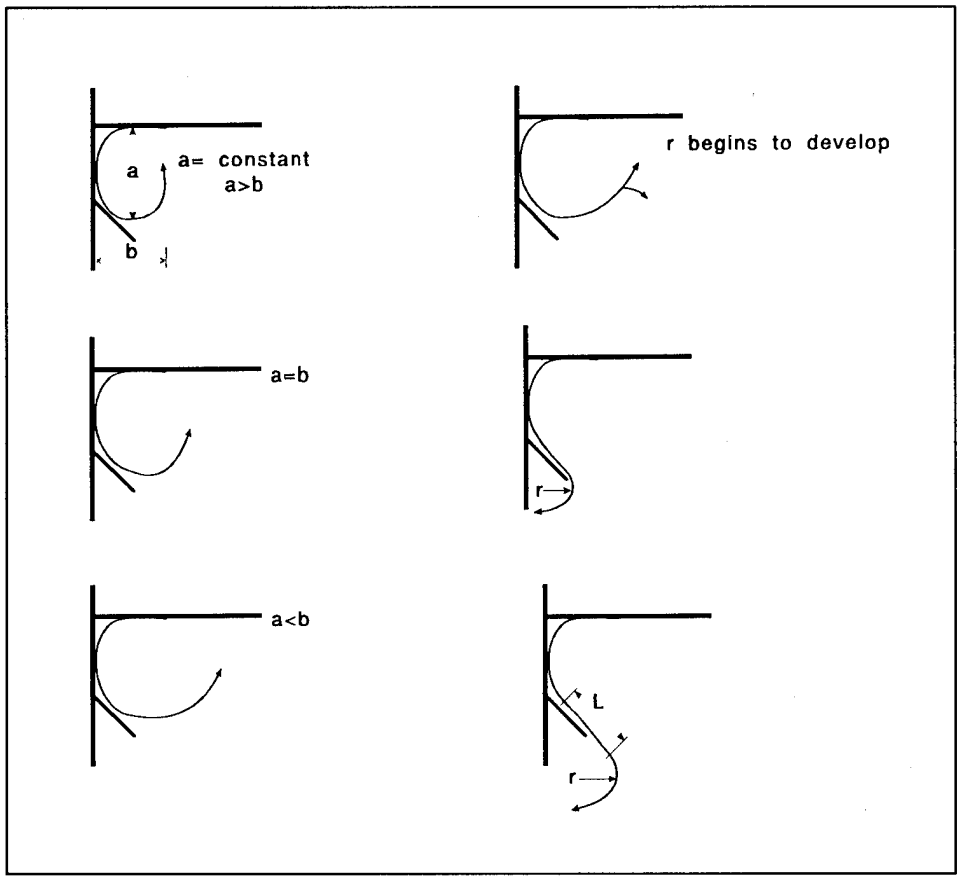

Figure 69. Interpretation of the evolution of the current/depositional pattern associated with increasing longshore current

In the fifth stage, the pattern resembles the tight "S" turns of a racetrack. The curvature of the elliptical shape has unwrapped and the "S" formation of the current pattern is confined by the jetty structure. The "S" formation is comprised of two arcs of radius *a* and *r* and midsectional line of length *L*, where *L* is a function of the length of the spur and the current velocity. The onshore component of the current split has diminished and the radius of the offshore component *r* has increased.

In stage six, *r* and *L* increase but are limited by processes outside the influence of the jetties.

This evolution process is based mainly on the trends identified in the model study, and can only be supported by the prototype for ebb tidal flows because flood tides were not documented in this study. In the prototype, during flood tides it is likely that flow patterns resemble the weaker longshore current conditions. Photographs of dye patterns and sediment plume patterns for flood tides indicate the flow pattern is most like stages one and two of the evolution described above.

6 Conclusions and Recommendations

Conclusions

Quantitative information on local currents in the nearshore region is very important for the planning, design, construction, and evaluation of coastal structures. Many methods exist to measure currents, including surface floats and/or dyes and arrays of stationary-mounted current meters; however, very few can satisfactorily perform the function of measuring near-bottom currents in adverse and dynamic nearshore environments.

The Airborne Coastal Current Measurement system proved to be an effective method for obtaining qualitative spatial understanding of bottom currents in hostile environments where boat operation is dangerous or where quick mobility is necessary. The system utilizes a helicopter as the support platform. A meter assembly including an electromagnetic current meter, an anchor, and a subsurface buoy is suspended by cable from the helicopter for data sampling approximately 1 m above the seabed. Current information is collected at several locations within a short period of time. Data collected are reduced to resultant current vectors and are presented as a sequence of vectors discrete in time and location. These vectors are plotted to create a mosaic from which local current patterns can be inferred.

The system was used at Siuslaw River, OR, to document currents near the entrance channel spur jetties. The system performed very well and met all of the study's requirements, sampling data at approximately 18 locations within an hour, operating in depths up to 7 m (23 ft), surviving in waves as high as 4 m (13 ft), and measuring currents over 1.6 m/s (5.2 ft/s). Capabilities of the system would have allowed it to measure currents as strong as 3 m/s (9.8 ft/s), and wave height and depth limitations were only constrained by the length of the cable used for the particular study. Data collected during the prototype field study were used to develop current vector mosaics and create visual interpretations of localized currents around spur jetties. Dye studies, aerial photos, and visual observations were used in support of the current information to develop the interpretations of the current patterns. For this site, on a qualitative level, it was determined that bottom currents bear close resemblance to

surface currents. Interpretations of the prototype current patterns were qualitatively compared with current-induced sediment tracer patterns documented in physical model testing completed prior to construction modifications to the existing entrance channel structures.

The first use of the system was at Siuslaw River, OR, in July 1990. Wind conditions during the study were very strong, directly out of the north. Current patterns during this period reflected a wind-dominated regime rather than a wave-dominated regime. From the vector mosaics of this study, no circulation patterns around the jetty spur were apparent. Although this prototype study did document conditions that occur at the Siuslaw River, the results were not compared with the physical model study due to the differences in the forcing climates.

An additional study was conducted at the same site during a 2-week period in September 1992, and included ground truthing with a stationary current meter located near the study site to substantiate airborne current measurements. Measurements taken by both meters compared closely. Averaged velocities for each of the meters differed by only 2 cm/s (0.79 in./s) in magnitude and 1 deg (0.02 rad) in direction. The variance is within the combined accuracy of the two instruments.

Four sampling intervals were conducted during the 2-week period. Two sampling intervals covered the high and low slack tidal periods and another two intervals were conducted during the ebb tide. Deepwater wave heights ranged from 0.8 to 2.2 m (2.6 to 7.2 ft) with breaker heights at the site of up to 3 m (9.8 ft), and the peak wave periods during the sampling intervals were 7 to 9 sec. The vector mosaics of these intervals captured circulation patterns induced by the alongshore current flowing by the spur jetties. Sampling interval I was conducted during the slack/low tide, and the current pattern interpretation displayed a split in the current at the end of the spur with a portion of the current turning toward shore and a portion of the current turning offshore. Sampling interval II was conducted during the slack/high tide and showed an eddy forming past the spur that turned toward the shore. Sampling intervals III and IV were conducted during the ebb tide. Both current pattern interpretations indicated the flow turned offshore past the jetty tip and then flowed parallel to the coast, and passed offshore of the jetty tips.

Comparisons revealed that, under certain conditions, the prototype structures deflected material away from the entrance channel as had been predicted by the physical model tests. Comparable prototype current and model sediment depositional patterns emerged. For all prototype conditions at the jetties, a rip current hugged very closely to the jetty trunk and spur. At the tip of the spur, different flow patterns occurred. These patterns can generally be described as circular eddies or "S"-shaped. The same patterns occurred in the models when the water depths were deep enough to allow a rip current to occur along the jetty. Prototype testing indicates that the current patterns take different forms for different strength alongshore currents and stages of the tide. For the model test, the different forms were also associated with the strength

of the alongshore current and were altered by changing water levels and wave conditions. Similarities exist between model and prototype current patterns for relative water levels and alongshore current strengths.

It is hypothesized for the prototype that the tidal flows combine with the longshore currents, depending upon flow direction, to either increase or decrease the longshore current for the ebbing and flooding tides, respectively.

Additionally, the different water levels due to the tides, in effect, change the length of the jetty trunk and the depth of water near the jetty spur. This may also influence the strength of the current and alter the current patterns near the jetties.

These field tests were conducted during high wave energy periods. During lower energy periods, different current patterns and less sediment movement are likely. Prototype dye studies conducted previously during very calm conditions indicated that, during an incoming tide, the current wraps around the jetty tip and flows directly into the channel. The physical model study indicated similar occurrences for the lower wave conditions.

Based on the model tests and field studies, a simplistic interpretation of the evolution process that the current patterns experience was developed. The interpretation assumes that a rip current exists along the jetty trunk and spur, and relates the changes in the current pattern past the spur tip to the current strength. The evolution process begins with the current forming a circular eddy that is deflected back to shore. As the current increases in strength the circular eddy uncoils and the flow resembles an "S" shape with larger radius curves and a longer midsection for stronger currents.

Recommendations

System operation

During operation of the Airborne Coastal Current Measurement system, communicating sampling locations to the helicopter crew and allowing the freedom to quickly alter the sampling pattern was difficult. The range pole method and following dye packets gave adequate results; however, using latitude/longitude coordinates and the helicopter's positioning equipment to horizontally position the helicopter for sampling may be another alternative to provide more uniform coverage of the study area.

The Airborne Coastal Current Measurement system could be used to measure waves outside the surf zone in order to estimate deepwater wave heights and periods for association with current patterns.

Spur jetty research

Further study of the spur jetties should investigate relationships among wave period and height, water level, and tidal flows, and the distance between shoreline and spur location, length of spur, and distance to jetty tip. The investigation should also evaluate whether tidal flows outside the jetties affect alongshore current velocities. Also to be considered is whether the direction the current pattern takes past the spur jetty tip is related to the rip current along the spur ending within or outside the surf zone.

References

Birkemeier, W. A., Hathaway, K. K., Smith, J. M., Baron, C. F., and Leffler, M. W. (1991). "DELILAH experiment: Investigator's summary report." Internal Working Document, Coastal Engineering Research Center, U.S. Army Engineer Waterway Experiment Station, Vicksburg, MS.

Bottin, R. R., Jr. (1981). "Siuslaw River Jetty extension study, Oregon." *Letter Report, September 1981*, Hydraulics Laboratory, U.S. Army Engineer Waterways Experiment Station, Vicksburg, MS.

_____. (1982). "Design for flood control, wave protection, and prevention of shoaling, Rogue River, Oregon; hydraulic model investigation," Technical Report HL-82-18, Hydraulics Laboratory, U.S. Army Engineer Waterways Experiment Station, Vicksburg, MS.

Chu, Y., and Nersesian, G. K. (1992). "Scour hole development and stabilization at Shinnecock and Moriches Inlets, New York." *Proceedings of Coastal Engineering Practice '92*. American Society of Civil Engineers, New York, 571-97.

Coastal Engineering Research Center. (1990). "Los Angeles and Long Beach Harbors Model Enhancement Program: Three-dimensional numerical model testing of tidal circulation," Technical Report CERC-90-16, Coastal Engineering Research Center, U.S. Army Engineer Waterways Experiment Station, Vicksburg, MS.

Dodd, N., Oltman-Shay, J., and Thornton, E. B. (1992). "Shear instabilities in the longshore current: A comparison of observation and theory," *Journal of Physical Oceanography* 22, 62-82.

Guza, R. T., and Thornton, E. B. (1978). "Variability of longshore currents." *Proceedings of 16th Coastal Engineering Conference*. Vol 1, American Society of Civil Engineers, New York, 756-75.

_____. (1980). "Local and shoaled comparisons of sea surface elevations, pressure, and velocities," *Journal of Geophysical Research* 85 (C3), 1524-30.

Guza, R. T., Thornton, E. B., and Christensen, N., Jr. (1986). "Observations of steady longshore currents in the surf zone," *Journal of Physical Oceanography* 16, 1959-69.

Hands, E. B. (1987). "Potential of seabed drifters for nearshore circulation studies." *Proceedings of Coastal Sediments '87.* Vol 1, American Society of Civil Engineers, New York, 865-80.

Hartman, G. L. (1977). "Jetty effects at the Siuslaw and Rogue Rivers." *Proceedings of Coastal Sediments '77.* Vol 1, American Society of Civil Engineers, New York, 287-304.

Horikawa, K., and Sasaki, T. (1972). "Field observations of nearshore current system." *Proceedings of the 13th Coastal Engineering Conference.* Vol 1, American Society of Civil Engineers, New York, 635-52.

Huntley, D. A., and Nummedal, D. (1978). "Velocity and stress measurements in a tidal inlet." *Proceedings of the 16th Coastal Engineering Conference.* Vol 2, American Society of Civil Engineers, New York, 1320-35.

InterOcean Systems, Inc. (1987). *S4 current meter user's manual.* InterOcean Systems, Inc., San Diego, CA.

Knoth, J. S., and Nummedal, D. (1977). "Longshore sediment transport using fluorescent tracer." *Proceedings of Coastal Sediments '77.* American Society of Civil Engineers, New York, 383-98.

Kraus, N. C., Isobe, M., Igarashi, H., Sasaki, T. O., and Horikawa, K. (1982). "Field experiments on longshore sand transport in the surf zone." *Proceedings of 18th Coastal Engineering Conference.* Vol 2, American Society of Civil Engineers, New York, 969-87.

McGehee, D. D., McKinney, J. P., and Dickey, M. S. (1989). "Los Angeles and Long Beach Harbors Model Enhancement Program; Tidal circulation prototype data collection effort; Vol I, Main text and Appendices A-C," Technical Report CERC-89-17, Coastal Engineering Research Center, U.S. Army Engineer Waterways Experiment Station, Vicksburg, MS.

McLellan, T. N., and Burke, C. E. "Site selection for nearshore berm construction, South Padre Island, Texas," in preparation, U.S. Army Engineer Waterways Experiment Station, Vicksburg, MS.

Mimura, N. (1988). "Measurement and observation of current." *Nearshore dynamics and coastal processes.* Edited by K. Horikawa, University of Tokyo Press, Japan, 423-32.

National Oceanic and Atmospheric Administration. (1990, 1992). "West coast of North and South America including Hawaiian Islands." *Tide Tables, 1990, High and Low Water Predictions,* U.S. Department of Commerce, Washington, DC, 827-29.

Pollock, C. B. "Helicopter-borne nearshore survey system, a valuable tool in difficult survey areas," in press, *Journal of Coastal Research.*

Pollock, C. B., Chesser, S., McGehee, D. D., and Livingston, C. R. "Siuslaw River Spur Jetties," in preparation, Coastal Engineering Research Center, U.S. Army Engineer Waterways Experiment Station, Vicksburg, MS.

Roberson, J. A., and Crowe, C. T. (1965). *Engineering fluid mechanics.* Houghton Mifflin Company, Boston, MA, 86-7.

Rosati, J. D., Gingerich, K. J., and Kraus, N. C. (1990). "SUPERDUCK surf zone sand transport experiment," Technical Report CERC-90-10, Coastal Engineering Research Center, U.S. Army Engineer Waterways Experiment Station, Vicksburg, MS.

Sallenger, A. H., Jr., Howard, P. C., Fletcher, C. H., III, and Howd, P. A. (1983). "A system for measuring bottom profile, waves, and currents in the high-energy nearshore environment," *Journal of Marine Geology* 51, 63-76.

Sasaki, T., and Sakuramoto, H. (1984). "Effect of rip current barrier on harbor shoaling." *Proceedings of 19th Coastal Engineering Conference.* American Society of Civil Engineers, New York, 2091-107.

Sasaki, T., Horikawa, K., and Hotta, S. (1976). "Nearshore current on a gently sloping beach." *Proceedings of 15th Coastal Engineering Conference.* American Society of Civil Engineers, New York, 626-44.

Smith, A. W. (1989). "Escape head vortices from groynes," *Shore and Beach,* July 1989, 32-3.

Thornton, E. B., and Guza, R. T. (1986). "Surf zone longshore currents and random waves: Field data and models," *Journal of Physical Oceanography* 16, 1165-78.

U.S. Army Engineer District, Portland. (1986). "Condition survey, Siuslaw River, Oregon Entrance. September 30, 1986," *Plate SL-1-396,* Operations Division, Portland, OR.

Scripps Institution of Oceanography. (1990). "Coastal Data Information Program, Monthly Report, July 1990," Monthly Summary Report No. 173, SIO REF. 90-25, University of California, San Diego (sponsored by U.S. Army Engineer Waterways Experiment Station and State of California Department of Boating and Waterways).

Scripps Institution of Oceanography. (1990). "Coastal Data Information Program, Monthly Report, September 1992," Monthly Summary Report No. 199, SIO REF. 92-28, University of California, San Diego (sponsored by U.S. Army Engineer Waterways Experiment Station and State of California Department of Boating and Waterways).

Whitford, D. J. (1988). "Wind and wave forcing of longshore currents across a barred beach," *Ph.D. diss.*, Naval Postgraduate School, Monterey, CA.

Whitford, D. J., and Thornton, E. B. (1988). "Longshore currents forcing at a barred beach." *Proceedings of 21st Coastal Engineering Conference.* No. 21, Vol 1, 77-90.

Wright, L. D., Boon, J. D., Kim, S. C., and List, J. H. (1991). "Modes of cross-shore sediment transport on the shoreface of the middle Atlantic Bight," *Marine Geology,* 96, 19-51.

Wright, L. D., Sonu, C. J., and Kielhorn, W. V. (1972). "Water-mass stratification and bed form characteristics in East Pass, Destin, Florida," *Marine Geology* 12, 43-58.

Appendix A
Data Analysis Programs

```
C*****************************************************************
C*                          VELDIR                               *
C*  This program calculates the mean velocity and an average direc- *
C*  tion (from the mean Northing and Easting current magnitudes)    *
C*  output from the S4 Current Meter.  The ASCII, Hexadecimal data  *
C*  must first be resolved and converted by using the "READS4.EXE"  *
C*  program (written in PASCAL).  Assuming data collection of 2 Hz  *
C*  (i.e. one sample every 1/2 second), this program will read a    *
C*  data set up to 12,000 samples or 1 hour and 40 minutes.         *
C*  Written 14 August 1992 by Greg Williams.                        *
C*****************************************************************
$Large
      Dimension depth(12000),north(12000),east(12000)
      Dimension d(50,300),n(50,300),e(50,300),avgstoptime(50)
      Dimension startavg(50),endavg(50),avgstarttime(50)
      Dimension lastgrppt(50),avgd(50),avgn(50),avge(50)
      Dimension grpstarttime(50),grpstoptime(50)
      Real depth,north,east,depthresh,d,n,e
      Real sumd,sume,sumn,sumcurr,avgcurr,avgd,avge,avgn,a
      Real ainitial,theta,tntheta
      Integer nofpts,npt,ngppt,ngp,avgstoptime,avgstarttime,lastgrppt
      Integer nofgrppts,endavg,startavg,grpstarttime,grpstoptime
      Integer snggpt, ngppts
C*****************************************************************
C*                       Variable Definitions                    *
C*                       ====================                    *
C*   -depth(x),north(x),east(x)-- 1-D arrays of READS4.EXE output  *
C*      data.  Raw data for input to this program.               *
C*   -d(x,y),n(x,y),e(x,y)-- 2-D arrays of the depth, north and east*
C*      currents after separating using the depth threshold where x *
C*      is Group Number and y is Point Number within the group.  *
C*   -avgstoptime(x),avgstarttime(x)--  Overall data time step at  *
C*      which averaging for calcualtions is stopped/started.     *
C*   -startavg(x),endavg(x)-- Number of points from 1st depthresh  *
C*      to first depth peak (where averaging begins) and number of  *
C*      points from last depth peak to last depthresh (where averag-*
C*      ing ends)                                                *
C*   -lastgrppt(x)-- Number of last group point (or number of points*
C*      within each group)                                       *
C*   -avgd(x),avgn(x),avge(x)-- Average of depth, north and east   *
C*      between the first and last depth peak                    *
C*   -grpstarttime(x),grpstoptime(x)-- Overall data time step at   *
C*      which each "group" was started ie. when depth thresholds   *
C*      crossed.                                                 *
C*   -ainitial-- Raw angle calculated from arctan(East curr/North  *
C*      curr).  The signs of a, east and north determines the    *
C*      azimuth (see equations in program)                       *
C*   -a-- Converted ainitial from radians to degrees             *
C*   -theta-- Azimuth determined from a, north and east as described*
C*      in Section 6 of the S4 manual.                           *
C*   -tntheta-- Angle corrected to true north for Siuslaw River    *
C*      entrance, +18.2 degrees (1992)                           *
C*****************************************************************
      Character*25 infile,outfile
      Character*70 line
      Write(*,*)'Please enter the input filename'
      read(*,90)infile
  90  format(A25)
      Write(*,*)'Please enter the output filename'
      read(*,90)outfile
```

```
      open(2,file=infile,status='old')
      open(3,file=outfile,status='unknown')
      write(3,897)
      write(3,899)
C*****Read the column titles
      read(2,91,end=95)line
  91  format(A70)
C*****Read data from "READS4.EXE" program in the format depth (meters),
C*****Northing and Easting
  95  do 100 i=1,12000
      read(2,*,end=150)depth(i),north(i),east(i)
 100  continue
 150  nofpts=i-1
      npt=0
      Write(*,*)'Please enter the depth threshold (f3.1)'
      read(*,92)depthresh
  92  format(f3.1)
C*****Using depth threshold criteria, put desired samples into groups
      do 200 ngp=1,50
           ngppt=0
  50       npt=npt+1
           if(npt.gt.nofpts)then
           goto 250
           endif
           if(depth(npt).ge.depthresh)then
              ngppt=ngppt+1
              d(ngp,ngppt)=depth(npt)
              n(ngp,ngppt)=north(npt)
              e(ngp,ngppt)=east(npt)
c              write(*,*)ngp, ngppt, d(ngp,ngppt), n(ngp,ngppt),
c     *e(ngp,ngppt)
           else
              goto 50
           endif
           if(depth(npt+1).lt.depthresh)then
              grpstoptime(ngp)=npt
              grpstarttime(ngp)=(npt-ngppt)+1
              lastgrppt(ngp)=ngppt
c              write(*,*)'Group Number=',ngp
c              write(*,*)'Number of Group Points=',ngppt
c      write(*,*)'grpStarttime=',grpstarttime(ngp),'grpStoptime=',
c     *grpstoptime(ngp)
              goto 200
           else
              goto 50
           endif
 200  continue
C*****Determine the starting and ending points for averaging by checking
C     for slope changes in the depth time series
c      write(*,*)'NUMBER OF GROUPS=',ngp-1
 250  ngpf=ngp-1
      do 400 j=1,ngpf
         sngppt=0
         do 300 sngppt=1,50
            if(d(j,sngppt).lt.d(j,sngppt+1))then
            goto 300
            elseif(d(j,sngppt).ge.d(j,sngppt+1))then
               startavg(j)=sngppt
               avgstarttime(j)=grpstarttime(j)+sngppt-1
c               write(*,*)'startavg(j)=',startavg(j)
```

```
c                write(*,*)'grpstarttime(j)=',grpstarttime(j)
c                write(*,*)'avgstarttime(j)=',avgstarttime(j)
                goto 400
              endif
 300  continue
 400  continue
      do 600 l=1,ngpf
      ngppts=lastgrppt(l)
 501        if(d(l,ngppts).lt.d(l,ngppts-1))then
            ngppts=ngppts-1
            goto 501
            elseif(d(l,ngppts).ge.d(l,ngppts-1))then
                 endavg(l)=lastgrppt(l)-ngppts-1
                 avgstoptime(l)=grpstoptime(l)-(lastgrppt(l)-ngppts)
c                 write(*,*)'endavg(l)=',endavg(l)
c                 write(*,*)'grpstoptime(l)=',grpstoptime(l)
c                 write(*,*)'avgstoptime(l)=',avgstoptime(l)
            endif
 600  continue
C*****Calculate average depth, northing and easting for each group
c      open(4,file='test.out',status='new')
      sumd=0
      sumn=0
      sume=0
      sumcurr=0
      do 700 igrp=1,ngpf
      nofgrppts=(avgstoptime(igrp)-avgstarttime(igrp))+1
      enddo=startavg(igrp)+nofgrppts-1
c      write(*,*)startavg(igrp),enddo
        do 800 jgrp=startavg(igrp),enddo
           sumd=sumd+d(igrp,jgrp)
           sumn=sumn+n(igrp,jgrp)
           sume=sume+e(igrp,jgrp)
           sumcurr=sumcurr+(n(igrp,jgrp)**2+e(igrp,jgrp)**2)**0.5
c           write(4,975)igrp, jgrp, sumd, sumn, sume, sumcurr
 800  continue
           avgcurr=sumcurr/nofgrppts
           avgd(igrp)=sumd/nofgrppts
           avgn(igrp)=sumn/nofgrppts
           avge(igrp)=sume/nofgrppts
c           write(*,*)'nofgrppts for avg=',nofgrppts
           ainitial=atan(avge(igrp)/avgn(igrp))
           a=ainitial*180/3.1416
               if(a.gt.0.0.and.avge(igrp).gt.0.0)then
               theta=a
               elseif(a.lt.0.0.and.avgn(igrp).gt.0.0)then
               theta=a+360.0
               elseif(avgn(igrp).lt.0.0.or.avge(igrp).lt.0.0)then
               theta=a+180.0
               endif
C*****Adjust direction to true north...add 18.2 degrees
         tntheta=theta+18.2
         write(3,900)avgstarttime(igrp),avgstoptime(igrp),
     *avgd(igrp),avgcurr,tntheta,avgn(igrp),avge(igrp)
      sumd=0
      sumn=0
      sume=0
      sumcurr=0
 700  continue
 897  format(' ',2x,'Avg Time (s)',32x,'Theta')
```

```
  899  format(' ',1x,'Start   End',5x,'Avg Depth',4x,'Avg Vel',3x,
     *'(w.r.t. TN)',3x,'Avg North',3x,'Avg East')
  900  format(' ',2i8,2x,f9.6,3x,f8.2,4x,f8.2,4x,f8.2,3x,f8.2)
  950  format(' ',2x,'Grp Num',1x,'Pt Num','Depth','North','East')
  951  format(' ',i4,3x,i5,3x,f5.2,3x,2f9.2)
c 975  format(' ',2i5,4f15.2)
      stop
      end
```

```
C*********************************************************************
C*             VELDIR90 adjusted for Jul 90 data set                 *
C*  This program calculates the mean velocity and an average direc- *
C*  tion (from the mean Northing and Easting current magnitudes)     *
C*  output from the S4 Current Meter.  The ASCII, Hexadecimal data   *
C*  must first be resolved and converted by using the "READS4.EXE"   *
C*  program (written in PASCAL).  Assuming data collection of 2 Hz   *
C*  (i.e. one sample every 1/2 second), this program will read a     *
C*  data set up to 12,000 samples or 1 hour and 40 minutes.          *
C*  Written 14 August 1992 by Greg Williams.                         *
C*********************************************************************
$Large
      Dimension depth(12000),north(12000),east(12000)
      Dimension d(50,300),n(50,300),e(50,300),avgstoptime(50)
      Dimension startavg(50),endavg(50),avgstarttime(50)
      Dimension lastgrppt(50),avgd(50),avgn(50),avge(50)
      Dimension grpstarttime(50),grpstoptime(50)
      Real depth,north,east,depthresh,d,n,e
      Real sumd,sume,sumn,sumcurr,avgcurr,avgd,avge,avgn,a
      Real ainitial,theta,tntheta
      Integer nofpts,npt,ngppt,ngp,avgstoptime,avgstarttime,lastgrppt
      Integer nofgrppts,endavg,startavg,grpstarttime,grpstoptime
      Integer snggpt, ngppts
C*********************************************************************
C*                        Variable Definitions                       *
C*                        ====================                       *
C*   -depth(x),north(x),east(x)-- 1-D arrays of READS4.EXE output    *
C*      data.  Raw data for input to this program.                    *
C*   -d(x,y),n(x,y),e(x,y)-- 2-D arrays of the depth, north and east*
C*      currents after separating using the depth threshold where x  *
C*      is Group Number and y is Point Number within the group.       *
C*   -avgstoptime(x),avgstarttime(x)--  Overall data time step at     *
C*      which averaging for calcualtions is stopped/started.          *
C*   -startavg(x),endavg(x)-- Number of points from 1st depthresh     *
C*      to first depth peak (where averaging begins) and number of   *
C*      points from last depth peak to last depthresh (where averag-*
C*      ing ends)                                                     *
C*   -lastgrppt(x)-- Number of last group point (or number of points*
C*      within each group)                                            *
C*   -avgd(x),avgn(x),avge(x)-- Average of depth, north and east      *
C*      between the first and last depth peak                         *
C*   -grpstarttime(x),grpstoptime(x)-- Overall data time step at      *
C*      which each "group" was started ie. when depth thresholds      *
C*      crossed.                                                      *
C*   -ainitial-- Raw angle calculated from arctan(East curr/North    *
C*      curr).  The signs of a, east and north determines the         *
C*      azimuth (see equations in program)                            *
C*   -a-- Converted ainitial from radians to degrees                  *
C*   -theta-- Azimuth determined from a, north and east as described*
C*      in Section 6 of the S4 manual.                                *
C*   -tntheta-- Angle corrected to true north for Siuslaw River       *
C*      entrance, +18.4 degrees (1990)                                *
C*********************************************************************
      Character*25 infile,outfile
      Character*70 line
      Write(*,*)'Please enter the input filename'
      read(*,90)infile
  90  format(A25)
      Write(*,*)'Please enter the output filename'
      read(*,90)outfile
```

```
      open(2,file=infile,status='old')
      open(3,file=outfile,status='unknown')
      write(3,897)
      write(3,899)
C*****Read the column titles
      read(2,91,end=95)line
  91  format(A70)
C*****Read data from "READS4.EXE" program in the format depth (meters),
C*****Northing and Easting
  95  do 100 i=1,12000
      read(2,*,end=150)depth(i),north(i),east(i)
 100  continue
 150  nofpts=i-1
      npt=0
      Write(*,*)'Please enter the depth threshold (f3.1)'
      read(*,92)depthresh
  92  format(f3.1)
C*****Using depth threshold criteria, put desired samples into groups
      do 200 ngp=1,50
           ngppt=0
  50       npt=npt+1
           if(npt.gt.nofpts)then
           goto 250
           endif
           if(depth(npt).ge.depthresh)then
              ngppt=ngppt+1
              d(ngp,ngppt)=depth(npt)
              n(ngp,ngppt)=north(npt)
              e(ngp,ngppt)=east(npt)
c              write(*,*)ngp, ngppt, d(ngp,ngppt), n(ngp,ngppt),
c     *e(ngp,ngppt)
           else
              goto 50
           endif
           if(depth(npt+1).lt.depthresh)then
              grpstoptime(ngp)=npt
              grpstarttime(ngp)=(npt-ngppt)+1
              lastgrppt(ngp)=ngppt
c              write(*,*)'Group Number=',ngp
c              write(*,*)'Number of Group Points=',ngppt
c      write(*,*)'grpStarttime=',grpstarttime(ngp),'grpStoptime=',
c     *grpstoptime(ngp)
              goto 200
            else
              goto 50
           endif
 200  continue
C*****Determine the starting and ending points for averaging by checking
C     for slope changes in the depth time series
c      write(*,*)'NUMBER OF GROUPS=',ngp-1
 250  ngpf=ngp-1
      do 400 j=1,ngpf
         sngppt=0
         do 300 sngppt=1,50
            if(d(j,sngppt).lt.d(j,sngppt+1))then
            goto 300
            elseif(d(j,sngppt).ge.d(j,sngppt+1))then
               startavg(j)=sngppt
               avgstarttime(j)=grpstarttime(j)+sngppt-1
c               write(*,*)'startavg(j)=',startavg(j)
```

```
c                write(*,*)'grpstarttime(j)=',grpstarttime(j)
c                write(*,*)'avgstarttime(j)=',avgstarttime(j)
                goto 400
              endif
 300  continue
 400  continue
      do 600 l=1,ngpf
      ngppts=lastgrppt(l)
 501        if(d(l,ngppts).lt.d(l,ngppts-1))then
            ngppts=ngppts-1
            goto 501
            elseif(d(l,ngppts).ge.d(l,ngppts-1))then
                endavg(l)=lastgrppt(l)-ngppts-1
                avgstoptime(l)=grpstoptime(l)-(lastgrppt(l)-ngppts)
c                write(*,*)'endavg(l)=',endavg(l)
c                write(*,*)'grpstoptime(l)=',grpstoptime(l)
c                write(*,*)'avgstoptime(l)=',avgstoptime(l)
            endif
 600  continue
C*****Calculate average depth, northing and easting for each group
c      open(4,file='test.out',status='new')
      sumd=0
      sumn=0
      sume=0
      sumcurr=0
      do 700 igrp=1,ngpf
      nofgrppts=(avgstoptime(igrp)-avgstarttime(igrp))+1
      enddo=startavg(igrp)+nofgrppts-1
c      write(*,*)startavg(igrp),enddo
        do 800 jgrp=startavg(igrp),enddo
           sumd=sumd+d(igrp,jgrp)
           sumn=sumn+n(igrp,jgrp)
           sume=sume+e(igrp,jgrp)
           sumcurr=sumcurr+(n(igrp,jgrp)**2+e(igrp,jgrp)**2)**0.5
c           write(4,975)igrp, jgrp, sumd, sumn, sume, sumcurr
 800  continue
           avgcurr=sumcurr/nofgrppts
           avgd(igrp)=sumd/nofgrppts
           avgn(igrp)=sumn/nofgrppts
           avge(igrp)=sume/nofgrppts
c           write(*,*)'nofgrppts for avg=',nofgrppts
           ainitial=atan(avge(igrp)/avgn(igrp))
           a=ainitial*180/3.1416
               if(a.gt.0.0.and.avge(igrp).gt.0.0)then
               theta=a
               elseif(a.lt.0.0.and.avgn(igrp).gt.0.0)then
               theta=a+360.0
               elseif(avgn(igrp).lt.0.0.or.avge(igrp).lt.0.0)then
               theta=a+180.0
               endif
C*****Adjust direction to true north...add 18.4 degrees
         tntheta=theta+18.4
         write(3,900)avgstarttime(igrp),avgstoptime(igrp),
     *avgd(igrp),avgcurr,tntheta,avgn(igrp),avge(igrp)
      sumd=0
      sumn=0
      sume=0
      sumcurr=0
 700  continue
 897  format(' ',2x,'Avg Time (s)',32x,'Theta')
```

```
 899  format(' ',1x,'Start   End',5x,'Avg Depth',4x,'Avg Vel',3x,
     *'(w.r.t. TN)',3x,'Avg North',3x,'Avg East')
 900  format(' ',2i8,2x,f9.6,3x,f8.2,4x,f8.2,4x,f8.2,3x,f8.2)
 950  format(' ',2x,'Grp Num',1x,'Pt Num','Depth','North','East')
 951  format(' ',i4,3x,i5,3x,f5.2,3x,2f9.2)
c 975  format(' ',2i5,4f15.2)
      stop
      end
```

```
C*********************************************************************
C*                          VELDIR-2.FOR                             *
C*  This program calculates the mean velocity and an average direc-  *
C*  tion (from the mean Northing and Easting current magnitudes)     *
C*  output from the S4 Current Meter.  The ASCII, Hexadecimal data   *
C*  must first be resolved and converted by using the "READS4.EXE"   *
C*  program (written in PASCAL).  Assuming data collection of 2 Hz   *
C*  (i.e. one sample every 1/2 second), this program will read a     *
C*  data set up to 12,000 samples or 1 hour and 40 minutes.          *
C*  One minute averages are calculated                               *
C*********************************************************************
C
C!!!!!!!!!!!!!!!!!!!!!!!!!!!!!!!!!!!!!!!!!!!!!!!!!!!!!!!!!!!!!!!!!!!!!!!
C  NOTE:  THIS PROGRAM WRITTEN TO READ THROUG SPIKES AND GIVE ONLY  !
C         1 MINUTE AVERAGES STARTING 3 SECONDS AFTER THE DEPTH      !
C         CRITERIA IS MET.
C!!!!!!!!!!!!!!!!!!!!!!!!!!!!!!!!!!!!!!!!!!!!!!!!!!!!!!!!!!!!!!!!!!!!!!!
$Large
      Dimension depth(12000),north(12000),east(12000)
      Dimension v(120)
      Real depth,north,east,theta,sumv,sumnorth,sumeast,sumdepth
      Real v,avgeast,avgnorth,avgv,avgdepth,a,ainitial
      Real endtime,starttime,depthresh,comthresh
      Integer nofpts
      Character*25 infile,outfile
      Character*70 line
      Write(*,*)'Please enter the input filename'
      read(*,90)infile
  90  format(A25)
      Write(*,*)'Please enter the output filename'
      read(*,90)outfile
      open(2,file=infile,status='old')
      open(3,file=outfile,status='unknown')
      write(3,897)
      write(3,899)
C*****Read the column titles
      read(2,91,end=95)line
  91  format(A70)
C*****Read data from "READS4.EXE" program in the format depth (meters),
C*****Northing and Easting
  95  do 100 i=1,12000
      read(2,*,end=150)depth(i),north(i),east(i)
 100  continue
 150  nofpts=i-1
      sumdepth=0
      sumv=0
      sumnnorth=0
      sumeast=0
      k=1
      write(*,*)'Please enter the depth threshold'
      read(*,92)depthresh
      write(*,*)'Please enter the depth comparison threshold'
      read(*,92)comthresh
  92  format(f3.1)
      do 200 j=1,nofpts
C*****Check depth threshold
      depthcheck=abs(depth(j)-depth(j+1))
      if(depth(j).gt.depthresh.and.depthcheck.le.comthresh)then
         if(k.lt.6)then
         k=k+1
```

```
          goto 200
          endif
          if(k.le.126)then
             v(j)=(north(j)**2.+east(j)**2.)**0.5
             sumv=sumv+v(j)
             sumnorth=sumnorth+north(j)
             sumeast=sumeast+east(j)
             sumdepth=sumdepth+depth(j)
c          write(*,*)sumnorth,sumeast,sumdepth
             k=k+1
             goto 200
          else
          avgnorth=sumnorth/120.
          avgeast=sumeast/120.
          avgv=sumv/120.
          ainitial=atan(avgeast/avgnorth)
          a=ainitial*180/3.1416
c          write(*,*)'ainitial=',ainitial,'   ','a =',a
                if(a.gt.0.0.and.avgeast.gt.0.0)then
                theta=a
                elseif(a.lt.0.0.and.avgnorth.gt.0.0)then
                theta=a+360.0
                elseif(avgnorth.lt.0.0.or.avgeast.lt.0.0)then
                theta=a+180.0
                endif
          avgdepth=sumdepth/120.
          endtime=(j-1)/2.
          starttime=(j-120)/2.
C     Adjust direction to true north...add 18.2 degrees
          tntheta=theta+18.2
          write(3,900)starttime,endtime,avgdepth,avgv,tntheta,avgnorth
     *,avgeast
          sumv=0
          sumnorth=0
          sumeast=0
          sumdepth=0
          k=1
          endif
       else
       k=1
       sumv=0
       sumnorth=0
       sumeast=0
       sumdepth=0
       endif
 200   continue
 897   format(' ',2x,'Time (s)',32x,'Theta')
 899   format(' ',1x,'Start   End',5x,'Avg Depth',4x,'Avg Vel',3x,
     *'(w.r.t. TN)',3x,'Avg North',3x,'Avg East')
 900   format(' ',2f7.1,2x,f9.6,3x,f8.2,4x,f8.2,4x,f8.2,3x,f8.2)
       stop
       end
```

```
program readS4;

{ Program modified 9/1/92 by Mike Carpenter to read tilt data.    }
{ Currently tilt data is simply ignored                           }
{ Changed result of Hex3ToDec and argument of Depth to longint    }
{ to eliminate 'rollover' problem at 4m depth when in 70m range   }
{ Modified Hex4ToDec and Hex3ToDec; sets result to 0 when out     }
{ of range characters are detected in data -- MC 9/10/92          }

uses crt;

var
 infile, outfile:                          text;
 N, E, D, Tx, Ty, temp, c:                 real;
 inchar, keychar:                          char;
 infilename, outfilename,
 Curr, Dep, Tilt:                  string;

 Function Hex3ToDec (Hex:string):integer;
  (*Converts a 12-bit hex string to a pascal integer*)
  var
   Dec: array [1..3] of integer;
   i, code : integer;
   BadData : boolean;

  begin
  BadData := false;
   for i:=1 to 3 do
    case Hex[i] of
     '0'..'9' : val (copy(Hex,i,1), Dec[i], code);
     'A'..'F' : Dec[i]:=Ord(Hex[i])-55;
     'a'..'f' : Dec[i]:=Ord(Hex[i])-87;
    else
     begin
     writeln ('Invalid character: ', Hex[i],' in hex data');
     BadData := true;
     end;
    end; (*case*)
    Dec[1]:=Dec[1] shl 8;
    Dec[2]:=Dec[2] shl 4;
    Hex3ToDec:=Dec[3]+Dec[2]+Dec[1];
    if BadData then Hex3ToDec := 0;
   end; (*Hex3ToDec*)

 Function Hex4ToDec (Hex:string):longint;
  (*Converts a 16-bit hex string to a pascal integer*)

   var
    Dec: array [1..4] of integer;
    i, code:integer;
    BadData : boolean;

   begin
   BadData := false;
```

```
    for i:=1 to 4 do
     case Hex[i] of
     '0'..'9' : val (copy(Hex,i,1), Dec[i], code);
     'A'..'F' : Dec[i]:=Ord(Hex[i])-55;
     'a'..'f' : Dec[i]:=Ord(Hex[i])-87;
    else
     begin
     writeln ('Invalid character: ', Hex[i],' in hex data');
     BadData := true;
     end;
    end; (*case*)
    Dec[1]:=Dec[1] shl 12;
    Dec[2]:=Dec[2] shl 8;
    Dec[3]:=Dec[3] shl 4;
    Hex4ToDec:=Dec[4]+Dec[3]+Dec[2]+Dec[1];
    if BadData then Hex4ToDec := 0;
    end;  (*Hex4ToDec*)

procedure header;

 begin
  writeln (outfile,'Depth (m)':15, 'N Current':15, 'E Current':15);
  writeln (outfile);
 end;

procedure Depth (DDDD:longint);

 begin
  D:= 70*DDDD/16383;
 end;

procedure ReadCur;

 var
  inchar:char;
  i:byte;

 begin
  Curr:='';
  repeat
   read (infile,inchar);
  until (inchar<>' ') and (ord(inchar)<> 13) and (ord(inchar)<>10);
  Curr:=Curr + inchar;
  for i:= 1 to 5 do
   begin
    read (infile,inchar);
    if (inchar=' ') then inchar:='0';
    Curr:=Curr+inchar;
   end;
 end;

 procedure ReadDep;
```

```
 var
  inchar:char;
  i:byte;

 begin
  Dep:='';
  repeat
   read (infile,inchar);
  until (inchar<>' ') and (ord(inchar)<> 13) and (ord(inchar)<>10);
  Dep:=Dep + inchar;
  for i:= 1 to 3 do
   begin
    read (infile,inchar);
    if (inchar=' ') then inchar:='0';
    Dep:=Dep+inchar;
   end;
 end;

 procedure ReadTilt;

 var
  inchar:char;
  i:byte;

 begin
  Tilt:='';
  repeat
   read (infile,inchar);
  until (inchar<>' ') and (ord(inchar)<> 13) and (ord(inchar)<>10);
  Tilt:=Tilt + inchar;
  for i:= 1 to 3 do
   begin
    read (infile,inchar);
    if (inchar=' ') then inchar:='0';
    Tilt:=Tilt+inchar;
   end;
 end;


procedure Vectors (NNN,EEE:integer);

 begin
  if NNN>=2048 then N:=(NNN-4096)/5;
  if NNN<2047 then N:=NNN/5;
  if EEE>=2048 then E:=(EEE-4096)/5;
  if EEE<2047 then E:=EEE/5;
 end;

begin
 write ('File for input?');
 readln (infilename);
 assign (infile,infilename);
```

```
 reset (infile);
 write ('File for output?');
 readln (outfilename);
 assign (outfile, outfilename);
 rewrite (outfile);
 header;
 repeat
  readcur;
  readdep;
  readtilt;
  readtilt;
  vectors (Hex3ToDec(copy(curr,1,3)),Hex3ToDec(copy(curr,4,3)));
  depth (Hex4ToDec(Dep));
  writeln (outfile, D:15:4, N:15:4, E:15:4);
 until eof(infile);
 close (infile);
 close (outfile);
end.
```

Appendix B
Current Vector Information

Appendix B
Current Vector Information

Point	Start Time		End Time		Current Meter Avg Depth, m	Current Mag, cm/s	Current Dir, deg	N-Vector, cm/s	E-Vector, cm/s	Start Point	
	1/2 sec	Clock	1/2 sec	Clock						X	Y
3 September 1992 Sampling Interval I											
1	866	10:47:13	1108	10:49:14	2.6	94.6	271.0	-28.0	-90.4	1042007	878364
2	3	10:51:01.5	120	10:52:00	3.0	132.7	238.7	-100.9	-86.1	1042007	878364
3	258	10:53:09	446	10:54:43	1.8	166.6	291.5	9.4	-166.4	1042007	878364
4	566	10:55:43	754	10:57:17	2.5	78.3	219.8	-72.8	-28.8	1042007	878364
5	950	10:58:55	1174	11:00:47	4.0	86.3	249.4	-54.1	-67.2	1042007	878364
6	1309	11:01:54.5	1473	11:03:16.5	4.7	51.3	243.9	-35.8	-36.7	1042007	878364
7	1635	11:04:37.5	1785	11:05:52.5	5.4	43.5	374.4	43.4	-2.9	1042007	878364
8	2578	11:12:29	2754	11:13:57	6.3	56.2	368.9	55.4	-9.1	1042007	878364
9	2871	11:14:55.5	3026	11:16:13	3.8	87.4	332.8	61.4	-62.2	1042007	878364
10	3136	11:17:08	3333	11:18:46.5	3.5	107.5	239.8	-80.4	-71.4	1042007	878364

(Sheet 1 of 6)

Appendix B (Continued)

Point	Start Time		End Time		Current Meter Avg Depth, m	Current Mag, cm/s	Current Dir, deg	N-Vector, cm/s	E-Vector, cm/s	Start Point	
	1/2 sec	Clock	1/2 sec	Clock						X	Y
11	3481	11:20:00.5	3649	11:21:24.5	5.8	80.6	349.8	70.9	-38.3	1042007	878364
12	3772	11:22:26	3859	11:23:09.5	6.5	33.3	49.7	28.4	17.4	1042007	878364
13	4040	11:24:40	4182	11:25:51	6.6	42.6	322.5	24.0	-35.2	1042007	878364
14	4648	11:29:44	4794	11:30:57	3.0	99.9	206.5	-98.9	-14.4	1042007	878364
15	4865	11:31:32.5	4995	11:32:37.5	3.2	78.3	262.7	-33.7	-70.7	1042007	878364
16	5132	11:33:46	5276	11:34:58	4.1	125.7	333.8	89.8	-87.9	1042007	878364
17	5358	11:35:39	5478	11:36:39	4.3	102.7	75.8	55.1	86.7	1042007	878364
18	5563	11:37:21.5	5687	11:38:23.5	3.5	50.7	276.5	-10.3	-49.6	1042007	878364
19	5801	11:39:20.5	6017	11:41:08.5	4.2	53.9	339.0	41.7	-34.1	1042007	878364
20	3	11:42:01.5	136	11:43:08	6.3	42.3	75.8	22.7	35.7	1042007	878364
21	230	11:43:55	326	11:44:43	7.1	22.1	112.0	-1.5	22.0	1042007	878364

(Sheet 2 of 6)

Appendix B (Continued)

Point	Start Time		End Time		Current Meter Avg Depth, m	Current Mag, cm/s	Current Dir, deg	N-Vector, cm/s	E-Vector, cm/s	Start Point	
	1/2 sec	Clock	1/2 sec	Clock						X	Y
9 September 1992 Sampling Interval II											
1	1	10:58:00.5	173	10:59:26.5	5.0	91.7	343.2	75.1	-52.6	1042007	878364
2	285	11:00:22.5	442	11:01:41	3.7	139.4	373.3	138.9	-11.9	1042007	878364
3	591	11:02:55.5	909	11:05:34.5	4.4	121.8	37.1	115.2	39.4	1042007	878364
4	1031	11:06:35.5	1190	11:07:55	5.7	90.9	107.1	1.8	90.9	1042007	878364
5	1390	11:09:35	1568	11:11:04	6.0	104.3	43.8	94.0	45.1	1042007	878364
6	2013	11:14:46.5	2263	11:16:51.5	5.5	117.6	283.5	-9.7	-117.2	1042007	878364
7	2371	11:17:45.5	2589	11:19:34.5	5.6	101.4	163.1	-83.0	58.3	1042007	878364
8	2719	11:20:39.5	2861	11:21:50.5	6.4	93.3	156.9	-70.1	61.7	1042007	878364
9	2960	11:22:40	3101	11:23:50.5	7.4	67.4	207.9	-66.4	-11.4	1042007	878364
10	3425	11:26:32.5	3609	11:28:04.5	4.0	136.3	369.0	134.6	-21.7	1042007	878364
11	3820	11:29:50	4090	11:32:05	4.5	113.3	29.0	111.3	21.1	1042007	878364

Appendix B (Continued)

Point	Start Time		End Time		Current Meter Avg Depth, m	Current Mag, cm/s	Current Dir, deg	N-Vector, cm/s	E-Vector, cm/s	Start Point	
	1/2 sec	Clock	1/2 sec	Clock						X	Y
12	4	11:33:02	147	11:34:13.5	3.9	101.3	24.9	100.6	11.9	1042007	878364
13	301	11:35:30.5	418	11:36:29	4.9	89.2	41.8	81.7	35.8	1042007	878364
Sampling Interval III											
1	83	13:21:41.5	261	13:22:10.5	3.8	74.5	282.8	-7.0	-74.1	1042007	878364
2	444	13:24:42	635	13:26:17.5	4.8	112.0	332.3	77.9	-80.5	1042007	878364
3	756	13:27:18	878	13:28:19	4.6	103.4	304.4	28.8	-99.3	1042007	878364
4	1005	13:29:22.5	1202	13:31:01	4.4	108.5	357.6	101.6	-38.2	1042007	878364
5	1339	13:32:09.5	1504	13:33:32	6.8	92.7	367.7	91.1	-17.0	1042007	878364
6	1614	13:34:27	1756	13:35:38	7.5	85.2	323.7	49.4	-69.4	1042007	878364
7	1883	13:36:41.5	2014	13:37:47	7.1	110.4	195.0	-110.3	6.1	1042007	878364
8	2156	13:38:58	2307	13:40:13.5	6.3	118.7	228.9	-102.0	-60.6	1042007	878364
9	2903	13:45:11.5	3033	13:46:16.5	5.7	108.9	359.7	103.2	-34.6	1042007	878364
10	3135	13:47:07.5	3299	13:48:29.5	3.8	94.9	326.9	59.4	-74.0	1042007	878364

Appendix B (Continued)

Point	Start Time		End Time		Current Meter Avg Depth, m	Current Mag, cm/s	Current Dir, deg	N-Vector, cm/s	E-Vector, cm/s	Start Point	
	1/2 sec	Clock	1/2 sec	Clock						X	Y
11	3818	13:52:49	3972	13:54:06	3.8	122.5	341.2	97.8	-73.8	1042007	878364
12	4308	13:56:54	4435	13:57:57.5	3.7	147.1	338.9	113.8	-93.2	1042007	878364
13	4681	14:00:00.5	4836	14:01:18	3.0	112.8	116.7	-16.8	111.6	1042007	878364
14	5005	14:02:42.5	5142	14:03:51	3.8	137.6	353.6	125.1	-57.3	1042007	878364
15	5729	14:08:44.5	5890	14:10:05	5.5	81.3	188.7	-80.1	13.4	1042007	878364
16	6390	14:14:15	6523	14:15:21.5	3.9	112.3	361.3	107.4	-32.6	1042007	878364
17	6657	14:16:28.5	6758	14:17:19	4.0	86.4	362.8	83.3	-23.0	1042007	878364
18	6911	14:18:35.5	7040	14:19:40	6.5	91.8	351.7	82.2	-41.0	1042007	878364
Sampling Interval IV											
1	202	15:43:41	326	15:44:43	1.8	132.2	268.9	-43.6	-124.8	1042007	878364
2	427	15:45:33.5	561	15:46:40.5	2.9	95.0	249.7	-59.1	-74.4	1042007	878364
3	680	15:47:40	871	15:49:15.5	4.3	98.9	246.8	-65.4	-74.1	1042007	878364
4	1504	15:54:32	1695	15:56:07.5	3.6	137.3	280.3	-18.9	-136.0	1042007	878364

Appendix B (Concluded)

Point	Start Time		End Time		Current Meter Avg Depth, m	Current Mag, cm/s	Current Dir, deg	N-Vector, cm/s	E-Vector, cm/s	Start Point	
	1/2 sec	Clock	1/2 sec	Clock						X	Y
5	2093	15:59:26.5	2373	16:01:46.5	4.6	124.8	361.4	119.5	-36.2	1042007	878364
6	2507	16:02:53.5	2665	16:04:12.5	4.6	149.4	312.9	62.3	-135.8	1042007	878364
7	2771	16:05:05.5	2905	16:06:12.5	5.5	150.7	292.5	11.3	-150.2	1042007	878364
8	3032	16:07:16	3199	16:08:39.5	6.0	122.5	291.3	6.7	-122.3	1042007	878364
9	3565	16:11:42.5	3731	16:13:05.5	3.3	160.8	188.9	-158.7	26.0	1042007	878364
10	3889	16:14:24.5	4057	16:15:48.5	3.4	160.7	349.2	140.6	-77.8	1042007	878364
11	4143	16:16:31.5	4261	16:17:30.5	6.3	108.0	305.9	32.8	-102.9	1042007	878364
12	4454	16:19:07	4616	16:20:28	6.9	110.0	282.8	-10.3	-109.5	1042007	878364
13	4826	16:22:13	4937	16:23:08.5	4.3	120.3	111.4	-6.8	120.2	1042007	878364
14[1]	5037	16:23:58.5	5157	16:24:58.5	5.1	81.0	308.0	27.4	-76.2	1042007	878364
15	5276	16:25:58	5426	16:27:13	6.9	101.0	289.2	1.7	-101.0	1042007	878364

(Sheet 6 of 6)

[1] Curr Mag, Curr Dir, N-vector, E-vector and End point adjusted based on visual observation and removal of some data points from the time series.

Appendix B
Vector Information

Point	Start Time		End Time		Current Meter Avg Depth, m	Current Mag, cm/s	Current Dir, deg	N-Vector, cm/s	E-Vector, cm/s	Start Point	
	1/2 sec	Clock	1/2 sec	Clock						X	Y
					18 July 1990	Sampling Interval I					
NA1	1117	9:53:18.5	1533	9:56:46.5	4.746	80.770	252.62	-47.4496	-65.3631	1041993	878776
NA2	1762	9:58:41	1956	10:01:18	6.490	72.300	316.90	34.4946	-63.5406	1042021	879298
NA3	2070	10:01:15	2230	10:02:35	6.412	74.370	176.40	-68.9539	27.8614	1041993	879493
NA4	3051	10:09:25.5	3337	10:11:48.5	5.349	76.300	250.24	-47.1441	-59.9927	1041991	879802
NA5	3489	10:13:04.5	3734	10:15:07	5.074	78.310	173.37	-70.9567	33.1302	1041971	880175
NA6	3947	10:16:53.5	4242	10:19:21	5.888	44.916	210.07	-43.9870	-9.0881	1042020	880703
NB1	5282	10:28:01	5440	10:29:20	8.073	66.100	299.65	12.8935	-64.8303	1041543	878792
NB2	5527	10:30:03.5	5702	10:31:31	5.286	57.414	260.91	-26.5000	-50.9325	1041541	879078
NB3	5817	10:32:28.5	6043	10:34:21.5	5.844	54.233	230.97	-45.7029	-29.1970	1041552	879431
NB4	6185	10:35:32.5	6333	10:36:46.5	6.292	78.980	145.52	-47.6700	62.9715	1041594	879929
NB5	6501	10:38:10.5	6900	10:41:30	7.083	54.220	32.64	52.5550	13.3334	1041571	880396

(Sheet 1 of 4)

Appendix B (Continued)

Point	Start Time		End Time		Current Meter Avg Depth, m	Current Mag, cm/s	Current Dir, deg	N-Vector, cm/s	E-Vector, cm/s	Start Point	
	1/2 sec	Clock	1/2 sec	Clock						X	Y
12	7065	10:42:52.5	7574	10:47:07.5							
NC1	7955	10:50:17.5	8318	10:53:19	8.377	69.208	291.01	3.1506	-69.1362	1041149	879308
NC2	8656	10:56:08	8947	10:58:33.5	6.286	55.220	232.08	-45.9489	-30.6259	1041251	879069
Sampling Interval II											
NE10	1380	13:56:30	1660	13:58:50	6.380	54.79	258.90	-26.9795	-47.6870	1039901	877876
NE11	1808	14:00:04	1944	14:01:12	7.501	61.57	232.68	-50.8766	-34.6761	1040054	878472
NE12	2086	14:02:23	2282	14:04:01	8.713	47.13	214.57	-45.2664	-13.1222	1040038	878729
NE13	2922	14:05:11	2571	14:06:25.5	9.318	52.23	246.78	-34.6879	-39.0477	1040195	879180
ND10	2789	14:08:14.5	2932	14:09:26	6.511	71.18	254.82	-39.3651	-59.3041	1040998	878717
ND11	3080	14:10:40	3221	14:11:50.5	6.892	48.55	238.49	-37.1423	-31.2658	1041005	879227
ND12	3342	14:12:51	3480	14:14:00	7.089	53.50	193.97	-53.3399	4.1360	1041116	879679
ND13	3611	14:15:05.5	3745	14:16:12.5	7.366	48.00	213.05	-46.4392	-12.1410	1041204	880140
NC10	3976	14:18:08	4118	14:19:19	6.925	102.11	272.61	-27.7913	-98.2553	1041165	878653

(Sheet 2 of 4)

Appendix B (Continued)

Point	Start Time		End Time		Current Meter Avg Depth, m	Current Mag, cm/s	Current Dir, deg	N-Vector, cm/s	E-Vector, cm/s	Start Point	
	1/2 sec	Clock	1/2 sec	Clock						X	Y
NC11	4215	14:20:07.5	4369	14:21:24.5	5.768	100.76	295.23	11.9915	-100.0439	1041257	879050
NC12	4509	14:22:34.5	4636	14:23:38	6.256	40.86	223.63	-36.9631	-17.4147	1041323	879582
NC13	4791	14:24:55.5	4941	14:26:10.5	7.087	39.42	221.43	-36.2784	-15.4211	1041348	880208
NC14	5096	14:27:28	5244	14:28:42	7.831	43.61	208.59	-42.9225	-7.7131	1041412	880782
NB10	5330	14:31:05	5670	14:32:15	6.848	98.79	277.80	-18.1649	-97.1056	1041530	878766
NB11	5792	14:33:16	6151	14:36:15.5	4.385	68.62	256.25	-36.5119	-58.0998	1041634	879064
NB12	6297	14:37:28.5	6428	14:38:34	5.553	46.23	226.06	-40.9477	-21.4593	1041545	879552
NB13	6567	14:39:43.5	6687	14:40:43.5	5.708	46.10	194.07	-45.9682	3.4840	1041708	880145
NB14	6862	14:40:41	7024	14:43:32	6.389	110.64	222.07	-101.3291	-44.4254	1041776	880767
NA10	7343	14:46:11.5	7476	14:47:18	3.019	84.32	281.13	-10.6750	-83.6415	1041976	878527
NA11	7582	14:48:11	7708	14:49:14	5.268	101.73	212.87	-98.5049	-25.4121	1041052	878896
NA12	7822	14:50:11	7955	14:51:17.5	5.879	68.25	234.18	-55.3718	-39.9002	1041991	879416
NA13	8143	14:52:51.5	8271	14:53:55.5	4.561	80.41	215.33	-76.9255	-23.4145	1041993	880187

Appendix B (Concluded)

Point	Start Time		End Time		Current Meter Avg Depth, m	Current Mag, cm/s	Current Dir, deg	N-Vector, cm/s	E-Vector, cm/s	Start Point	
	1/2 sec	Clock	1/2 sec	Clock						X	Y
NA14	8460	14:55:30	8718	14:57:39	6.577	46.44	201.07	-46.3896	-2.1622	1041964	881264
NH1	9070	15:00:35	9210	15:01:45	2.173	108.18	78.98	53.1383	94.2297	1041835	878363
Sampling Interval III 19 July 1990											
NA1	1612	8:20:26	1819	8:22:09.5	4.203	198.31	310.29	73.9459	-184.0078	1041996	878286
NA2	1940	8:23:10	2125	8:24:42.5	2.670	104.36	287.91	-0.8954	-104.3562	1041979	878514
NA3	2272	8:25:56	2427	8:27:13.5	3.650	98.10	251.85	-58.4106	-78.8151	1041989	878738
NA4	2536	8:28:08	2724	8:29:42	5.362	82.66	203.89	-82.2810	-7.9067	1042038	878968
NA5	2873	8:30:56.5	3051	8:32:25.5	6.045	74.90	183.63	-72.4240	19.0992	1042020	879270
NA6	3214	8:33:47	3552	8:36:36	5.258	82.42	231.68	-68.9032	-45.2262	1042000	879274
NA7	3656	8:37:28	3934	8:39:47	4.475	68.28	216.72	-64.8204	-21.4588	1041999	880092
NA8	4118	8:41:19	4555	8:44:57.5	5.218	94.46	240.54	-70.0427	-63.3775	1042002	880507
NA9	4688	8:46:04	4892	8:47:46	5.624	163.52	240.45	-121.4140	-109.5328	104125	880905
NB1	5893	8:56:06.6	6227	8:58:53.5	4.686	102.13	376.18	102.0531	-3.9616	1041534	878603

(Sheet 4 of 4)

Appendix C
Notation

a = Dimension of curvature (onshore/offshore)

b = Dimension of curvature (alongshore)

E = Easting component of the current vector

i = Sample number

L = Length of mid-section of "S"

N = Northing component of the current vector

n = Number of samples

r = Radius of curvature

V_{avg} = Magnitude of the resultant vector average

θ_{init} = Resultant vector angle of the average vector components

θ_{degree} = Resultant vector angle relative to magnetic north

REPORT DOCUMENTATION PAGE

Form Approved
OMB No. 0704-0188

1. AGENCY USE ONLY *(Leave blank)*

2. REPORT DATE
September 1995

3. REPORT TYPE AND DATES COVERED
Report 2 of a series

4. TITLE AND SUBTITLE
Effectiveness of Spur Jetties at Siuslaw River, Oregon; Report 2, Localized Current Flow Patterns Induced by Spur Jetties: Airborne Current Measurement System and Prototype/Physical Model Correlation

5. FUNDING NUMBERS

6. AUTHOR(S)
Cheryl E. Pollock

7. PERFORMING ORGANIZATION NAME(S) AND ADDRESS(ES)
U.S. Army Engineer Waterways Experiment Station
3909 Halls Ferry Road, Vicksburg, MS 39180-6199

8. PERFORMING ORGANIZATION REPORT NUMBER
Technical Report CERC-95-14

9. SPONSORING/MONITORING AGENCY NAME(S) AND ADDRESS(ES)
U.S. Army Corps of Engineers
Washington, DC 20314-1000

10. SPONSORING/MONITORING AGENCY REPORT NUMBER

11. SUPPLEMENTARY NOTES
Available from National Technical Information Service, 5285 Port Royal Road, Springfield, VA 22161.

12a. DISTRIBUTION/AVAILABILITY STATEMENT
Approved for public release; distribution is unlimited.

12b. DISTRIBUTION CODE

13. ABSTRACT *(Maximum 200 words)*

The development of an airborne current measurement system that can provide a near-synoptic view of near-bottom currents in extremely hostile wave and current environments is described. A helicopter is used as the support platform from which an electromagnetic current meter is suspended by cable to within one meter of the sea floor. The helicopter hovers overhead while data acquisition is accomplished at each spatial location. Maneuvering ease of the helicopter above the sea surface allows the system to be operated in almost any wave or current environment, around structures, or in dynamic bathymetry. The ability of the helicopter to move quickly from point to point allows nearshore bottom currents to be measured at several locations in a short period of time. Because the meter is not deployed at a stationary location, the use of only one current meter is required, and in situ deployment problems with scour or burying are alleviated. To demonstrate the capabilities of the system, data obtained under high-energy wave conditions at the structured entrance to the Siuslaw River, Florence, OR, are presented, and prototype current patterns are compared with results from sediment tracer tests performed in a previous physical model test.

14. SUBJECT TERMS
Coastal engineering—Oregon—Florence—Siuslaw River
Current measurements
Currents
Current/structure interaction
Spur jetties

15. NUMBER OF PAGES
117

16. PRICE CODE

17. SECURITY CLASSIFICATION OF REPORT	18. SECURITY CLASSIFICATION OF THIS PAGE	19. SECURITY CLASSIFICATION OF ABSTRACT	20. LIMITATION OF ABSTRACT
UNCLASSIFIED	UNCLASSIFIED		